

OPTICAL ABSORPTION OF  $\text{Pb}_x\text{Cd}_{1-x}\text{S}$  THIN FILMS PREPARED BY CHEMICAL BATH  
DEPOSITION

BY

YAW SARFO KANTANKA, BSc. Physics (Hons.)

A Thesis submitted to the Department of Physics, Kwame Nkrumah University of  
Science and Technology, in partial fulfillment of the requirement for the degree of  
MASTER OF PHILOSOPHY (SOLID STATE PHYSICS)

Department of Physics,

College of Science

MAY, 2013

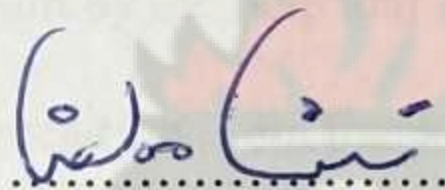


## DECLARATION

I hereby declare that this submission is my own work towards the M.Sc. and that, to the best of my knowledge, it contains no material previously published by any person nor material which has been accepted for the award of any other degree of the University, except where due acknowledgment has been made in the text.

KNUST

Yaw Sarfo Kantanka



24/10/2013

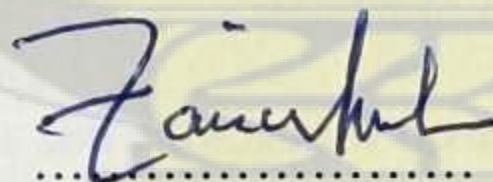
Student

Signature

Date

Certify by;

Prof. F. Boakye



25/10/2013

Supervisor

Signature

Date

Certify by;

Prof. S. K. Danuor



25/10/2013

Head of Department

Signature

Date



## ACKNOWLEDGEMENT

My foremost thanks and gratitude is to the ALMIGHTY and EVER MERCIFUL GOD who has carried me on his wings and given me the strength, knowledge and self- confidence to complete this work.

Furthermore, I express my sincere appreciation to my thoughtful and motivating supervisor, Professor Francis Boakye for his guidance and effective supervision in carrying out this thesis. For that, I am grateful

My work has seen its successful completion by the help and support provided me by various individuals and with a deep sense of appreciation, i am thankful to Dr. Kofi Ampong and Mr. Nkrumah of the Department of Physics, KNUST , Dr. Twumasi of the Department of Chemistry, KNUST.

I will also like to thank some Teaching Assistants namely James, Charles and Lommo who helped me in the preparative stage and analysis of my samples.

My heartfelt gratitude goes to my parents and siblings for their prayers and support.

Finally, my sincere gratitude goes to my benefactors: Mr. and Mrs. Adu for their monetary support for this program.



## ABSTRACT

Lead cadmium sulphide thin films with varying composition were successfully deposited from chemical baths containing lead acetate, cadmium acetate, thiourea and ammonia (as the basic medium). The thin films obtained using this method were smooth, uniform adherent bright yellow in colour and changed to black with increasing lead content. The crystal structure was studied using powder X-ray diffraction (XRD). The results showed reflection peaks at  $26.200^\circ$ ,  $44.221^\circ$ ,  $52.340^\circ$  and  $80.042^\circ$  corresponding respectively to the (111), (220), (311) and (422) planes of the cubic structured CdS thin film. Also, reflection peaks at  $26.200^\circ$ ,  $30.271^\circ$ ,  $43.491^\circ$  and  $50.206^\circ$  corresponds respectively to the (111), (200), (220) and (311) planes of the cubic structured PbS thin films. Optical absorption spectroscopy was used to investigate some optical properties of the films. The films were annealed in air at  $200^\circ\text{C}$  and  $300^\circ\text{C}$  for 75 minutes and the effect of annealing on the optical structure were studied.. The band gap analysed from optical absorption spectroscopy varied linearly with composition between that of CdS (2.36 eV) and PbS (1.60 eV) for the as-deposited samples whiles the annealed at  $300^\circ\text{C}$  samples varied from (2.30 eV) for CdS to (1.58 eV) for PbS. The decrease in band gap after thermal annealing is an indication of improved crystallinity in the samples.



## Table of Contents

<b>Declaration</b>	<b>i</b>
<b>Acknowledgement</b>	<b>ii</b>
<b>Abstract</b>	<b>iii</b>
<b>Table of Contents</b>	<b>iv</b>
<b>List of Tables</b>	<b>vii</b>
<b>List of Figures</b>	<b>viii</b>
<b>List of Symbols and Acronyms</b>	<b>x</b>

<b>1.0 INTRODUCTION</b>	<b>1</b>
1.1 Semiconductor Materials.....	4
1.2 Objectives of Project.....	6
1.3 Project Objectives.....	8
1.4 Structure of Thesis.....	8
<b>2.0 LITERATURE REVIEW</b>	<b>9</b>
2.1 Semiconductor Alloy and a Compound.....	9
2.2 Thin Films.....	11
2.3 Thin Film Deposition.....	13
2.3.1 Chemical Deposition.....	13
2.3.2 Physical Deposition.....	15
2.4 Chemical Bath Deposition.....	19
2.4.1 Basic Principles of Chemical Bath Deposition.....	22
2.4.2 Substrates and Substrate Preparation.....	24
2.5 Annealing.....	25
2.5.1 Irradiation Annealing.....	25



2.5.2 Recrystallization Annealing.....	26
2.5.3 Pulsed Annealing of Semiconductors.....	26
2.6 Crystal Structure of Some Important II-IV-VI Semiconductor Materials.....	28
2.6.1 Lead Sulphide.....	28
2.6.2 Cadmium Sulphide.....	29
2.7 Review of Lead Cadmium Sulphide Thin Films Prepared by CBD.....	31

### 3.0 THEORY 37

3.1 Energy Band Theory.....	37
3.2 Classification of Solids.....	40
3.2.1 Crystalline Semiconductors.....	41
3.2.2 Polycrystalline Semiconductors.....	43
3.2.3 Amorphous Semiconductors.....	45
3.3 Optical Absorption Spectroscopy.....	52
3.3.1 Optical Properties of semiconductors.....	53
3.3.2 Fundamental Absorption in Direct and Indirect Band Gap Semiconductors.....	56
3.3.3 Optical Absorption and Band Gap.....	58
3.4 X-ray Diffraction.....	60

### 4.0 EXPERIMENTAL DETAILS 63

4.1 Methodology.....	63
4.2 Substrate Preparation.....	63
4.3 Reagents.....	64
4.3.1 Standard Solution of 0.5M Lead Acetate.....	64
4.3.2 Standard Solution of 0.5M Cadmium Acetate.....	65



4.3.3 Standard Solution of 1M Thiourea.....	65
4.4 Chemical Equations for the Deposition Process.....	65
4.4.1 Decomposition of Thiourea.....	65
4.4.2 Decomposition of Lead and Cadmium Acetate.....	66
4.5 Sample Preparation.....	67
4.6 Measurement of the Absorption Spectra.....	68
4.7 Thermal Annealing.....	70
4.8 X-Ray Diffraction Measurements.....	71
<b>5.0 RESULTS AND DISCUSSION</b>	<b>73</b>
5.1 Results of the Optical Absorption Spectra.....	73
5.2 Determination of the Optical Band Gap.....	74
5.3 Effect of Thermal Annealing on the Optical Properties.....	78
5.4 X-Ray Diffraction Patterns of the Thin Films.....	81
<b>6.0 CONCLUSIONS AND RECOMMENDATIONS</b>	<b>84</b>
6.1 Conclusions.....	84
6.2 Recommendations.....	85

## REFERENCES



## LIST OF TABLES

**Table 4.1:** Summary of deposition conditions.....67

**Table 5.1:** Summary of variation of band gap with increasing Pb ion content for  $\text{Pb}_x\text{Cd}_{1-x}\text{S}$ ...80





LIST OF FIGURES

**Figure 1.1:** Relationship between Photonics and Key Technologies.....3

**Figure 1.2:** Specific application of Photonics.....3

**Figure 2.1:** Crystal Structure of Lead Sulphide.....29

**Figure 2.2:** Crystal structure of Cadmium Sulphide.....30

**Figure 3.1:** Oversimplified diagram of a Band of Energy.....38

**Figure 3.2:** Schematic Band Diagrams for an Insulator, Semiconductor and a Metal.....39

**Figure 3.3:** Schematics of the three general types of Structural orders.....41

**Figure 3.4:** Two dimensional view of the Structure of Amorphous and Crystalline solid.....46

**Figure 3.5:** Density of State of a Crystalline Semiconductor.....48

**Figure 3.6:** Area of mobility between Valence and Conduction bands.....50

**Figure 3.7:** Schematic diagram of a two dimensional continuous random network of atoms having various bonding coordination.....51

**Figure 3.8:** Absorption coefficient plotted as a function of photon energy in a typical semiconductor.....55

**Figure 3.9:** Direct and Indirect electron transitions in semiconductors.....58

**Figure 3.10:** Schematic for X-Ray Diffraction.....60



<b>Figure 3.11:</b> Illustration of Bragg’s Law of Diffraction.....	61
<b>Figure 3.12:</b> Schematic of the rotating crystal method of X-Ray Diffraction.....	61
<b>Figure 4.1:</b> Diagram of the Experimental set-up for Chemical Bath Deposition.....	68
<b>Figure 4.2:</b> Schematic diagram of a single-beam Spectrophotometer.....	69
<b>Figure 4.3:</b> A Shimadzu UV-VIS Spectrophotometer.....	70
<b>Figure 5.1:</b> A plot of Absorbance vrs Wavelength for $Pb_xCd_{1-x}S$ .....	74
<b>Figure 5.2:</b> Plot of $(Ah\nu)^2$ vrs $h\nu$ for $Pb_xCd_{1-x}S$ as-deposited thin films.....	75
<b>Figure 5.3:</b> Plot of $(Ah\nu)^2$ vrs $h\nu$ for $Pb_{0.1}Cd_{0.9}S$ .....	76
<b>Figure 5.4:</b> A plot of band gap energy (eV) against composition (x).....	77
<b>Figure 5.5:</b> Optical Absorption Spectra of the as-deposited and annealed $Pb_{0.1}Cd_{0.9}S$ thin film.....	78
<b>Figure 5.6:</b> A plot showing the decreasing band gap of $Pb_{0.1}Cd_{0.9}S$ as its annealed in air.....	79
<b>Figure 5.7:</b> X-Ray Diffraction pattern of $Pb_{0.1}Cd_{0.9}S$ (as-deposited).....	81
<b>Figure 5.8:</b> X-Ray Diffraction pattern of $Pb_{0.15}Cd_{0.85}S$ (as-deposited).....	82
<b>Figure 5.9:</b> X-Ray Diffraction pattern of $Pb_{0.25}Cd_{0.75}S$ (as-deposited).....	83



## LIST OF SYMBOLS AND ACRONYMS

A Absorbance

$\alpha$  Absorption coefficient

CBD Chemical Bath Deposition

CdS Cadmium Sulfide

CVD Chemical Vapour Deposition

DOS Density of States

$K_i$  Stability constant of a complex ion

$h$  Planck constant

IR Infrared

$k$  Wave vector, Extinction coefficient

$\lambda$  Wavelength

JCPDS Joint Committee On Powder Diffraction Standards

MBE Molecular Beam Epitaxy

PbS Lead Sulphide

$\rho$  Resistivity

IP Ionic product

T Transmittance

UV Ultraviolet

$\nu$  Photon frequency

VIS Visible Spectrum

$x, y$  Compositional parameters/an integer number in polyacetylene

XRD X-Ray Diffraction

$K_{sp}$  Solubility constant



## CHAPTER ONE

### 1.0 INTRODUCTION

There is no doubt that semiconductors changed the world beyond anything that could have been imagined before them. Although people have probably always needed to communicate and process data, semiconductors have it possible for this task to be performed easily and under infinitely less time compared to the period where vacuum tubes were used for most electronic technology with its attendant shortcomings of unwanted heat generation, size and high cost.

The arrival of optical communications, personal computers, and digital television around the world has placed a heavy burden on materials and devices for signal transmission and processing. In telecommunication, the benefits of optical techniques for signal processing and transmission have already changed our lives in a major way by giving us access to the information superhighway (Simmons and Potter, 2000).

According to Busch, 1983 the term “semiconducting” was used for the first time by Alessandro Volta in 1782. The development of studies in semiconductor materials is traced from its beginnings with Michael Faraday in 1833 who noticed that the resistance of silver sulfide decreased with temperature, which was different than the dependence observed in metals (Laeri et al., 2003) to the production of the first

silicon transistor in 1954, which heralded the age of silicon electronics and microelectronics. An extensive quantitative analysis of the temperature dependence of the electrical conductivity of  $\text{Ag}_2\text{S}$  and  $\text{Cu}_2\text{S}$  was published in 1851 by Johann Hittorf (Busch, 1983). Prior to the advent of band theory, work was patchy and driven by needs of technology. However, the arrival of this successful quantum theory of solids, together with a concentration on the growth of pure silicon



and germanium and an understanding of their properties, saw an explosion in activity in semiconductor studies that has continued to this day.

During the recent decades, advances in semiconductor materials resulted in the development of a wide range of electronic and optoelectronic devices that affected many aspects of the technological society. From semiconductors to microelectronic and optoelectronic devices for information applications, these advances and applications were catalyzed by an improved understanding of the interrelationship between different aspects (i.e., structure, properties, synthesis and processing, performance, and characterization of materials) of this multidisciplinary field (Yacobi, 2004).

At the same time, an intense research effort is currently under way to integrate multiple optical technologies onto a single chip. In this chip, there will be a system in which optical signals are generated by micro-lasers, shaped by thin-film digital lenses, and coupled into optical waveguide channels by nonlinear optical switches for transmission. Within the same chip, there will also be optical logic gates where the optical signals can be analyzed and holographic data storage media where information can be stored. Incorporating all these functions into a single computer chip is no longer beyond our reach (Simmons and Potter, 2000).

These advances are not possible without a good understanding of the optical characteristics of photonic materials and its role in the future will expand even further when photonics finds its way into new applications in transportation, medicine, biotechnologies, environmental pollution detection, conservation and power production (Ralf, 2001).



Figure 1.1 and Figure 1.2 show the connection between key technologies and photonics, and their applications respectively.

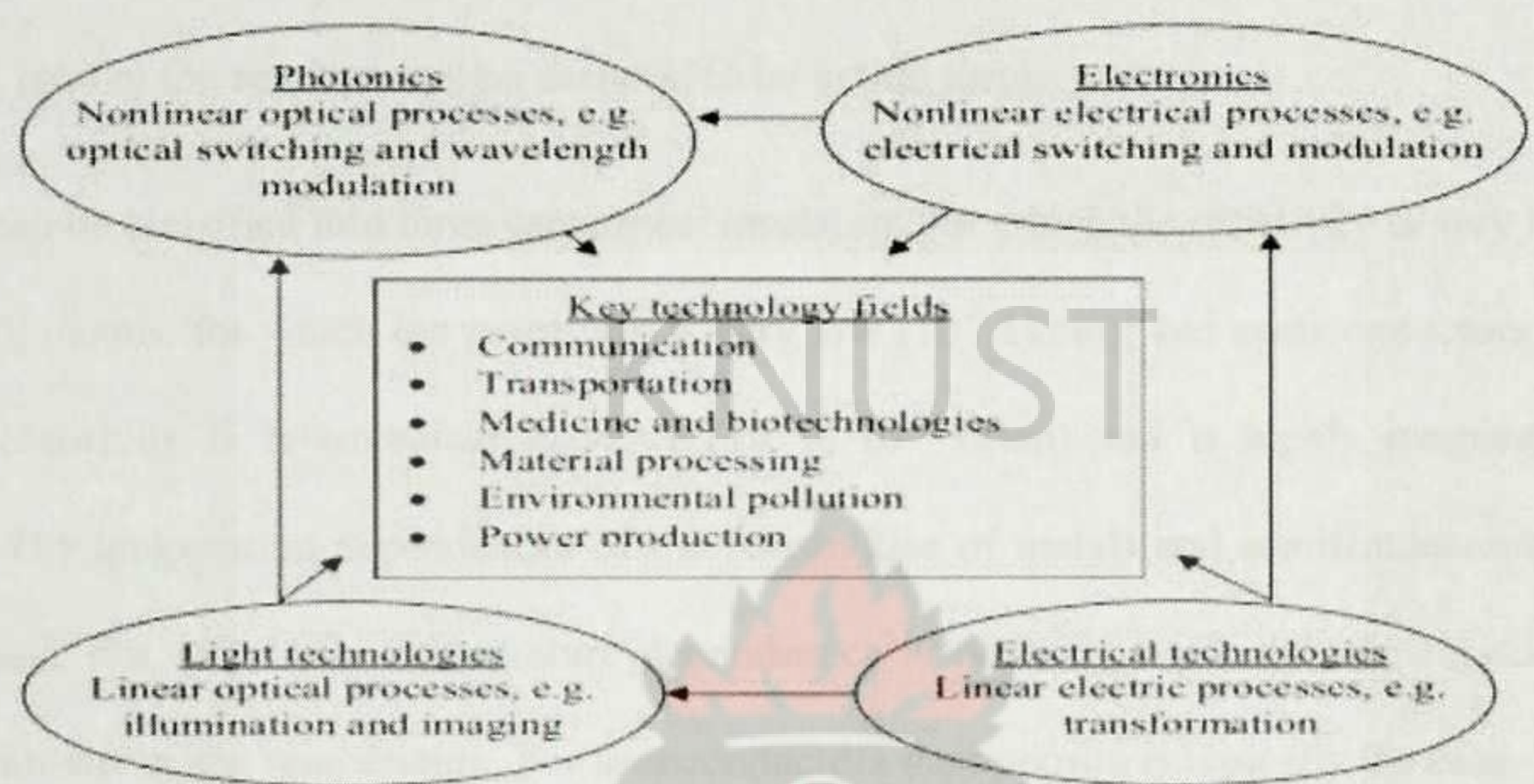


Figure 1.1: Relationship between Photonics and Key Technologies (Ralf, 2001). The arrows show the direction of the knowledge.

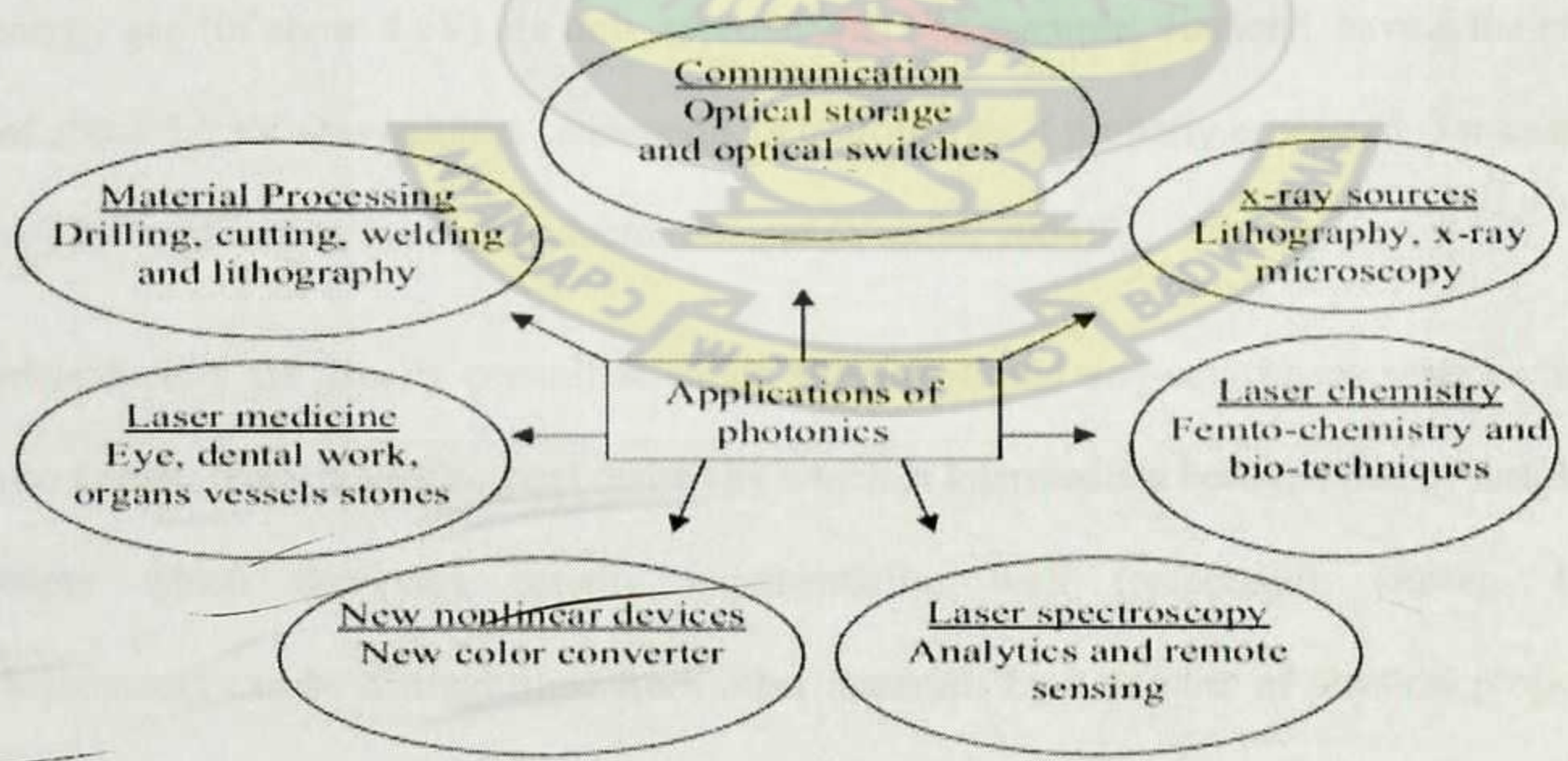


Figure 1.2: Specific Applications of Photonics (Ralf, 2001).



## 1.1 SEMICONDUCTOR MATERIALS

The selection of an opto-electronic or photonic material for a particular application requires a firm knowledge and understanding of the electronic and optical properties of the material. Many applications require the semiconducting material to be in thin form.

“Materials can be classified into three categories: insulators, for which the resistivity is very high ( $10^{12} \Omega\cdot\text{cm}$ ); metals, for which the resistivity is very low ( $10^{-6} \Omega\cdot\text{cm}$ ); and semiconductors, for which the resistivity is intermediate in value ( $10^6 - 10^{-3} \Omega\cdot\text{cm}$ ) and is highly temperature dependent. The temperature dependences of the resistivities of metals and semiconductors are quite different. For metals the temperature dependence is typically weak and the resistivity increases with increasing temperature. For semiconductors the opposite is typically the case. The temperature dependence is strong and the resistivity for the most part decreases with increasing temperature (Balkanski and Wallis, 2000). It should be noted, however, that for semiconductors the boundaries for both the resistivity (between about  $10^{-3}$  and  $10^9 \Omega\cdot\text{cm}$ ) and the upper limit of the energy gap (of about 4 eV) are only approximate. For example, diamond, having the energy gap of about 5.5 eV also exhibits semiconducting properties if properly processed (for example, doping) for applications in semiconductor devices (Yacobi, 2004)”.

“Semiconductors are usually crystalline solids although liquid and amorphous semiconductors are also known. They have electrical resistivity which is intermediate between that of metals and insulators which decreases usually exponentially, with temperature (Juster, 1963). Semiconductors can be distinguished from other materials by a number of physical properties, one of the most important of which is the electrical resistivity  $\rho$  or the difficulty with which an electric current can pass through the material under the influence of an electric field”.



Semiconductors are mostly classified by their elemental composition or aggregation of some elements to form compounds. The most widely used elemental semiconductors are the two elements lying in Group IV of the periodic table, Si and Ge. Both have the diamond cubic structure. The coordination is tetrahedral and bonding is essentially covalent. The size of their energy gap increases with the strength of bonding. Semiconducting compounds of Group III-V (eg. AlAs, GaAs, GaP, GaN, InP, and InSb) possess the sphalerite structure which is closely related to the diamond cubic structure. Also, Group II-VI semiconducting compounds (eg. ZnS, ZnSe, ZnTe, CdS, CdSe, and CdTe) possess the wurzite structure except CdTe which has the sphalerite structure. Group IV-VI compounds (eg. PbS, PbSe, and PbTe) has the halite (cubic) structure (Rose et al., 1965).

In addition to these elemental and binary semiconductors, materials such as ternary alloys; for example,  $\text{Al}_x\text{Ga}_{1-x}\text{As}$ ,  $\text{GaAs}_{1-x}\text{P}_x$ , and  $\text{Hg}_{1-x}\text{Cd}_x\text{Te}$  and quaternary alloys; for example,  $\text{Ga}_x\text{In}_{1-x}\text{As}_y\text{P}_{1-y}$  with “tunable” (adjustable) properties are also used in specific device applications. The subscript x and y are composition parameters. Organic compounds which are semiconductors include anthracene,  $\text{C}_{14}\text{H}_{10}$ , and polyacetylene  $(\text{CH})_x$  (Yacobi, 2004; Balkanski and Wallis, 2000). This work focuses on some optical properties of a ternary alloy of the Group II-VI and IV-VI i.e  $\text{Pb}_x\text{Cd}_{1-x}\text{S}$  thin films deposited by the chemical bath technique. This thesis primarily is of interest because of their application in optoelectronic and photovoltaic devices.

The potential applications of ternary based materials in electronic and optoelectronic devices are vast, but have received little attention until recently due to the cheap and wide availability of silicon based alternatives. However as the use of silica as an electronic/optoelectronic material is



rapidly approaching its physical limitations, research into ternary materials is receiving increasing attention around the world (Kasap, 2002).

Although much has been learnt in the past about the physics of semiconductors, new developments are still coming thick and fast and in the materials area there is still tremendous need for progress. For many applications and to observe many interesting properties semiconductors must be prepared with a purity and structural perfection greatly exceeding that attainable in other materials. To produce transistor action, for example, silicon and germanium purer and more perfect than any other known materials are regularly being manufactured for commercial production (Dunlap W.C., 1961).

## 1.2 OBJECTIVES OF PROJECT

Thin films of lead and cadmium sulphide have attracted considerable interest because of their wide applications in optoelectronic devices. These materials are promising photovoltaic materials as their variable band gap could be adjusted to match the ideal band gap (1.5 eV) required for achieving a most efficient solar cell (Nayak and Acharya, 1985).

The ternary semiconductor thin films are considered to be an important technological material due to its prime applications in various optical and electronic devices. The II-VI and IV-VI group compound materials having specific physical properties like high efficiency, high optical absorbance and direct band gap, are considered to be potential materials in respect for a wide spectrum of optoelectronic applications such as photo detectors, photovoltaic devices, photo-electrochemical cells (Razykov, 1989), lasers, IR devices, solar control coatings (Elabd and Steckl, 1980).



These materials can be deposited in thin film form by various methods, such as electro-deposition (Molin and Diksar,1995), spray pyrolysis (Elango et al.,2003), vacuum deposition (Das and Bhat,1990), chemical bath deposition (Choudhary et al.,2005), successive ionic layer and reaction [SILAR] (Nicolou and Dupuy,1990) and sol-gel methods (Karanjai and Dashupta,1998). Among them the chemical bath deposition method is very simple, convenient for large area deposition on substrates of different materials, size and shape and it is inexpensive. Especially, one of the attractive features of the chemical bath deposition process is the ease with which the alloys can be generated without the use of any sophisticated instrumentation and process control (Seghaier et al., 2006).

Although extensive studies of the electrical and optical properties of  $Pb_{1-x}Cd_xS$  have been made by many researchers, these films generally have been prepared by chemical bath deposition from solution with high lead molar fraction in solution ( $0 \leq x \leq 0.2$ ). Among the numerous papers, the investigation by Skyllas-Kazacos et al., 1985 is the only one which gives detailed data on high cadmium mole fraction in solution.

Their analysis shows that a monotonic decrease in the band gap of the semiconductor alloys was obtained as the Pb ratio was increased, and the composition of films was very close to the composition of the deposition mixture.



### 1.3 SPECIFIC PROJECT OBJECTIVES

This present research work is based on the following objectives:

- To optimize various parameters to synthesize the ternary  $\text{Pb}_x\text{Cd}_{1-x}\text{S}$  thin films by chemical bath deposition method.
- To investigate the optical absorbance of the ternary alloy i.e  $\text{Pb}_x\text{Cd}_{1-x}\text{S}$  thin films deposited by the chemical bath technique.
- To investigate the effect of thermal annealing and increasing composition of Pb on the optical band.
- To investigate the structure of the ternary alloy through XRD technique to make them suitable candidate for various optoelectronic and nano device application.

### 1.4 STRUCTURE OF THESIS

The thesis is organized into six chapters: The first chapter gives an introduction to the impact of semiconductor research over the years, classification of semiconductors and how new semiconductor materials including ternary and quaternary alloys and more specifically  $\text{PbCdS}$  are being developed and used. The chapter also states the specific research objectives and finally describes the structure of the thesis. The second chapter gives detailed review of literature on group II-VI and IV-VI semiconductor alloys with emphasis on the optical and transport properties of  $\text{Pb}_x\text{Cd}_{1-x}\text{S}$  ternary alloy deposited with different methods under different conditions. The third chapter treats the relevant theory. Methodology and materials used in doing this research are presented in the fourth chapter, while the fifth chapter deals with results in graphical format and in-depth discussion of results. In the sixth chapter conclusions and recommendations are made.



## CHAPTER TWO

### 2.0 LITERATURE REVIEW

#### 2.1 SEMICONDUCTOR ALLOY AND A COMPOUND

Semiconductor materials are nominally small band gap insulators with its defining property being the ability to be doped with impurities that alter its electronic properties in a controllable way. Because of their varying applications in devices like transistors and lasers, the search for new and improved semiconductor materials is an important field of study in materials science. Most commonly used semiconductor materials are crystalline inorganic solids. These materials are classified according to the periodic table groups of their constituent atoms.

Different semiconductor materials differ in their properties. Thus, in comparison with silicon, compound semiconductors (alloys) have both advantages and disadvantages (Ohring, 1998). In principle, the electronic and optical properties of semiconductor materials are tunable by varying their shapes and sizes (Yang and Leiber, 1996). So it is one of the desired goals in materials science to have precise control of the morphology of semiconductor materials.

“An alloy is a combination, either in solution or compound, of two or more elements. The resulting alloy substance generally has properties significantly different from those of its components”.

A chemical compound is a substance consisting of two or more chemical elements that are chemically combined in fixed proportions. The ratio of each element is usually expressed by chemical formula. For example, water is a compound consisting of two hydrogen atoms bonded to an oxygen atom ( $\text{H}_2\text{O}$ ). The atoms within a compound can be held together by a variety of



interactions, ranging from covalent bonds to electrostatic forces in ionic bonds. A continuum of bond polarities exists between the purely covalent and ionic bonds. For example,  $\text{H}_2\text{O}$  is held together by polar covalent bonds.  $\text{NaCl}$  is an example of an ionic compound.

Simply, an alloy is formed from a physical mixture of two or more substances, while a compound is formed from a chemical reaction. An alloy crystal is sometimes called a mixed crystal or a solid solution. For example,  $\text{GaAs}$  is a compound consisting of Ga atoms bonded to As atoms. It is not an alloy.  $\text{Al}_x\text{Ga}_{1-x}\text{As}$  is an alloy compound consisting of AlAs and GaAs with a mole ratio of  $x:(1-x)$ . The bonds in GaAs and AlAs are not adequately described by any of these extreme types, but have characteristics intermediate to those usually associated with the covalent and ionic terms. The bonds in diamond, C-C, can be described by the covalent bond term only. It is an elemental semiconductor, not a compound semiconductor. Similarly, Si and Ge are elemental semiconductors. Like  $\text{Al}_x\text{Ga}_{1-x}\text{As}$ ,  $\text{Si}_x\text{Ge}_{1-x}$  ( $0 \leq x \leq 1.0$ ) is an alloy or compound semiconductor (Adachi, 2009). Binary alloys are made by mixing similar elements such as Si and Ge, for example, to form  $\text{Ge}_x\text{Si}_{1-x}$ . Ternary alloy is an alloy made up of three different chemical elements; usually two cations and an anion. Ternary alloys of compound semiconductors can be obtained by substituting an element such as Al for the homologous element Ga in GaAs to form  $\text{Ga}_{1-x}\text{Al}_x\text{As}$ . Alternatively, one can mix the non-metal constituents by substituting S for Se in ZnSe to give  $\text{ZnS}_x\text{Se}_{1-x}$ . Quaternary alloys result if both the metal and nonmetal constituents are mixed to give, for example,  $\text{Ga}_x\text{Al}_{1-x}\text{P}_y\text{As}_{1-y}$ . The band gap of an alloy is a continuous function of composition. In ternary alloys, the variation with composition is linear if the two constituents that are varied have nearly the same atomic radii and the same bonding strength to the third constituent (Adachi, 2009; Balkanski and Wallis, 2000).



## 2.2 THIN FILMS

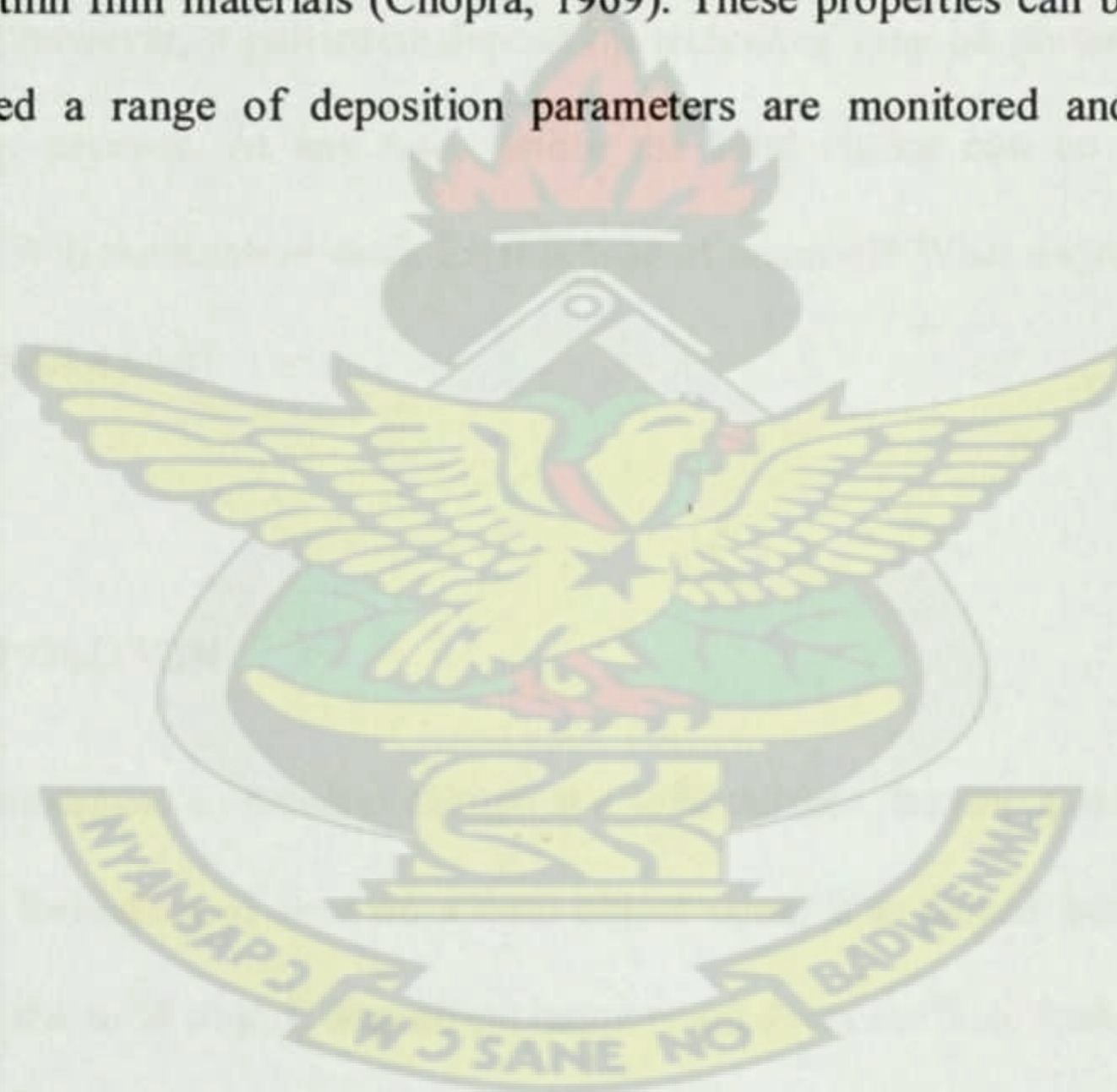
Thin film is a branch that deals with very thin structural layers of different materials. In recent years, thin film science has been grown worldwide into a major research area. The importance of thin film coating leads breakthrough in microelectronics, optics and nano technology (Venables et al., 1984). The film science and technology plays an important role in high technological industries. Thin film technology has been developed primarily for the need of the integrated circuit industry. The demand for development of smaller and smaller devices with higher speed especially in new generation of integrated circuits requires advanced materials and new processing techniques suitable for future giga scale integration (GSI) technology. In this regard, physics and technology of thin films can play an important role to achieve this goal. The production of thin films for device purposes has been developed over the past 40 years. Thin films as a two dimensional system are of great importance to many real-world problems. Their material costs are very small as compared to the corresponding bulk material and they perform the same function when it comes to surface processes. Thus, knowledge and determination of the nature, functions and new properties of thin films can be used for the development of new technologies like solar cells (Poortmans and Arkipov, 2006), sensors (Joachim et al., 2004), optical applications (Mereno et al., 2005), electronic engineering (Okimura, 1980) ferroelectrics (Moazzami, 1992) etc.

According to Chopra et al., (2004), a thin film is a material created *ab initio* by the random nucleation and growth process of individually condensing / reacting atomic / ionic / molecular species on a substrate. The structural, chemical, metallurgical and physical properties of such materials are strongly dependent on a large number of deposition parameters and may also be thickness dependent. When compared with the bulk material, physical properties of thin films on



substrate may strongly differ, depending especially on development of morphology and structure. Features like grain size, shape, orientation and others are determined to a large extent at an early stage of nucleation and growth and can be influenced by deposition conditions (Vossen, 1991).

Thin films are a layer of material ranging from fractions of a nanometer (monolayer) to several micrometers in thickness (Wikipedia) and thus are best defined in terms of the birth processes rather than by thickness. The atomistic, random nucleation and growth processes bestow new and exotic properties to thin film materials (Chopra, 1969). These properties can be controlled and reproduced, provided a range of deposition parameters are monitored and controlled precisely.





## 2.3 THIN FILM DEPOSITION

Thin film deposition is any technique for depositing a thin film of material onto a substrate or onto previously deposited layers. "Thin" is a relative term, but most deposition techniques allow layer thickness to be controlled within a few tens of nanometers, and some allow one layer of atoms to be deposited at a time. "Deposition techniques fall into two broad categories, depending on whether the process is primarily chemical or physical (Advincula and Knoll, 2011)".

Usually, the choice of deposition method is made after the material has been selected. In a limited number of cases, however, a particular deposition technique may be preferred if it fits more easily into a larger process. At any rate, before the final choice can be made, three questions must be asked: Will the method work for this type of material? What degree of control will it allow? How much will it cost?

### 2.3.1 CHEMICAL DEPOSITION

"Here, a fluid precursor undergoes a chemical change at a solid surface, leaving a solid layer. An everyday example is the formation of soot on a cool object when it is placed inside a flame. Since the fluid surrounds the solid object, deposition happens on every surface, with little regard to direction; thin films from chemical deposition techniques tend to be *conformal*, rather than *directional*".

Chemical deposition is further categorized by the phase of the precursor:

- Plating relies on liquid precursors, often a solution of water with a salt of the metal to be deposited. Some plating processes are driven entirely by reagents in the solution (usually



for noble metals), but by far the most commercially important process is electroplating. It was not commonly used in semiconductor processing for many years, but has seen resurgence with more widespread use of chemical-mechanical polishing techniques.

- Chemical solution deposition (CSD) or chemical bath deposition (CBD) uses a liquid precursor, usually a solution of organometallic powders dissolved in an organic solvent. This is a relatively inexpensive, simple thin film process that is able to produce stoichiometrically accurate crystalline phases. This technique is also known as the sol-gel method because the 'sol' (or solution) gradually evolves towards the formation of a gel-like diphasic system.
- Spin coating or spin casting, uses a liquid precursor, or sol-gel precursor deposited onto a smooth, flat substrate which is subsequently spun at a high velocity to centrifugally spread the solution over the substrate. The speed at which the solution is spun and the viscosity of the sol determines the ultimate thickness of the deposited film. Repeated depositions can be carried out to increase the thickness of films as desired. Thermal treatment is often carried out in order to crystallize the amorphous spin coated film. Such crystalline films can exhibit certain preferred orientations after crystallization on single crystal substrates.
- Chemical vapour deposition (CVD) generally uses a gas-phase precursor, often a halide or hydride of the element to be deposited. In the case of MOCVD, an organometallic gas is used. Commercial techniques often use very low pressures of precursor gas.
  - Plasma enhanced CVD (PECVD) uses an ionized vapour, or plasma, as a precursor. Unlike the soot example above, commercial PECVD relies on



electromagnetic means (electric current, microwave excitation), rather than a chemical reaction, to produce a plasma.

- Atomic layer deposition (ALD) uses gaseous precursor to deposit conformal thin films one layer at a time. The process is split up into two half reactions, run in sequence and repeated for each layer, in order to ensure total layer saturation before beginning the next layer. Therefore, one reactant is deposited first, and then the second reactant is deposited, during which a chemical reaction occurs on the substrate, forming the desired composition. As a result of the stepwise, the process is slower than CVD, however it can be run at low temperatures, unlike CVD.

### 2.3.2 PHYSICAL DEPOSITION

Physical deposition uses mechanical, electromechanical or thermodynamic means to produce a thin film of solid. An everyday example is the formation of frost. Since most engineering materials are held together by relatively high energies, and chemical reactions are not used to store these energies, commercial physical deposition systems tend to require a low-pressure vapour environment to function properly; most can be classified as physical vapour deposition (PVD).

The material to be deposited is placed in an energetic, entropic environment, so that particles of material escape its surface. Facing this source is a cooler surface which draws energy from these particles as they arrive, allowing them to form a solid layer. The whole system is kept in a vacuum deposition chamber, to allow the particles to travel as freely as possible. Since particles



tend to follow a straight path, films deposited by physical means are commonly *directional*, rather than *conformal*.

Examples of physical deposition include:

- A thermal evapourator uses an electric resistance heater to melt the material and raise its vapour pressure to a useful range. This is done in a high vacuum, both to allow the vapour to reach the substrate without reacting with or scattering against other gas-phase atoms in the chamber, and reduce the incorporation of impurities from the residual gas in the vacuum chamber. Obviously, only materials with a much higher vapour pressure than the heating element can be deposited without contamination of the film. Molecular beam epitaxy is a particularly sophisticated form of thermal evaporation.
  - An electron beam evapourator fires a high-energy beam from an electron gun to boil a small spot of material; since the heating is not uniform, lower vapour pressure materials can be deposited. The beam is usually bent through an angle of  $270^\circ$  in order to ensure that the gun filament is not directly exposed to the evapourant flux. Typical deposition rates for electron beam evaporation range from 1 to 10 nanometres per second.
  - In molecular beam epitaxy (MBE), slow streams of an element can be directed at the substrate, so that material deposits one atomic layer at a time. Compounds such as gallium arsenide are usually deposited by repeatedly applying a layer of one element (i.e., gallium), then a layer of the other (i.e., As), so that the process is chemical, as well as physical. The beam of material can be generated by either



physical means (that is, by a furnace) or by a chemical reaction (chemical beam epitaxy).

- Sputtering relies on a plasma (usually a noble gas, such as argon) to knock material from a "target" a few atoms at a time. The target can be kept at a relatively low temperature, since the process is not one of evaporation, making this one of the most flexible deposition techniques. It is especially useful for compounds or mixtures, where different components would otherwise tend to evaporate at different rates. Note, sputtering's step coverage is more or less conformal. It is also widely used in the optical media. The manufacturing of all formats of CD, DVD, and BD are done with the help of this technique. It is a fast technique and also it provides a good thickness control. Presently, nitrogen and oxygen gases are also being used in sputtering.
- Pulsed laser deposition systems work by an ablation process. Pulses of focused laser light vaporize the surface of the target material and convert it to plasma; this plasma usually reverts to a gas before it reaches the substrate.
- Cathodic arc deposition (arc-PVD) which is a kind of ion beam deposition where an electrical arc is created that literally blasts ions from the cathode. The arc has an extremely high power density resulting in a high level of ionization (30–100%), multiply charged ions, neutral particles, clusters and macro-particles (droplets). If a reactive gas is introduced during the evaporation process, dissociation, ionization and excitation can occur during interaction with the ion flux and a compound film will be deposited.
- Electrohydrodynamic deposition (Electrospray deposition) is a relatively new process of thin film deposition. The liquid to be deposited, either in the form of nano-particle



solution or simply a solution, is fed to a small capillary nozzle (usually metallic) which is connected to a high power source. The substrate on which the film has to be deposited is connected to the ground terminal of the power source. Through the influence of electric field, the liquid coming out of the nozzle takes a conical shape (Taylor cone) and at the apex of the cone a thin jet emanates which disintegrates into very fine and small positively charged droplets under the influence of Rayleigh charge limit. The droplets keep getting smaller and smaller and ultimately get deposited on the substrate as a uniform thin layer (Wikipedia).

Despite the existence of these large variety of deposition techniques, searching for the most reliable and economic deposition technique has always been the main goal.

Chemical bath deposition (CBD) offers a simple and inexpensive route to deposit semiconductor nanostructures and thin films, but lack of fundamental understanding and control of the underlying chemistry has limited its versatility. CBD is traditionally performed in a batch reactor, requiring only a substrate to be immersed in a supersaturated solution of aqueous precursors such as metal salts, complexing agents and pH buffers. Highlights of CBD include low cost, operation at low temperature and atmospheric pressure and scalability to large area substrates (McPeak, 2010). Chemical bath deposition is becoming an important deposition technique for thin films of compound materials like chalcogenides (Hodes,2002).



## 2.4 CHEMICAL BATH DEPOSITION

One of the earliest reports of the use of CBD was in the preparation of lead sulphide and lead selenide thin films for use as photoconductive detectors during World War II (Lokande, 1991; Lincot et al., 1999). Since then, CBD has become an attractive method due to its suitability for large scale deposition and the ability to deposit onto polymer substrates. It is characterized by simple formulation, ease of set up and low temperature requirements. The process generally operates under ambient conditions and has the potential to replace expensive and equipment intensive techniques. In CBD, the thin film forms when the substrate is immersed into a dilute, generally alkaline, solution containing metal ions and an appropriate source of chalcogenide ions. Complexation of the metal ions enables the rate of the reaction to be controlled. The chalcogen anion is usually generated by the decomposition or hydrolysis of an organic or inorganic precursor.

Despite the advances that have been made using CBD, the full development of the technology has been hampered by poor understanding of the relationships between process chemistry and film structure, factors that are dependent on the properties of the bath and deposition precursors. The process is sensitive to precursor concentrations and to the substrate used (Mane and Lokhande, 2000; Kaur et al., 1980; Rieke and Bentjen, 1993). The optimal deposition parameters are generally different for each compound deposited.

Although there have been numerous papers published reporting the preparation of chalcogenide thin films using CBD, Kaur et al. (1980), point out that the process has remained recipe oriented with little understanding of the kinetics of the process. With a few exceptions, this is also true regarding the mechanistic understanding of the process. There is therefore a need for careful



investigation of the CBD process and identification of the conditions that favour high quality coherent deposits.

For a long time, CBD was then essentially limited to PbS and PbSe. It was not until 1961 that deposition of CdS, now the most widely studied material in CBD was explicitly reported by Mokrushin and Tkachev, (1961). Over the past decade CBD has experienced an increased level of interest. A simple literature search in the Web of Science for chemical bath deposition shows a steady increase in publications over the past decade from 53 publications in the year 2000 to 211 publications in 2009. This renaissance in CBD has been primarily fueled by a need to deposit large area semiconductor films and nanowire arrays for inexpensive photovoltaic devices (McPeak, 2010).

The range of materials deposited by CBD was gradually extended particularly in the 1980's to include sulphides and selenides of many metals, some oxides and also many ternary compounds. Chemical deposition received a major impetus after CdS films, chemically deposited onto CdTe and later onto CuInSe<sub>2</sub> films, was shown to give superior photovoltaic (PV) cells compared with the previously evaporated CdS.

The preparation of ternary compounds by CBD has been undertaken in several ways. The simplest method is to prepare bi-layers of two different chalcogenide materials such as Bi<sub>2</sub>S<sub>3</sub>-Cu<sub>x</sub>S (Nair et al., 1993), PbS-CdS (Orozco-Teran et al., 1999) and PbS-Cu<sub>x</sub>S (Nair and Nair, 1989). Formation of the ternary chalcogenide then occurs by interaction of the two layers during annealing process.



For example, Oladeji and Chow prepared the  $\text{Cd}_{1-x}\text{Zn}_x\text{S}$  by growing thin layers of zinc sulphide and cadmium sulphide by CBD, which were subsequently annealed to form the ternary compound (Oladeji and Chow, 2005).

CBD can also be used in conjunction with other techniques to form ternary compounds. For example, Bindu et al. (2002, 2003) combined CBD with vacuum evaporation in order to provide a less toxic pathway to the production of indium selenide ( $\text{In}_2\text{Se}_3$ ) and copper indium selenide ( $\text{CuInSe}_2$ ) (Bindu et al., 2002, 2003). Indium or indium and copper were evaporated sequentially onto CBD selenium thin films, and the resulting films annealed at temperatures up to 723 K to form the binary or ternary compound.

CBD ternary chalcogenides can also be prepared by the combination of all reactants in a single bath. This method was used by Pentia et al. to synthesize the ternary chalcogenide cadmium lead sulphide ( $\text{Cd}_x\text{Pb}_{1-x}\text{S}$ ) on glass substrates (Pentia et al., 2004). Using a range of Cd:Pb ratios, the metal ions were stabilized with EDTA (ethylenediaminetetraacetic acid) in an alkaline solution to form  $[\text{Cd}(\text{EDTA})]^{2-}$  and  $[\text{Pb}(\text{EDTA})]^{2-}$  complexes. As the metal complexes dissociated, metal ions released slowly in solution reacted with sulphide ions formed from the decomposition of thiourea.

The resulting films were annealed in air at 100 °C, and showed a variance in crystallinity which was dependent on the value of x. It was noted that for  $0.4 > x > 0.8$  ternary chalcogenide films were formed, but for  $x \sim 0.5$ , the resulting films were a mixture of cadmium sulphide and lead sulphide.



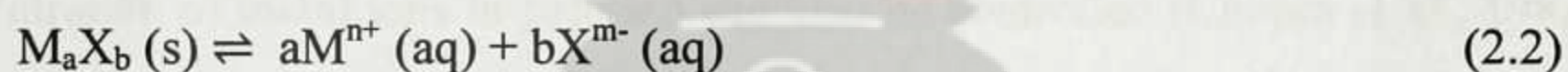
### 2.4.1 BASIC PRINCIPLES OF CHEMICAL BATH DEPOSITION

The basic principles behind the CBD process are similar to those for all precipitation reactions, and are based on the relative solubility of the product. The equilibrium concentration of ions in solution is defined by the solubility (SP) expression (equation 2.1):

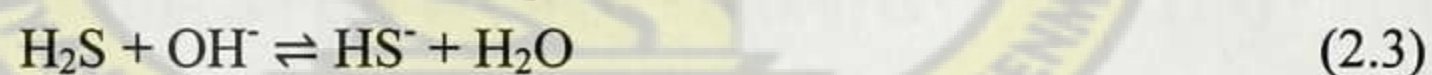
$$K_{sp} = [M^{n+}]^a [X^{m-}]^b \quad (2.1)$$

where  $K_{sp}$  is the solubility constant and  $[M^{n+}]^a [X^{m-}]^b$  is the ionic product (IP).

a moles of  $M^{n+}$  ions and b moles of  $X^{m-}$  ions are formed from a mole the solid as in equation (2.2).



The preparation of metal sulphides by introducing  $S^{2-}$  ions into an aqueous solution of a metal salt to effect chemical precipitation is well established.  $S^{2-}$  ions can be generated in-situ by the hydrolysis of hydrogen sulphide gas in aqueous solution (Chopra et al., 1982). The equations for this hydrolysis are presented in equations 2.3 and 2.4:



The sulphide ions formed in equation 2.4 react with the metal ions in solution to produce the metal sulphide. Precipitation occurs when the ionic product,  $IP > K_{sp}$ .

In the CBD, this process is modified such that precipitation is controlled to eliminate or reduce spontaneous precipitation. The first method of controlling the reaction is by complexing the



metal ions such that only a controlled number of free ions are available. As the complex dissociates, the following equation applies (assuming a metal ion with a charge of 2+):

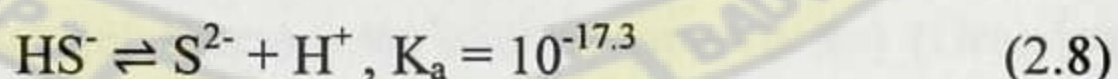
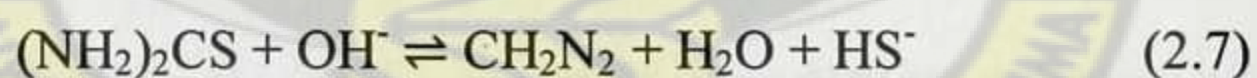


At any given temperature, the concentration of free metal ions is given by equation 2.6

$$K_i = [M^{2+}][A] / [M(A)^{2+}] \quad (2.6)$$

In this equation,  $K_i$  is the stability constant of the complex ion. A complex with a small  $K$  value is most stable, and will therefore have a lower concentration of metal ions in solution than one with a higher constant. By controlling the concentration and temperature of the complexing reagent, the concentration of metal ions in solution can also be controlled (Chopra et al., 1982). If these ions can be generated at a surface, then it leads to CBD of a film.

The second method of controlling the reaction is by the slow generation of chalcogen ions in solution. Thiourea is frequently chosen as the sulphide ion source for metal sulphides and is considered to produce sulphide ions according equations 2.7 and 2.8 (Chopra et al., 1982).



Equation 2.8 can also be written in terms of hydroxide ion concentration:

$HS^- + OH^- \rightleftharpoons S^{2-} + H_2O$ ,  $K_a = 10^{-3.3}$ . In the mildly alkaline solutions with pH~11, which is the pH of many chemical baths for CBD, the sulphide ion concentration can be written in terms of  $[HS^-]$ , giving  $[S^{2-}] = 10^{-4.3}[HS^-]$ . This shows that most of the sulphur ions will be present in the form of  $HS^-$  rather than  $S^{2-}$  (Hodes, 2003). Pentia et al. proposed that the main factors that



control the generation of  $M^{2+}$  and  $S^{2-}$  precursors were: precursor concentration, pH and temperature (Pentia et al., 2004).

#### 2.4.2 SUBSTRATES AND SUBSTRATE PREPARATION

One of the advantages of the CBD thin films is the range of substrates that can be used on which films deposit. This is shown by the wide range of substrates that have been used for lead cadmium sulphide thin film deposition. The main criteria for substrate selection are that the growing film will attach to the substrate and that the substrate will not dissolve in the chemical bath.

Glass substrates are commonly used; microscope slides for small scale projects and glass sheets for large scale projects (Gadave and Lokhande, 1993). Glass generally has been immersed in a vertical position in the bath solution, although with large coating areas, two sheets have been supported with a set distance between them and the CBD solution filled in the gap (Nair et al., 1991, 2001).

The use of other substrates have also been tried. Various polymer substrates were also used: 25  $\mu\text{m}$  Kapton polyimide (Cardoso et al., 2001), modified low density polyethylene (LDPE) (Kunita et al., 2002), transparent polyester sheets (overhead transparencies) (Grozdanov et al., 1994, 1995), PPMA (polymethylmethacrylate) sheets (Hu and Nair, 1996).

PET (polyethylene terephthalate) films (Yamamoto et al., 1993) and PES (polyethersulphone) (Nair et al., 2001). The polymer substrates were commonly floated on top of the CBD solution during the deposition process. Other materials include PZT (ferroelectric piezoelectric transducer) films (Grozdanov, 1995), iron, steel, aluminium, zinc and copper (Varkey, 1989).



The preparation of substrates is a critical aspect that can contribute to film adherence. Several cleaning regimes have been proposed. Glass substrates have been cleaned with detergent, chromic acid, rinsed with water and dried (Nair and Nair, 1989), ultrasonically cleaned (Gadave and Lokhande, 1993), or treated in a solution of tin(II)chloride (Nair et al., 1998). Overhead transparencies have been ultrasonically cleaned, soaked in tin(II)chloride, washed with water and dried in air (Grozdanov et al., 1995).

KNUST

## 2.5 ANNEALING

“Annealing is heat treatment of materials at elevated temperatures aimed at investigating or improving their properties. Material annealing can lead to phase transitions, recrystallization, polygonization, homogenization, relaxation of internal stresses, removal of after effects of cold plastic deformation (strain hardening), annihilation and rearrangement of defects and so on. The results of annealing depend significantly on its kinetics: the rate of heating and cooling and the time of exposure at a given temperature”.

### 2.5.1 IRRADIATION ANNEALING

This is the annealing of defects in a crystal stimulated by nuclear radiations. Both impurity atoms and other defects formed prior to irradiation, as well as radiation-induced defects take part in the process. When radiation doses are large, annealing lowers the rate of accumulation of the defects, particularly if the intensities are high enough.



Irradiation annealing mechanisms are related to the processes of radiation-induced diffusion of defects, to atomic restructuring triggered by collisions of external particles with crystal atoms and also the small dose effect (Poole, C.P.Jr., 2004).

### **2.5.2 RECRYSTALLIZATION ANNEALING**

This is heating a solid to a temperature that provides full recrystallization within a given time period. Recrystallization annealing is used to lower the dislocation density, to change texture, to form a polycrystal structure and thereby to bring the physical and chemical properties of a solid to a level characteristic of an unhardened annealed state. Conditions for this annealing of deformed materials are chosen using recrystallization diagrams which provide the dependences of the temperatures for the beginning and end of the initial recrystallization on the degree of strain for a given processing duration.

### **2.5.3 PULSED ANNEALING OF SEMICONDUCTORS**

This is a high temperature treatment of semiconductor specimens which is characterized by sharp fronts of heating  $\tau_h$  and cooling  $\tau_c$ , in practice without holding the temperature at the maximum value. Values of  $\tau_h$  and  $\tau_c$  vary over a wide range. As a rule, they are set by the conditions of conserving the bulk properties, without noticeable diffusion of impurities, and this provides the possibility of fusing surface layers while conserving the crystal structure of the bulk. The process duration is from 10-12 s to several seconds. For pulses shorter than a few microseconds the most efficient results are achieved with exciting pulse energies sufficient for melting the surface layer. For longer pulses the target heating is almost uniform due to thermal conductivity. Particularly important results were obtained by combining pulsed annealing with ion implantation of



impurities. The nonequilibrium introduction of impurities together with nonequilibrium annealing is the most efficient technique for obtaining highly doped, structurally perfect semiconducting layers. The pulsed annealing method is widely used for the restoration of a crystal structure disturbed during ion bombardment (Poole, C.P.Jr., 2004).





## 2.6 CRYSTAL STRUCTURE OF SOME IMPORTANT II-IV-VI SEMICONDUCTOR MATERIALS

II-VI semiconductor materials show the structural duality and can be formed as either sphalerite (cubic, zinc blende type) or wurzite (hexagonal type) (Bouroushian et al., 1997) while IV-VI semiconductor materials generally have rock salt structure (NaCl). This section examines the crystal structure of II-IV-VI semiconductors namely; lead sulphide, cadmium sulphide and lead cadmium sulphide.

### 2.6.1 LEAD SULPHIDE

Lead(II) sulphide is an inorganic compound with the formula PbS. PbS, also known as galena, is the principal ore and most important compound of lead (Patnaik and Pradyot, 2003). Like the related materials PbSe and PbTe, PbS is a semiconductor (Vaughan and Craig, 1978). In fact, lead sulfide was one of the earliest materials to be used as a semiconductor (Hogan, 2011).

PbS is a semiconductor material belonging to IV-VI group with a direct narrow band gap (0.41 eV) (Kanazawa and Adachi, 1998; Joshi et al., 2004) which falls in the near infra – red spectrum at room temperature. Lead sulphide salt is dark in color with molar mass of 239.30 g/mol and density of 7.6 g/cm<sup>3</sup>. It also has a melting point of 1118 °C and boiling point of 1281 °C. PbS has a halite structure (cubic) with an all face centered lattice type and eight (8) atoms in its unit cell. Also it has a lattice constant,  $a = 5.936 \text{ \AA}$  (Wikipedia).



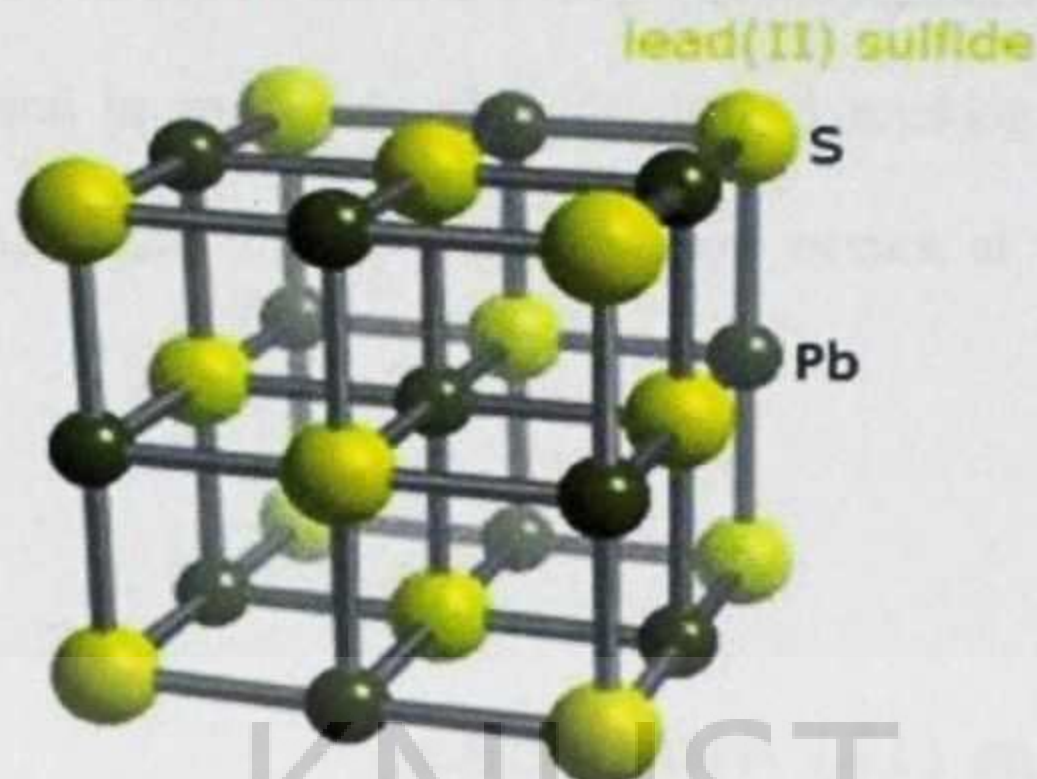


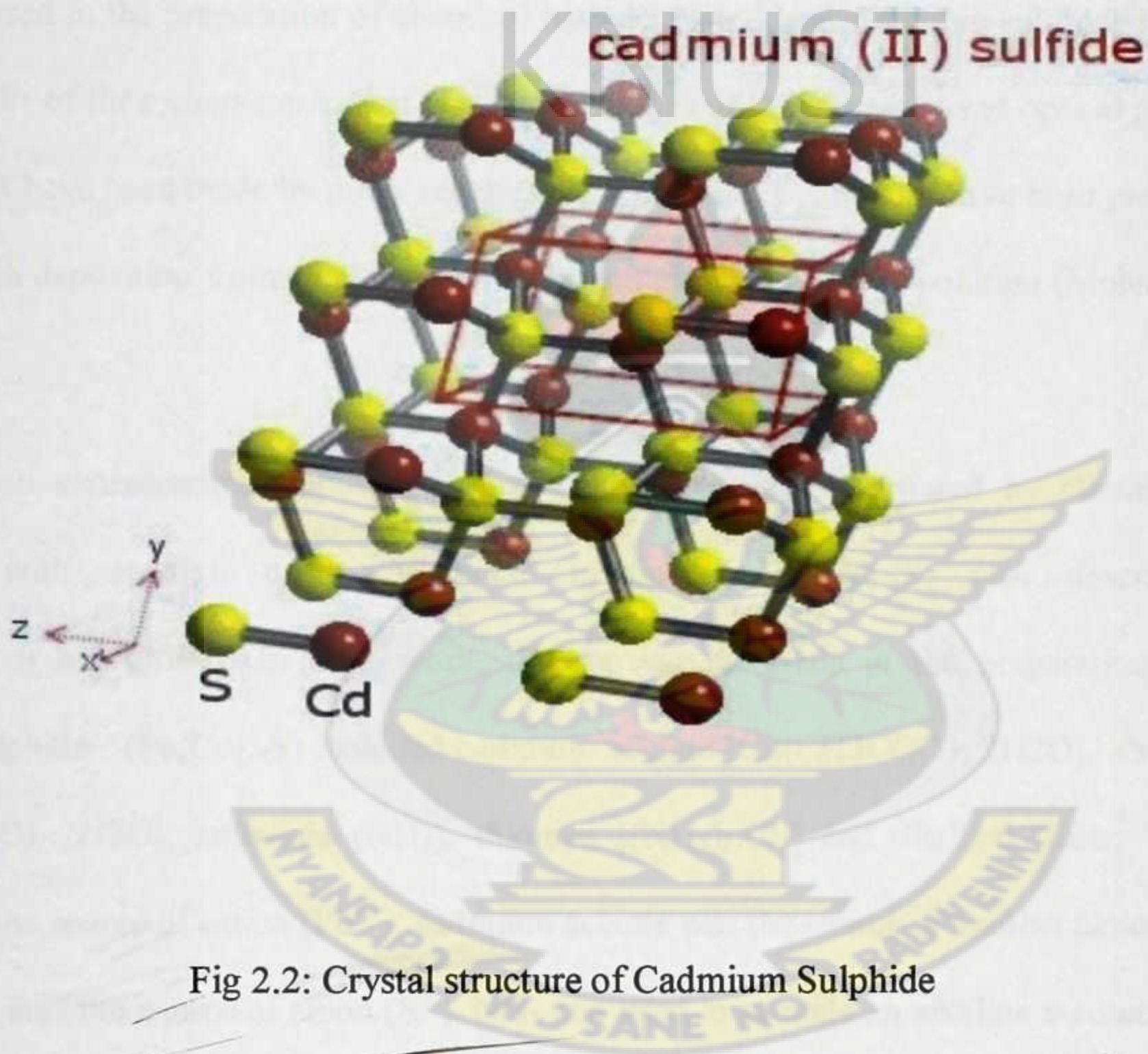
Fig 2.1: Crystal structure of Lead Sulphide

### 2.6.2 CADMIUM SULPHIDE

. CdS is yellowish – orange in color with a molar mass of 144.48g/mol and a density of 4.82g/cm<sup>3</sup>. Also, it has a melting point of 1750 °C at a pressure of 10 MPa and boiling point of 980 °C (Wikipedia). CdS is an important semiconductor with a direct wide band gap of 2.42 eV which falls in the visible spectrum at room temperature. It exists in two crystallographic phases namely, the  $\alpha$  and  $\beta$  – phases. The  $\alpha$ -phase of CdS is a wurtzite structure. This structure is hexagonal with  $a = 4.1348 \text{ \AA}$  and  $b = 6.77490 \text{ \AA}$ . The  $\beta$ -phase is zinc blende with an f.c.c structure with  $a = 5.818 \text{ \AA}$  (Boakye and Nusenu, 1996). This structure may be regarded as two interpenetrating face centered lattices of the elements with the corner of one located at the position  $\frac{1}{4} \frac{1}{4} \frac{1}{4}$  of the other as in the diamond structure. The zinc blende structure is related to the wurtzite structure which has one kind of atom on c.p.h positions and the other at intermediate



positions corresponding to tetrahedral voids where each atom is surrounded symmetrically by four atoms of the other kind (Barrett and Massalski, 1966). The hexagonal layers are stacked in one sequence in the wurtzite and in another in zinc blende and stacking faults are frequent (Jagodzinski, 1949). The wurtzite-zinc blende transformation occurs at the temperature of 1000°C (Wyckoff, 1963).





## 2.7 REVIEW OF LEAD CADMIUM SULPHIDE THIN FILMS PREPARED BY CHEMICAL BATH DEPOSITION

Recently, the greatest interest and effort in the CBD of ternary semiconductors has been focused on lead cadmium sulphide (Pb,Cd)S. This literature review summarizes some of the various techniques used in the preparation of chemical bath deposited lead cadmium sulphide thin films and the results of their characterization. Extensive studies of the electrical and optical properties of  $\text{Pb}_{1-x}\text{Cd}_x\text{S}$  have been made by many researchers. These films generally have been prepared by chemical bath deposition from solution with high lead molar fraction in solution (Mohammed et al., 2009).

The first well characterized deposition of (Pb,Cd)S alloy film prepared by chemical bath deposition with a high cadmium molar fraction ( $\text{Pb}_x\text{Cd}_{1-x}\text{S}$ ) was described by Mohammed et al., (2009). In their work, the starting materials in the preparation of lead cadmium sulphide ( $\text{Pb}_x\text{Cd}_{1-x}\text{S}$ ) included cadmium acetate  $[\text{Cd}(\text{CH}_3\text{COO})_2 \cdot 2\text{H}_2\text{O}]$ , lead acetate  $[\text{Pb}(\text{CH}_3\text{COO})_2 \cdot 2\text{H}_2\text{O}]$ , ammonia ( $\text{NH}_3$ ), thiourea  $[(\text{NH}_2)_2\text{CS}]$  and distilled water. The lead acetate was the source of cation ( $\text{Pb}^{2+}$ ), cadmium acetate was the source of another cation ( $\text{Cd}^{2+}$ ), and thiourea was the source of anion ( $\text{S}^{3-}$ ).  $\text{NH}_3$  was used to provide an alkaline medium needed for maximum growth. The deposition process started with the mixing of the lead and cadmium acetate with ammonia. The solution was made up to 100 ml with distilled water and heated up to 50 °C. The glass substrate was immersed vertically and then 20 ml thiourea was added drop by drop and the bath was slowly heated up to 75 °C and kept at this temperature for 75 minutes.



Subsequently, the substrates were taken out, washed with distilled water and dried. The glass slide substrates in our study were ultrasonically cleaned.

Structural and morphological analysis of the thin film using XRD with a scan over a range of  $10^\circ \leq 2\theta \leq 90^\circ$  diffractograms revealed the polycrystalline nature of the films, irrespective of Pb mole fraction over the whole range. Both CdS and PbS exhibit hexagonal wurtzite and cubic zinc blend structure. Such results are reported by Deshmukh. et al (Deshmukh et al., 1994). Increasing the mole fraction of lead was accompanied by the appearance of lead oxide planes. The dominant peaks were (111) and (200) reflections. Additionally, there existed a plane at  $2\theta = 89^\circ$ , which does not belong to either PbS or CdS. Thus, there must be an inter-metallic formation of the kind  $(\text{Pb}_x\text{Cd}_{1-x}\text{S})$  in the composition.

Optical studies to determine the band gap showed that the plots exhibited two well defined absorption edges for all values of (x). The first absorption edge at (2.4 eV) corresponds to the fundamental optical transition in CdS. The fundamental optical transitions of PbS (0.41 eV) is not observed in these films, presumably because of complete alloying of PbS with CdS forming a uniphase ternary inter-metallic compound of the type  $\text{Pb}_x\text{Cd}_{1-x}\text{S}$ . It seems that the band gap 'corresponding to the low photon energy' decreased monotonically with the film composition parameter x. The band gap decreases from 2.4 eV for CdS to less than 1.3 eV for the  $\text{Pb}_x\text{Cd}_{1-x}\text{S}$  inter-metallic. Thus, decrease in optical gap is mainly attributed to the alloying of PbS with CdS, in agreement with the behavior shown previously (Skylas-Kazacos et al., 1985).

Barote et al., (2011) worked on synthesizing and characterization of  $\text{Cd}_{1-x}\text{Pb}_x\text{S}$  ( $0 \leq x \leq 1$ ) thin films. Cadmium sulphate, lead sulphate and thiourea were used as the basic starting materials. Triethanolamine (TEA) was used as complexing agent. For good quality deposits the various



preparative parameters such as deposition temperature, time, speed of substrate rotation and pH of the reaction mixture were optimized to 80 °C, 60 min., 65 rpm and 10.5±0.1 respectively. The 'as-grown' samples were characterized through structural, surface morphological, compositional, optical, electrical and thermoelectric studies. The colour of 'as-grown' samples went on changing from orange yellow to black with increase in composition parameter 'x' from 0 to 1. The thickness of the samples went on increasing with the composition parameter 'x'. The X-ray diffractograms of 'as-grown' samples exhibited polycrystalline nature with presence of cubic phases for CdS and PbS and hexagonal phase for CdS alone. The crystal size determined from XRD and SEM micrographs was observed to increase with 'x' up to 0.175 and later on it decreased. The energy dispersive analysis by X-rays (EDAX) revealed that films are cadmium rich. Films with crystallite size in the range 7-17 nm can be obtained. EDAX studies showed that films were non-stoichiometric. The optical study at room temperature revealed high coefficient of absorption ( $10^4 \text{ cm}^{-1}$ ) with a direct allowed type of transition with band gap energy decreasing continuously from 2.47 eV to 0.49 eV with varying composition parameter 'x'. The electrical resistivity measurements revealed semiconducting nature of the film and it is found that the resistivity of the film decreases with increase in 'x' up to 0.175 and further it increases up to  $x = 1$ .

Barote et al. (2011) conducted further research on this ternary alloy by analyzing the effect of various preparative parameters such as bath composition, pH of reaction solution, deposition temperature and time, speed of the substrate rotation, role of complexing agent on the growth process for the optimization of good quality films over a composition range of ( $x = 0.00, 0.20, 0.40, 0.60, 0.80, 1.00$ ), Cadmium sulphate, lead sulphate and thiourea were used as the basic source materials.



It was observed that, the film growth can be affected by changing the composition parameter  $x$  of the reaction solution. The change in bath composition can alter the processes of homogeneous nucleation and heterogeneous nucleation and ultimately the growth of thin films (Format and Lincot, 1995). The hydroxide species plays an important role in film formation and acts as nucleation centers on the substrates. The proper amount of hydroxy species in bath solution enhances the film growth and gives good quality film. If the bath contains low concentration of bath ingredients it generally favors the nucleation in early stage. Also the bath concentration plays an important role, when bath contains high concentration the films formed were thicker and for low concentration the films were thin, non-uniform and non-homogeneous. This indicates that there is lack of required number of ionic species for better quality film. Above certain concentration when rate of reaction becomes high and precipitation also becomes important leading to lesser amount CdS/PbS on the substrate and hence lowers the thickness (Kitaev et al., 1965).

The thin film formation depends on the pH of the reaction mixture and pH depends on OH ions. By the observation of Kaur et al. (Kaur et al., 1980), the decomposition of chalcogen is stimulated by presence of solid phase such as cadmium hydroxide and lead hydroxide. At the experimental conditions it was found that good quality CdPbS thin films can be deposited at pH ranging between 9.5 - 11.5. At this condition the alkaline hydrolysis and sulphur source release  $S^{2-}$  ions. The reactivity of hydroxide ions with metal ions is affected when pH of the solution is decreased. The decrease in pH results in porous, non-reflecting, powdery and weakly adhered thin films on the substrates. Increasing the pH value above 9.5, nonporous, uniform, smooth, tightly adherent and reflecting thin films are obtained. At higher pH metal ion concentration will



be lower and the reaction rate will be slow. With an increase in pH as the metal ion concentration decreases, the rate of film formation decreases (Hankare et al., 2006).

It was observed that at room temperature no film formation takes place. It may be due to at low temperature almost all the metal ions are in a complex-bound state, there may not be free ions for film formation. When temperature of bath container is increased to 80 °C good quality and adherent CdPbS films were deposited on glass substrates. Variation of film thickness with temperature showed that the terminal layer thickness increased with increase in temperature linearly up to 80 °C and above 80 °C it decreases. It is clear that at 80 °C, thermal energy is sufficient to make ions free from bound complex state which increases the rate of film formation. Above 80 °C the reaction gave precipitation rather than film which settled down at the bottom of container, as a result layer thickness of CdPbS thin films was found to be decreased (Hankare et al., 2006). It is observed that film growth is time-dependent and is initially quasi-linear, and after 60 minutes it saturates. It may be due to the fact that the volumetric ion concentration to surface substrate ratio decreases as time increases and finally results in a terminal layer thickness (Hankare et al., 2006). So in the study, CdPbS thin films were deposited for 60 minute time period.

The speed of the substrate rotation affects the film formation process. In case of CdPbS, the speed of substrate rotation is moderated to 65 rpm to obtain sufficient layer thickness and quality film. When the rotation speed is decreased, thick porous and non-sticky film was formed, while at a speed greater than 65 rpm very thin adherent, reflecting film deposition was formed.

The deposition of thin film on glass surface is an adsorption phenomenon. Film formation occurs by combination of released metal ions from complex metal ion source and chalcogen source. In



the present study triethanolamine is used as the complexing agent. With the help of triethanolamine complexed metal ion can be made free in alkaline medium of pH value  $10.5 \pm 0.1$ . It helps to limit the hydrolysis of the metal ion and impart some stability to bath otherwise it undergoes rapid hydrolysis and precipitation. If less amount of triethanolamine is used fast precipitation occurs, when excess triethanolamine is used less number of ions are available for film formation, so thinner films are formed (Mondal et al., 1983). In the present study pH of solution is optimized at  $10.5 \pm 0.1$  for good quality films.





## CHAPTER THREE

### 3.0 THEORY

#### 3.1 ENERGY BAND THEORY

In solid-state physics, the electronic band structure (or simply band structure) of a solid describes those ranges of energy, called energy bands, that an electron within the solid may have (allowed bands) and ranges of energy, called forbidden bands, which it may not have. Band theory models the behavior of electrons in solids by postulating the existence of energy bands. It successfully uses a material's band structure to explain many physical properties of solids, such as electrical resistivity and optical absorption.

Bands may also be viewed as the large-scale limit of molecular orbital theory. The electrons of a single isolated atom occupy atomic orbitals, which form a discrete set of energy levels. If several atoms are brought together into a molecule, their atomic orbitals split into separate molecular orbitals each with a different energy. This is due to the Pauli Exclusion Principle, which says that electrons that are close together must have different sets of quantum numbers (energy). This produces a number of molecular orbitals proportional to the number of valence electrons. When a large number of atoms (of order  $10^{20}$  or more) are brought together to form a solid, the number of orbitals becomes exceedingly large. Consequently, the difference in energy between them becomes very small. Thus, in solids the levels form continuous bands of energy rather than the discrete energy levels of the atoms in isolation. However, some intervals of energy contain no orbitals, no matter how many atoms are aggregated, forming band gaps.

Within an energy band, energy levels can be regarded as a near continuum for two reasons. First, the separation between energy levels in a solid is comparable with the energy that electrons



constantly exchange with phonons (atomic vibrations). Second, this separation is comparable with the energy uncertainty due to the Heisenberg uncertainty principle, for reasonably long intervals of time. As a result, the separation between energy levels is of no consequence (Wikipedia, energy band structure).



Figure 3.1: An extremely oversimplified diagram of a *band* of energy. Z represent one atom with an arbitrary energy level. When more and more Z atoms interact to form a crystal lattice, they all have energy levels that are practically degenerate in energy. Thus, all of these energy levels become a *band*, which is represented by the energy levels encased by the box (Neamen, 2006).

The band represents a kind of electronic highway allowing electrons to move throughout the solid, thereby conducting electricity. For this to occur, however, the band cannot be empty or



filled with electrons. Only if the band is partially filled can a net flow of electrons occur, corresponding to an electrical current.

The band containing the valence electrons is known as the valence band. The band of unoccupied orbitals is known as the conduction band. Conduction occurs when electrons are promoted from the valence band to the conduction band, where they can move throughout the solid. The energy separation between the valence and conduction bands is known as the band gap energy.

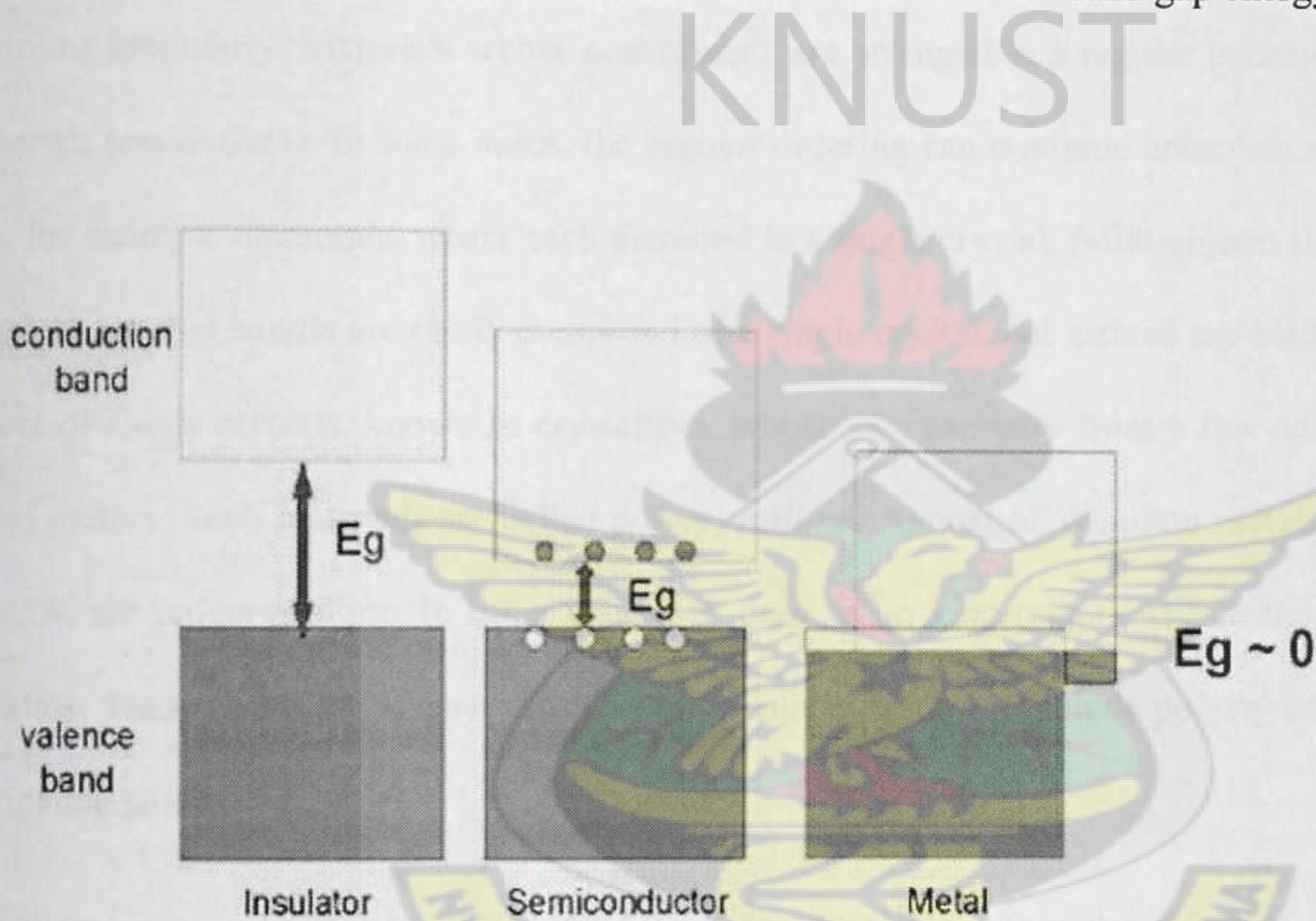


Fig 3.2: Schematic band diagrams for an insulator, a semiconductor, and a metal

The band gap energy,  $E_g$ , shown as the double-headed arrow, is the separation between the top of the valence band and the bottom of the conduction band. The size of the band gap decreases in passing from an insulator to a semiconductor to a metal, where it is effectively zero. Electron-



hole pairs are shown for a semiconductor as filled circles (electrons) in the conduction band and open circles (holes) in the valence band (<http://mrsec.wisc.edu/Edetc/background/LED/>).

### 3.2 CLASSIFICATION OF SOLIDS

The atoms, molecules or ions which make up a solid may be arranged in an orderly repeating pattern, or irregularly. Materials whose constituents are arranged in a regular pattern are known as crystals (*crystalline*). In some cases, the regular ordering can continue unbroken over a large scale, for example diamonds, where each diamond is a single crystal. Solid objects that are large enough to see and handle are rarely composed of a single crystal, but instead are made of a large number of single crystals, known as crystallites, whose size can vary from a few nanometers to several meters. Such materials are called *polycrystalline*. Almost all common metals, and many ceramics, are polycrystalline. In other materials, there is no long-range order in the position of the atoms. These solids are known as *amorphous* solids; examples include polystyrene and glass (Wikipedia, solid)

Each type is characterized by the size of an ordered region within the material. An ordered region is spatial volume in which atoms or molecules have a regular geometric arrangement or periodicity. Figure 3.3 shows the three structural orders (Neamen, 2003). It should be noted that the majority of semiconductors used in electronic applications are crystalline materials, although some polycrystalline and amorphous semiconductors have found a wide range of applications in various electronic devices, (Yacobi, 2004).



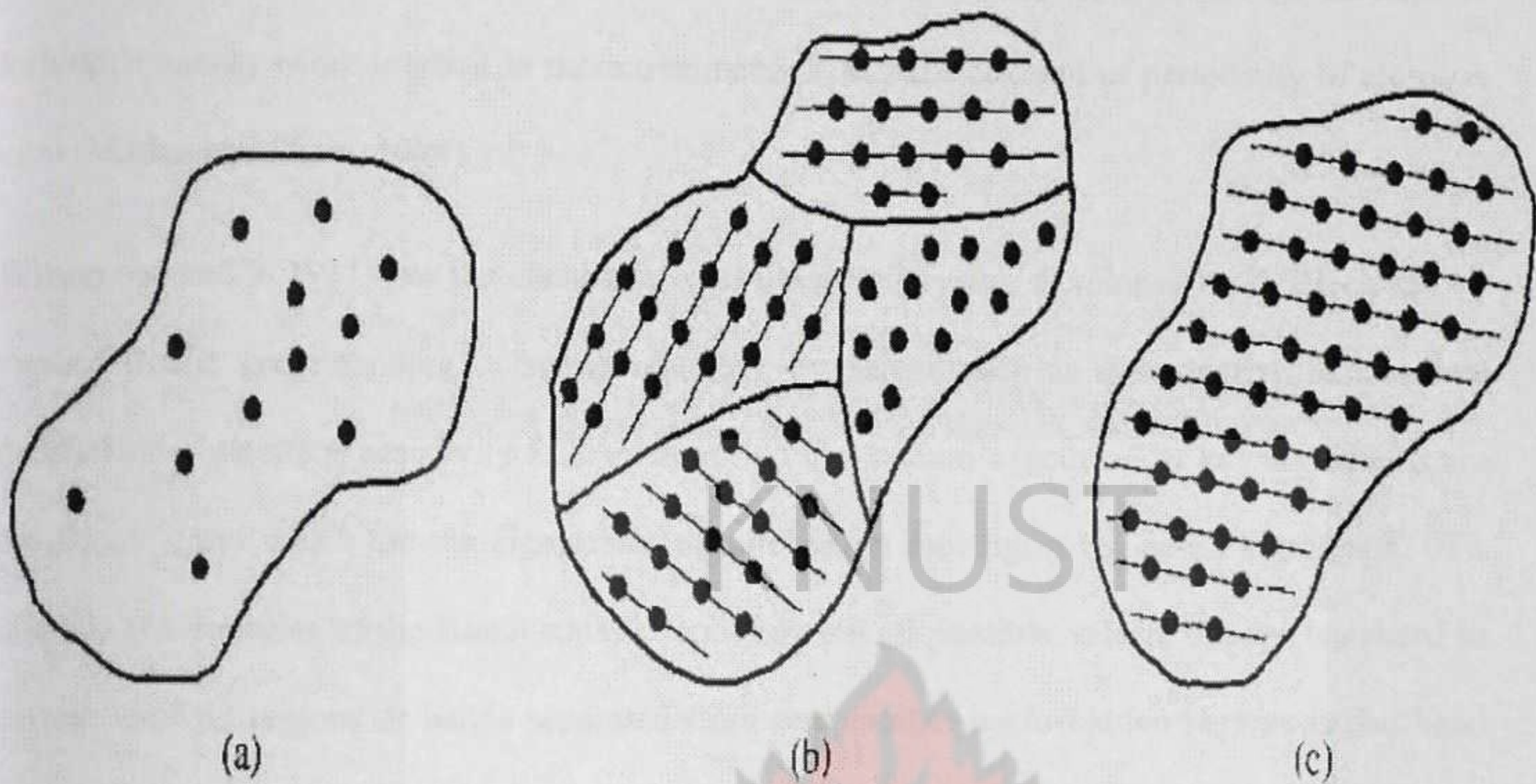


Figure 3.3: Schematics of the three general types of structural orders: (a) amorphous (b) polycrystalline, (c) crystalline.

### 3.2.1 CRYSTALLINE SEMICONDUCTORS

We can distinguish the crystalline state from the existence of the long-range order in three dimensions or from the arrangement of atomic structure, in crystalline material the atomic structure repeats itself in a periodical way.

The major success of solid state physics has been the theoretical prediction of the behavior of metals, insulators and semiconductors. The success of the energy band theory has relied on the derivation of the  $E - k$  (energy – wave vector) relationship which involves the consideration of a periodic array of atoms and the derivation of Bloch wave functions, from which the classes of



energy states available to electrons and holes can be predicted. This leads to the concept of forbidden energy band. Implicit in these treatments is that the concept of periodicity of atoms is vital (Madan and Shaw, 1988).

Wilson showed in 1931 how the electronic band theory of crystals developed by F. Bloch can be applied to the understanding of semiconductors. Properties such as the negative temperature coefficient of electrical resistivity follow naturally from Wilson's theory. The key ingredients are the Bloch states which are the eigenstates of an electron moving in the periodic potential of a crystal. The energies of the Bloch states cannot take on all possible values, but are restricted to certain allowed regions or bands separated from one another by forbidden regions called band gaps or energy gaps. Band theory and its outcome-effective mass theory-has allowed us to understand the difference between metals, insulators and semiconductors and how electrons respond to external forces in solids (Balkanski and Wallis, 2000; Singh, 2003).

It is well known that the great success of the 20th century, the transistor, is based upon the periodicity of materials with particular emphasis on one element, silicon. Indeed, with the great success of the transistor based upon the crystal structure of germanium and silicon, we entered the historical era where achieving crystalline perfection over a very large distance became the *sine qua non* of materials science.

The electronic band structure of crystalline semiconductors is substantially different from that in the amorphous semiconductors. In crystalline materials, the periodicity of the atomic structure and the presence of long-range order result in a band structure with allowed and forbidden electronic levels, with sharp band edges and a fundamental energy gap separating valence band from the conduction band. In amorphous semiconductors, there is still a fundamental energy gap



based on the short-range bonding between the atoms; however, the sharp band edges of the crystalline semiconductor are replaced in the amorphous materials by exponential band tails due to localised states related to the structural disorder (i.e., bond length and bond angle deviations that broaden the distribution of electronic states); in addition, defects (i.e., dangling bonds) introduce electronic levels in the energy gap (Yacobi, 2004).

From observations and measurements we find that it is the regular crystalline structure that leads to certain special properties and behavior of the associated materials (Korvink and Greiner, 2002). The advantage of crystalline material is that, in general, its electrical properties are superior to those of a nonsingle-crystal material, since grain boundaries tend to degrade the electrical characteristics (Neamen, 2003).

### **3.2.2 POLYCRYSTALLINE SEMICONDUCTORS**

Most real crystalline solids have discontinuities in the regular arrangement of atoms. They are known as polycrystalline materials. Their structure consists of lots of individual crystals called grains. The area where grains meet is called the grain boundary ([www.southampton.ac.uk](http://www.southampton.ac.uk)). The size and orientation of grains has a major influence on the mechanical properties of a material. They have a high degree of order over many atomic or molecular dimensions. These ordered regions or single-crystal regions only vary in size and orientation with respect to one another (Neamen, 2003).

These semiconductors can be further classified as (i) microcrystalline and nanocrystalline materials that are usually prepared as thin films and (ii) large grain materials in the form of sliced ingots and sheets. The grain size in polycrystalline materials depends on the substrate



temperature during thin film growth, the thickness of the film and also on post-growth annealing treatment of the film. It is important to consider here that many solids are incorrectly described as being amorphous, but are in fact microcrystalline or nanocrystalline with small crystallite sizes which fail to give crystalline X-ray diffraction patterns. However, often these materials can be confirmed as crystalline using electron diffractions, with lattice images routinely obtained from particles in the range of 5 nm. The grain boundaries generally have an associated space-charge region controlled by the defect structure of the material and the grain boundaries are paths for the rapid diffusion of impurities affecting various properties of polycrystalline materials. An important consequence of the presence of potential barriers on grain boundaries in a polycrystalline semiconductor is the increase of its electrical resistivity. One of the important processes is the decoration of grain boundaries, that is, the process in which precipitates of impurity elements segregate to the boundaries.

In general, the grain boundaries introduce allowed levels in the energy gap of a semiconductor and act as efficient recombination centers for the minority carriers. This effect is important in minority-carrier devices, such as photovoltaic solar cells and it is expected that some of the photo generated carriers will be lost through recombination on the grain boundaries. Typically, the efficiency of the device will improve with increasing grain size. In this context, the columnar grain structure (i.e., grains in a polycrystalline material extend across the wafer thickness) is more desirable as compared to the material containing fine grains that do not extend from back to front of a device structure. In order to prevent significant grain boundary recombination of the minority carriers, it is also desirable that the lateral grain sizes in the material be larger than the minority carrier diffusion length. It should also be mentioned that the possible preferential diffusion of dopants along the grain boundaries and or precipitates of impurity elements



segregated at the boundaries may provide shunting paths for current flow across the device junction. It should also be noted that hydrogen passivation of grain boundaries in polycrystalline silicon devices, such as photovoltaic cells, is an effective method of improving their photovoltaic performance efficiency. This improvement is associated with the mechanism similar to that of the passivation of dangling bonds in amorphous silicon (Yacobi, 2004; Gellings and Bouwmeester, 1997)

KNUST

### 3.2.3 AMORPHOUS SEMICONDUCTORS

All solids that do not have long range periodicity in their arrangement of its atoms can be termed as amorphous or “structureless”. They are best defined when compared to a crystalline solid which has a distinctive regular spatial arrangement of atoms throughout the whole material. In fact they are often simply referred to as non-crystalline materials. Although their structure appears random over the long range, an amorphous substance still has a high degree of short range spatial order in its atomic structure. This is because individual atoms in an amorphous solid must still fulfill their requirement for valence bonding. However, unlike their crystalline counterpart, there are some small deviations in the bonding angles between adjacent atoms and this leads to a disruption of the periodicity in the material. Figure 3.4 illustrates the difference between a crystalline and an amorphous solid.



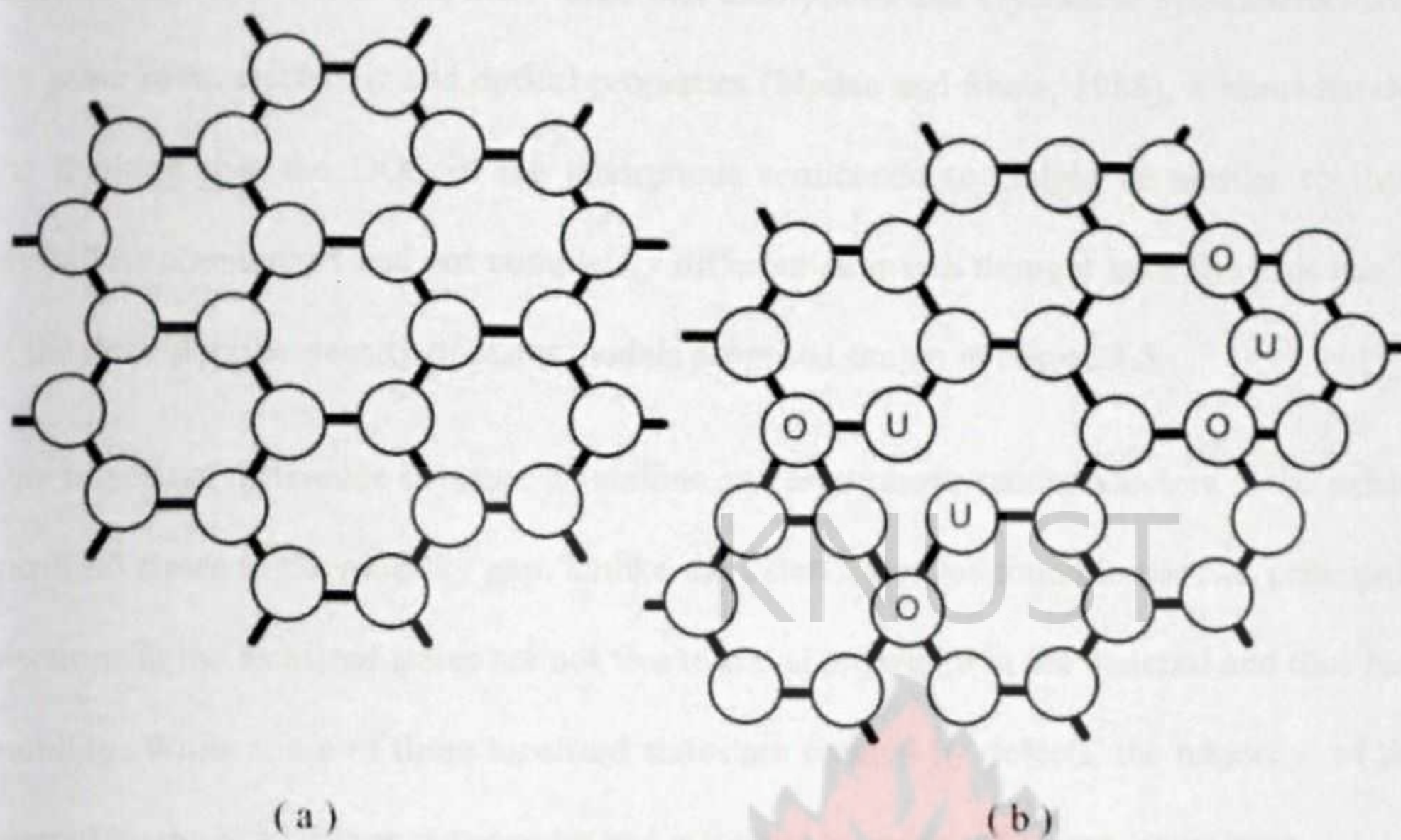


Figure 3.4: Two dimensional representation of the structure of (a) a crystalline solid and (b) an amorphous solid.

Although an amorphous semiconductor is a non-crystalline material, the band theory of amorphous semiconductors is closely related to its crystalline counterpart. The theory was called the band theory because when quantum mechanics was applied to a crystal, bands of allowable energy states were brought into existence. Besides these bands of allowable states, which are often grouped into two principle bands labeled as the valence and conduction bands, there is also a band gap separating the two bands where no electron states can exist. Very often the density of states (DOS) diagram is used to explain or predict the properties of a material in the band theory. It denotes the number of electron states per unit energy per electron a material will have at an energy level and is used successfully to describe many of the characteristic found in a crystalline



semiconductor. When it was discovered that amorphous and crystalline semiconductors shared the same basic electronic and optical properties (Madan and Shaw, 1988), it immediately led to the thinking that the DOS of the amorphous semiconductor might be similar to that of its crystalline counterpart and not completely different as it was thought initially. This can be seen in the three popular density of states models proposed shown in Figure 3.5.

One important difference between crystalline and amorphous semiconductors is the existence of localized states in the mobility gap. Unlike the extended states found in the two principal bands, electrons in the localized states are not free to travel anywhere in the material and thus have zero mobility. While some of these localized states are created by defects, the majority of them are created by the loss of long range order and is unique to solids which are amorphous.





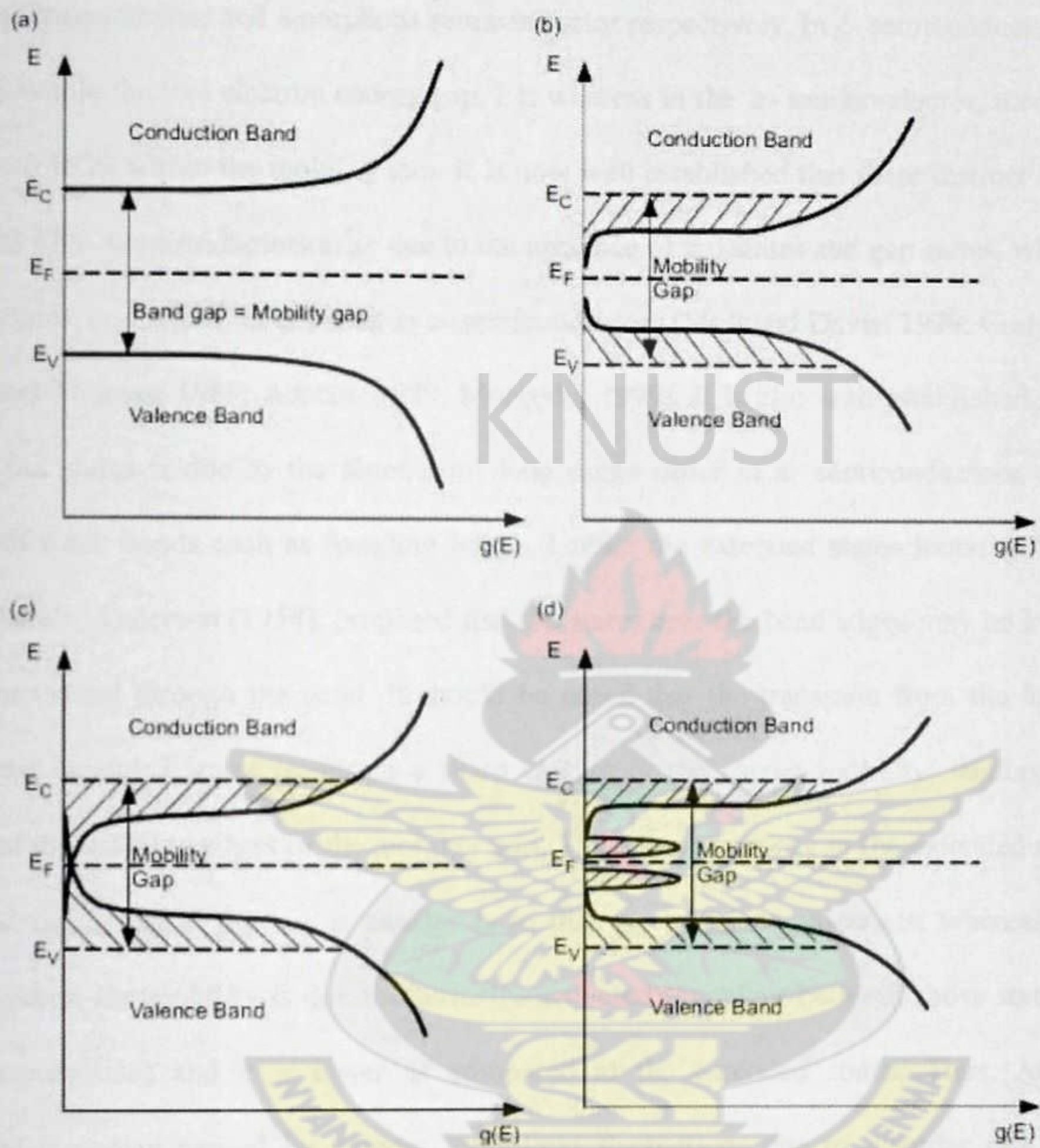


Figure 3.5: (a) DOS of a crystalline semiconductor; (b) DOS models proposed by Mott (1967), (c) DOS models proposed by Cohen et al. (1969), and (d) DOS models proposed by Marshall and Owen (1971). The hatched regions denote localized states. Note: the x-axis in all the 4 figures is logarithmic.



Figures 3.5(a) and (b) show schematically typical features of density of states (DOS) of a crystalline semiconductor and amorphous semiconductor respectively. In c- semiconductor, there is no DOS within the free electron energy gap,  $E_g$ , whereas in the a- semiconductor, there exists a non – zero DOS within the mobility gap. It is now well established that these distinct features of the DOS of a- semiconductors arise due to the presence of tail states and gap states, which are localized states, and which do not exist in c- semiconductors (Mott and Davis, 1979; Cody, 1984; Overhof and Thomas, 1989; Adachi, 1999; Morigaki, 1999). It is also well established that the origin of tail states is due to the absence of long range order in a- semiconductors, and the presence of weak bonds such as dangling bonds. Unlike the extended states found in the two principal bands, Anderson (1958), proposed that the states near the band edges may be localized and do not extend through the solid. It should be noted that the transition from the localized states to the extended states results in a sharp change in the carrier mobility, leading to the presence of the mobility edges or the mobility gap. The carrier mobility in the extended states is higher and the transport process is analogous to that in crystalline materials; whereas in the localized states, the mobility is due to thermally-activated tunneling between those states (i.e., *hopping conduction*) and it is lower as compared to the extended states. Thus, Anderson localization transition caused by random local field fluctuations due to disorder can lead to “mobility edges” rather than band edges as illustrated in Figure 3.6 and hence, rather than an energy gap one has a mobility gap separating localised and nonlocalised or extended states (Kittel, 2005; Yacobi, 2004; Petterson and Bailey, 2005).

Two distinct classes of amorphous semiconductors are widely studied: tetrahedrally-bonded amorphous solids such as silicon and germanium and chalcogenide glasses. The latter are



multicomponent solid of which one major constituent is a “chalcogen” element—sulphur, selenium, or tellurium (Kittel, 2005).

The tetrahedrally-bonded materials have properties similar to those of their crystalline forms, provided the dangling bonds defects are compensated with hydrogen. They can be doped with small amount of chemical impurities and their conductivity can be sharply modified by injection of free carriers from a metallic contact. By contrast, the chalcogenide glasses are largely insensitive to chemical impurities and to free carrier injection.

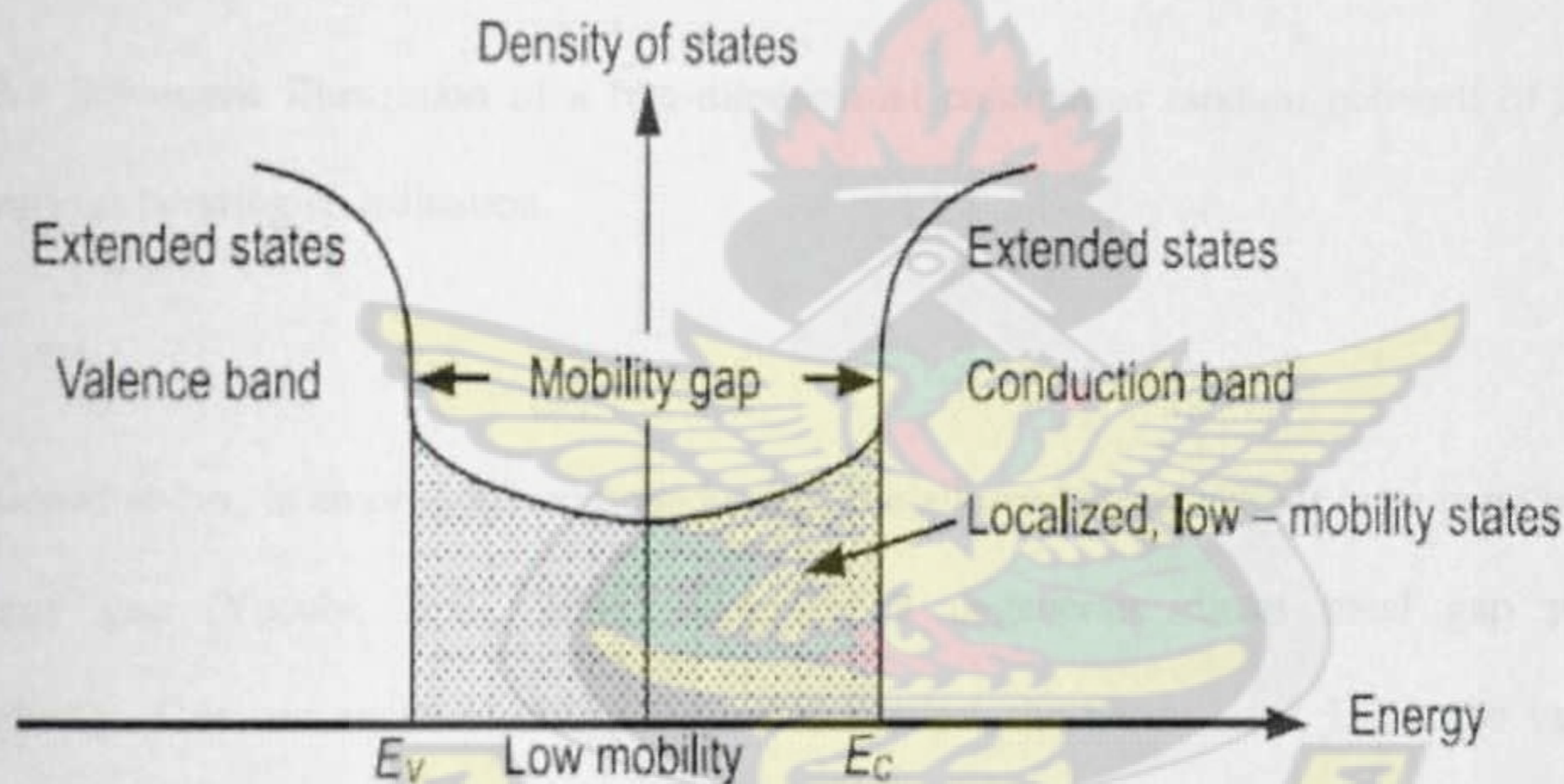


Figure 3.6. Area of mobility between valence and conduction bands

In amorphous materials, defects are of different kind as compared to crystalline materials. In the case of amorphous materials, the main defects are those related to the deviations from the average coordination number, bond length and bond angle; other defects include, e.g., dangling bonds, deviations from an optimal bonding arrangement and microvoids.



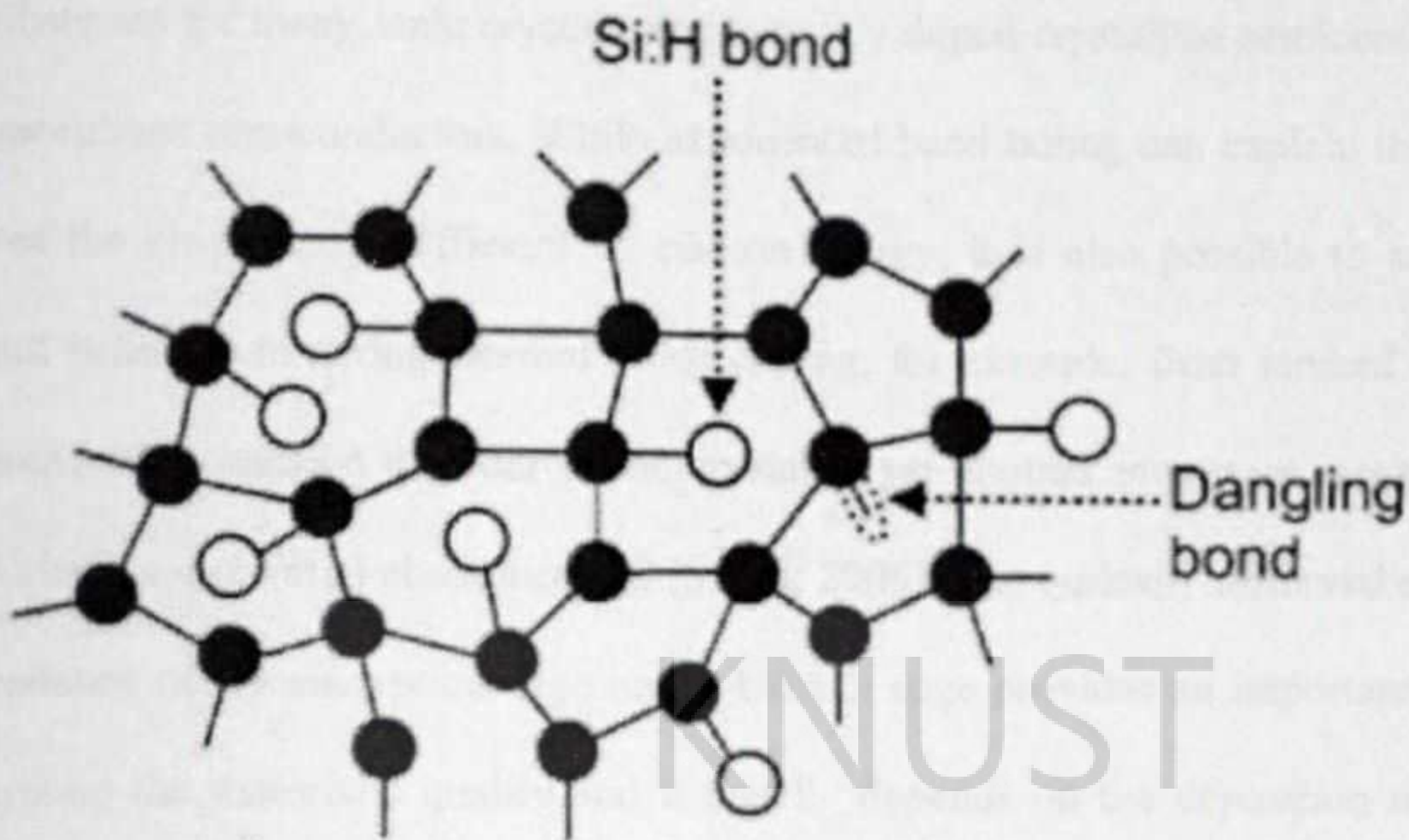


Figure 3.7 Schematic illustration of a two-dimensional continuous random network of atoms having various bonding coordination.

As mentioned above, in amorphous semiconductors, the allowed energy bands have band tails in the energy gap (Yacobi, B.G., 2004). Consider a degenerate direct band gap p-type semiconductor. One can excite electrons from states below the Fermi level,  $E_f$ , in the valence band where the band is nearly parabolic, to tail states below conduction band edge,  $E_c$ , where the density of states decreases exponentially with energy into the band gap, away from  $E_c$ . Such excitations lead to absorption coefficient,  $\alpha$ , depending exponentially on photon energy,  $h\nu$ , a dependence that is usually called the Urbach rule, given by

$$\alpha = \alpha_0 \exp [(h\nu - E_0)/\Delta E] \quad (3.1)$$

where  $\alpha_0$  and  $E_0$  are material- dependent constants and  $\Delta E$ , called the Urbach width, is also a material-dependent constant. The Urbach rule was originally reported for alkali halides.



It has been observed for many ionic crystals, degenerately doped crystalline semiconductors and almost all amorphous semiconductors. While exponential band tailing can explain the observed Urbach tail of the absorption coefficient vs. photon energy, it is also possible to attribute the absorption tail behavior to strong internal fields arising, for example, from ionized dopants or defects. Temperature-induced disorder in the crystal is yet another important mechanism that leads to an Urbach exponential absorption tail (Singh, 2006). The typically observed exponential energy dependence of the absorption edge or the Urbach edge provides an important parameter for characterizing the material's quality and it usually depends on the deposition method and deposition conditions. Thus as already noted above, in amorphous materials the exponential band tails are related to the structural disorder, i.e., bond length and bond angle deviations that broaden the distribution of electronic states; hence, the slope of the Urbach edge can be related to the material's quality (Street, 1991).

### 3.3 OPTICAL ABSORPTION SPECTROSCOPY

The study of the electromagnetic spectrum of elements is called Optical Spectroscopy. Electrons exist in energy levels within an atom. These levels have well defined energies and electrons moving between them must absorb or emit energy equal to the difference between them. In optical spectroscopy, the energy absorbed to move an electron to a more energetic level and/or the energy emitted as the electron moves to a lower energy level is in the form of a photon (a particle of light). Because this energy is well-defined, an atom's identity can be found by the energy of this transition. The wavelength of light can be related to its energy. It is usually easier to measure the wavelength of light than to directly measure its energy.



Optical spectroscopy can be further divided into absorption, emission, and fluorescence (Wikipedia, atomic spectroscopy).

In a semiconductor there exist allowed energy bands. Thus, there will be a range of photon energies that can be absorbed. Thus by inserting a slab of semiconductor material at the output of a monochromator and studying the changes in the transmitted radiation, one can discover all possible transitions an electron can make and learn much about the distribution of states.

### **3.3.1 OPTICAL PROPERTIES OF SEMICONDUCTORS**

In order to understand the optical behavior of films, one must become familiar with the optical constants of materials, their origins; magnitudes and how they depend on the way films are processed. The unifying concept that embraces all optical properties is the interaction of electromagnetic radiation with the electrons of the material. On this basis, optical properties are interpretable from what we know of the electronic structure and how it is affected by atomic structure, bonding, impurities, and defects (Ohring, 1992).

Optical properties of semiconductors typically consist of their refractive index  $n$  and extinction coefficient  $k$  or absorption coefficient  $\alpha$  (or equivalently the real and imaginary parts of the relative permittivity) and their dispersion relations, that is their dependence on the wavelength,  $\lambda$ , of the electromagnetic radiation or photon energy  $h\nu$ , and the changes in the dispersion relations with temperature, pressure, alloying, impurities, etc (Singh, 2006)



The process of absorption in semiconductors can have a variety of mechanisms by which electrons (and holes) absorb optical energy. Most of these processes can occur in quantum wells, wires, and dots, as well as in bulk material and they include;

1- Band-to-band: an electron in the valence band absorbs a photon with enough energy to be excited to the conduction band, leaving a hole behind.

2- Band-to-exciton: an electron in the valence band absorbs almost enough energy to be excited to the conduction band. The electron and hole it leaves behind remain electrically "bound" together, much like the electron and proton of a hydrogen atom.

3- Band-to-impurity or impurity to band: an electron absorbs a photon that excites it from the valence band to an empty impurity atom or from an occupied impurity atom to the conduction band.

4- Free carrier: an electron in the conduction band, or hole in the valence band, absorbs a photon and is excited to a higher energy level within the same set of bands (i.e., conduction or valence).

In quantum structures there can be photon absorption due to carriers being excited between the quantum levels within the same band (termed "intra-band"), as well as between the various quantum levels in one band and those in another "(inter-band").

5- Inter-band: inter-band transitions can occur between conduction and valence bands, or between different valence bands (light-hole, heavy-hole, and spin-off). There are transitions can be active for either polarization of the light, depending on the symmetries of the respective bands

(Rnjdar and Ali, 2006)



Singh (2006), showed a typical relationship between the absorption coefficient and photon energy observed in a crystalline semiconductor where the various possible absorption processes are illustrated in Figure 3.8.

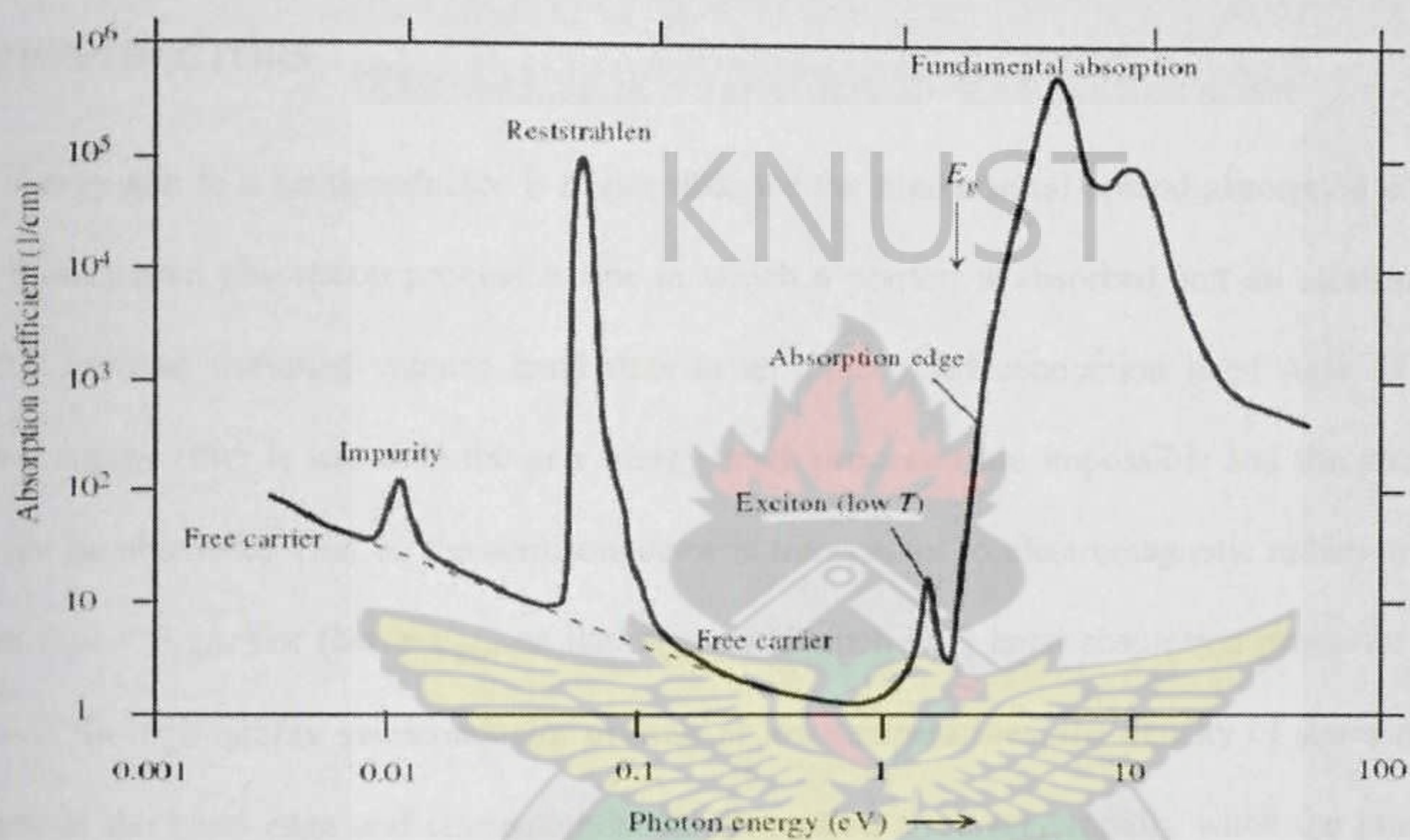


Figure 3.8: Absorption coefficient is plotted as a function of the photon energy in typical semiconductor to illustrate the various possible absorption processes.

The important features in the  $\alpha$  vs.  $h\nu$  behaviour as the photon energy increases can be classified in the following types of absorptions: (a) Reststrahlen or lattice absorption in which the radiation is absorbed by vibrations of the crystal ions, (b) free-carrier absorption due to the presence of free electrons and holes, an effect that decreases with increasing photon energy, (c) an impurity absorption band (usually narrow) due the various dopants, (d) exciton absorption peaks that are usually observed at low temperatures and are close to the fundamental absorption



edge and (e) band-to-band or fundamental absorption of photons, which excites an electron from the valence to the conduction band (Singh, 2006).

### 3.3.2 FUNDAMENTAL ABSORPTION IN DIRECT AND INDIRECT BANDGAP SEMICONDUCTORS

The energy gap in a semiconductor is responsible for the fundamental optical absorption edge. The fundamental absorption process is one in which a photon is absorbed and an electron is excited from an occupied valence band state to an unoccupied conduction band state. If the photon energy ( $\hbar\omega$ ) is less than the gap energy, such processes are impossible and the photon will not be absorbed. That is, the semiconductor is transparent to electromagnetic radiation for which ( $\hbar\omega < E_{\text{gap}}$ ). For ( $\hbar\omega > E_{\text{gap}}$ ) on the other hand, such inter band absorption processes are possible. In high quality semiconductor crystals at low temperatures, the density of states rises sharply at the band edge and consequently the absorption rises very rapidly when the photon energy reaches the gap energy. Observation of the optical absorption edge is the most common means of measuring the energy gap in semiconductors (Rnjdar and Ali, 2006). However, because the transitions are subject to certain selection rules (i.e. there are some restrictions based on the E-k diagrams), the estimation of the energy gap from the “absorption edge” is not a straightforward process even if competing absorption processes can be accounted for.

There are two types of optical transition associated with the fundamental absorption process, namely, direct and indirect band-to-band transitions, as shown in Figure 3.9 a and b. Since the photon momentum is small compared with the crystal momentum, the absorption process should essentially conserve the electron momentum, i.e.,  $\hbar k$ . The direct (or vertical) transition shown in



Figure 3.9a is the dominant absorption process taking place in a direct band gap semiconductor like GaAs and InP where the conduction band minimum and the valence band maximum are located at the same  $k$ -value in the reciprocal space. Thus, the transition results from the direct interaction of a photon with an electron. Direct band gap materials are generally efficient emitters and absorbers of optical energy because it's easy for electrons to move between the conduction and valence band without having to acquire or give off  $k$ . In an indirect band gap semiconductor (e.g., Si, Ge and GaP), the conduction band minimum and the valence band maximum are not located at the same  $k$ -value in the reciprocal space as shown in Figure 3.9b. An electron cannot go from one band to another simply by absorbing a photon of energy close to the band gap, because the photon cannot supply adequate wave vector. The electron needs to acquire both energy and wave vector to make the transition in indirect materials. Therefore, the indirect optical transition induced by photon absorption is usually accompanied by the simultaneous absorption or emission of a phonon to conserve momentum; the probability of such a process is substantially lower compared with direct transitions (Li, 2006). Therefore, in general, fundamental absorption in indirect gap semiconductors is relatively weaker as compared with the direct gap materials.



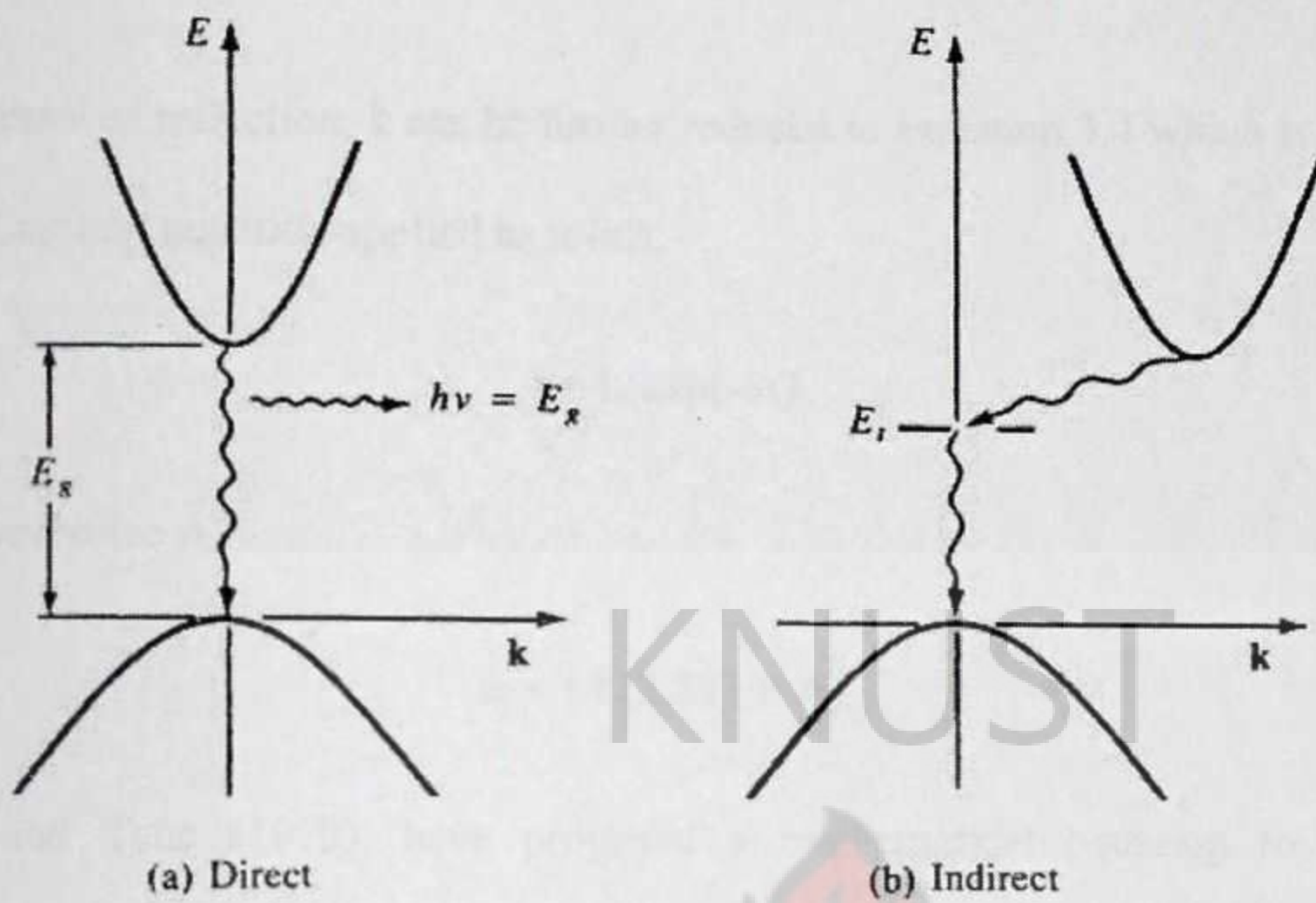


Figure 3.9: Direct and indirect electron transitions in semiconductors (a) Direct transition with accompanying photon emission; (b) indirect transition via a defect level.

### 3.3.3 OPTICAL ABSORPTION AND BAND GAP

Absorption is expressed in terms of a coefficient,  $\alpha(h\nu)$  which is defined as the relative rate of decrease in light intensity along its propagation path. The absorption coefficient  $\alpha$ , can be derived from transmission or absorption measurements. If  $I_0$  is an incident light intensity,  $I$  is the transmitted light intensity and  $R$  is the reflectivity, then the transmission,  $T = I / I_0$  can be written as (neglecting interference)

$$T = (1-R)^2 \exp(-\alpha t) / 1-R^2 \exp(-2\alpha t) \quad (3.2)$$

where  $t$  is the thickness of the material. For large  $\alpha t$ , this expression can be reduced to



$$T = (1-R)^2 \exp(-\alpha t) \quad (3.3)$$

and, in the absence of reflection, it can be further reduced to Equation 3.4 which is also described as the Beer – Lambert equation applied to solids.

$$I = I_0 \exp(-\alpha t) \quad (3.4)$$

In terms of absorbance A,

$$\alpha = 1/t (2.303 \times A) \quad (3.5)$$

Mott, Davis and Tauc (1979), have proposed a mathematical equation to represent the relationship between optical energy gap and the energy of the incident photon as:

$$\alpha h\nu = A(h\nu - E_g)^n \quad (3.6)$$

where A is a constant,  $E_g$  is the optical energy gap and n is an index which could take different values according to the electronic transition. The value of n is 1/2 or 3/2 for direct allowed and direct forbidden transitions respectively. For indirect transitions, n is 2 or 3 for indirect allowed and indirect forbidden transition respectively.

The energy band gap is determined by extrapolating the linear portion of  $(\alpha h\nu)^2$  vs  $h\nu$  to the energy axis at  $(\alpha h\nu)^2 = 0$ . The intercepts of these plots on the energy axis gives the energy band gap. (Tauc, 1974; Yacobi, 2004).

Alternatively and with specific reference to this work, band gap energy and transition can be derived from mathematical treatment of data from optical absorbance versus wavelength with the Stern (1963), relationship of near – edge absorption.

$$A = [k(h\nu - E_g)]^{n/2} / h\nu \quad (3.7)$$



where  $\nu$  is the frequency,  $h$  is the Planck's constant,  $k$  equals a constant while  $n$  carries the value of either 1 or 4. The band gap,  $E_g$ , could be obtained from a straight line plot of  $(Ah\nu)^{2/n}$  as a function of  $h\nu$ . Extrapolation of the line to the base line, where the value of  $(Ah\nu)^{2/n}$  is zero, will give the energy band gap. A linear trend is apparent where  $n$  in the Stern relationship equals 4.

### 3.4 X – RAY DIFFRACTION

X-ray diffraction technique is the most suitable, non-destructive and most precise method for crystal structure analysis and atomic spacing. It is simple because no elaborate sample preparation is required (Chopra and Das, 1983; Schroder, 1998).

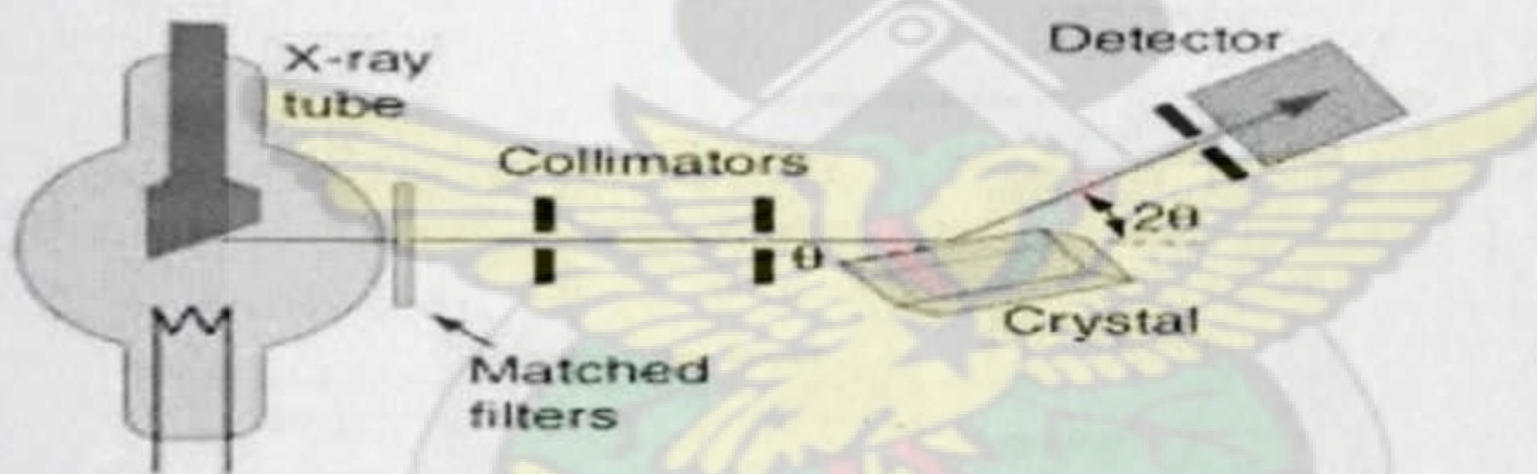


Figure 3.10: Schematic for X-ray Diffraction (Wikipedia/braggs law).

A monochromatic beam of x-ray that falls upon a crystal is scattered in all directions within it, but owing to the regular arrangement of the atoms, in certain directions the scattered waves constructively interfere with one another while in others they interfere destructively. Constructive interference takes place only between scattered rays, which obey the Bragg law:  $\lambda = 2d\sin\theta$ , where  $\lambda$  is the wavelength of the x-ray beam incident upon a crystal at angle  $\theta$  with family of planes whose spacing is  $d$ .



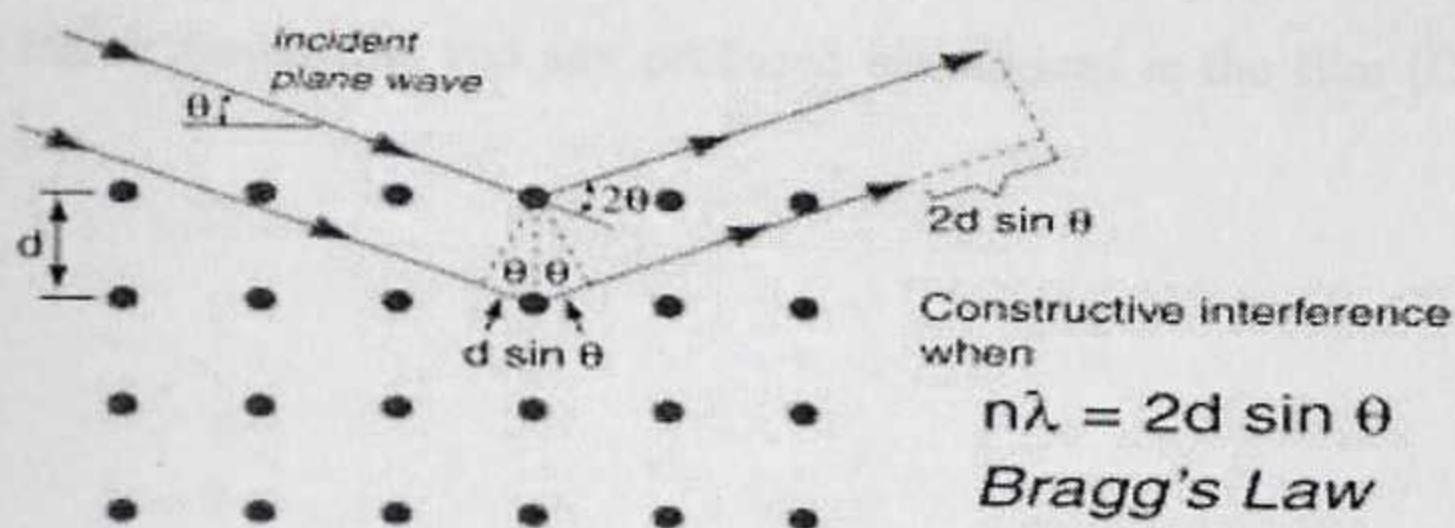


Figure 3.11: Illustration of Bragg's law of diffraction (Wikipedia / bragg's law)

In the case of the rotating crystal method, a crystal is mounted with one of its axes or some important crystallographic direction, normal to monochromatic x-ray beam. As the crystal rotates a particular set of lattice planes will make the correct Bragg angle for reflection of the monochromatic incident beam (Cullity, 1978).

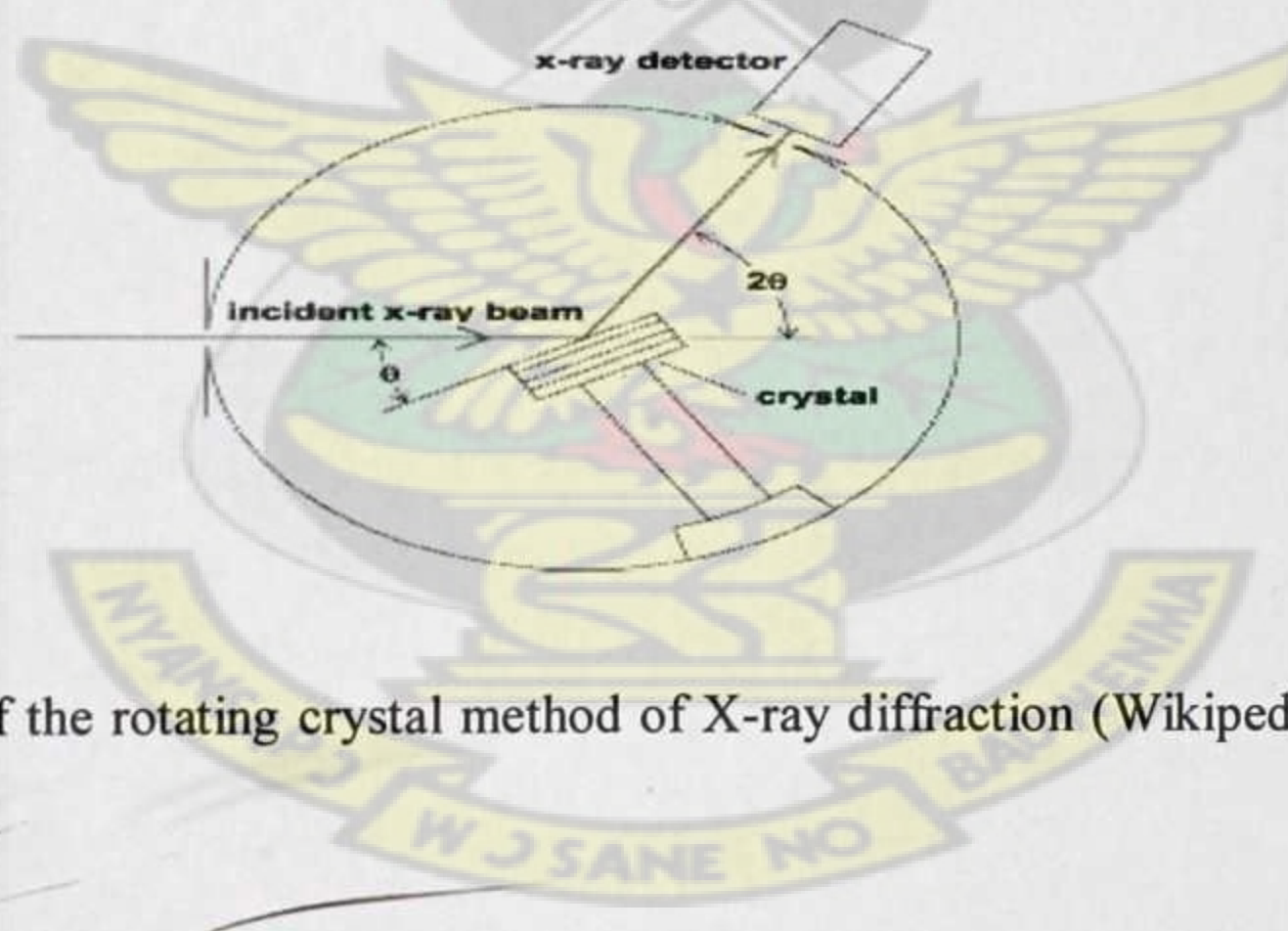


Figure 3.12: Schematic of the rotating crystal method of X-ray diffraction (Wikipedia, rotating crystal method).

Improved detection methods for x-rays, the availability of commercial monochromators and intense micro – focus x-ray sources have made x-ray diffraction methods applicable to film as thin as 50 Å. The method is generally applied to films thickness of several hundred Å (Chopra, 1969; Eckertova, 1977). Analysis of the diffraction patterns obtained and comparison with standard ASTM data can reveal the existence of different crystallographic phases, their relative



abundance, the lattice parameters and any preferred orientations in the film (Chopra and Das, 1983).

KNUST





## CHAPTER FOUR

### 4.0 METHODOLOGY

#### 4.1 EXPERIMENTAL DETAILS

The method of preparing or depositing a material can profoundly affect the phase composition, thermal stability and morphology which in turn can influence the functional behaviour of the material (Ramasamy et al., 2011). Also, one has to keep in mind that the high sensitivity of the film properties to deposition parameters can produce a multitude of undesired results thus thin film materials must be treated with due respect and understanding (Chopra et al., 2004).

#### 4.2 SUBSTRATE PREPARATION

The preparation of substrates is a critical aspect that can contribute to film adherence. Although thin films can be deposited by CBD on any surface, there will be certain obvious exceptions such as substrates that are unstable in the deposition solution or “dirty” substrates (Dekker, 2002). A clean surface is one that contains no significant amount of undesirable material (Mattox, 1978). Cleaning is defined as the removal, by physical and or chemical means of soil that could interfere with the preparation of the desired material. Soil is matter on the surface whose chemical characteristics are different from those being formed. The types of soils mostly encountered are fingerprint oils, metal oxides, dirt, etc. (Beal, 1978). Cleanliness and preparation of substrates is essential for success in thin film work. Condensation rate and adhesion of the deposit are critically dependent of conditions on the surface. Even a thin layer of grease can have such a gross effect on a molecular scale as to alter completely the characteristics of the layer. It is



therefore important that prior to the deposition of the semiconducting thin film the substrate, in this case microscope glass is cleaned thoroughly to remove any undesirable substance from it.

In this work, the microscope glass slides were left in nitric acid ( $\text{HNO}_3$ ) for 24 hours to remove any form of dirt, grease or other contaminants. They were then soaked in ethanol and later rinsed with de-ionized water before use. After cleaning, the slides were kept in a desiccator; this stops any movement and possible contamination.

### 4.3 REAGENTS

The starting materials in the preparation of lead cadmium sulphide ( $\text{Pb}_x\text{Cd}_{1-x}\text{S}$ ) consisted of the following: Cadmium acetate  $[\text{Cd}(\text{CH}_3\text{COO})_2 \cdot 2\text{H}_2\text{O}]$ : 99% purity, Lead acetate  $[\text{Pb}(\text{CH}_3\text{COO})_2 \cdot 2\text{H}_2\text{O}]$  : 98% purity, Ammonia ( $\text{NH}_3$ ), Thiourea  $[(\text{NH}_2)_2\text{CS}]$ : 99% purity all from B.D.H Laboratory Chemicals Division, (Poole – England) and distilled water. The lead acetate was the source of cation ( $\text{Pb}^{2+}$ ), cadmium acetate was the source of another cation ( $\text{Cd}^{2+}$ ), thiourea was the source of anion ( $\text{S}^{3-}$ ).  $\text{NH}_3$  was used to provide an alkaline medium needed for maximum growth.

#### 4.3.1 STANDARD SOLUTION OF 0.5 M LEAD ACETATE $[\text{Pb}(\text{CH}_3\text{COO})_2 \cdot 2\text{H}_2\text{O}]$

Lead acetate salt (9.03 g) was measured into a 50 ml volumetric flask and diluted to the meniscus level with distilled water. The solution was stirred using a magnetic stirrer to prevent precipitates from forming. The resulting solution had a concentration of 0.5 M.



#### 4.3.2 STANDARD SOLUTION OF 0.5 M CADMIUM ACETATE $[\text{Cd}(\text{CH}_3\text{COO})_2 \cdot 2\text{H}_2\text{O}]$

Cadmium acetate salt (13.32 g) was measured into a 100 ml volumetric flask and diluted to the meniscus level with distilled water. The solution was stirred to prevent precipitates from forming. The resulting solution had a concentration of 0.5 M.

#### 4.3.3 STANDARD SOLUTION OF 1 M THIOUREA $[(\text{NH}_2)_2\text{CS}]$

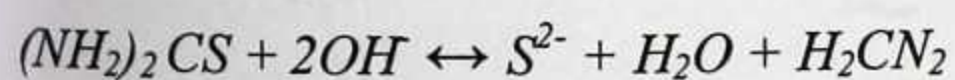
Thiourea salt (19.03 g) was measured into a 250 ml volumetric flask and diluted to the meniscus level with distilled water. The solution was stirred to prevent precipitates from forming. The resulting solution had a concentration of 1 M.

#### 4.4 CHEMICAL EQUATIONS FOR THE DEPOSITION PROCESS

The lead acetate was the source of cation ( $\text{Pb}^{2+}$ ), cadmium acetate was the source of another cation ( $\text{Cd}^{2+}$ ), and thiourea was the source of anion ( $\text{S}^{3-}$ ).  $\text{NH}_3$  was used to provide an alkaline medium needed for maximum growth.

##### 4.4.1 DECOMPOSITION OF THIOUREA

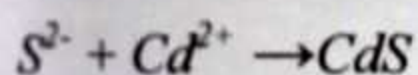
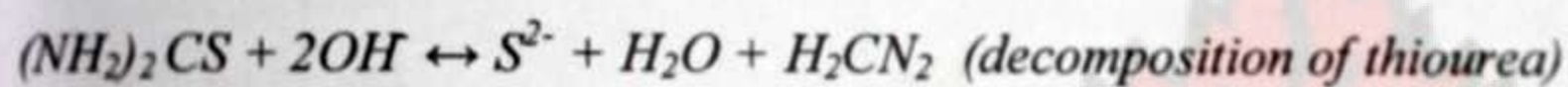
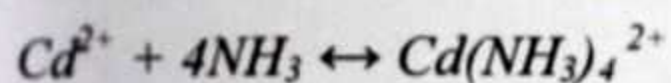
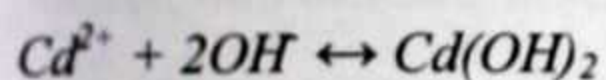
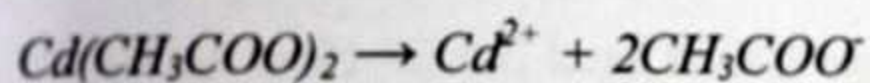
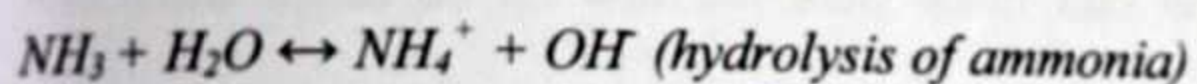
Thiourea has been used for a long time as an analytical reagent to precipitate metal sulphides. Thiourea is frequently chosen as the sulphide ion source for metal sulphides over a wide range of pH and is often used as a precursor for CBD in mildly alkaline solutions.



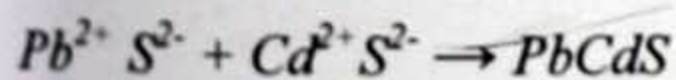
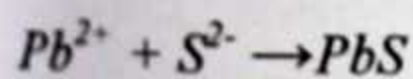
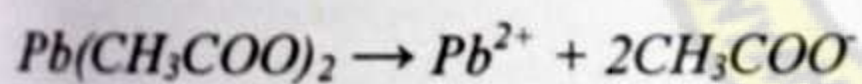


#### 4.4.2 DECOMPOSITION OF LEAD AND CADMIUM ACETATE

The reaction taking place is typically as follows;



The lead acetate salt equally goes through the same decomposition process as the cadmium acetate.





4.5 SAMPLE PREPARATION

The deposition steps start with mixing lead and cadmium acetate with ammonia. The solution was made up to 80 ml with distilled water and heated up to 50 °C. The glass substrate was immersed vertically and then 20 ml thiourea was added drop by drop and the bath was slowly heated up to 75 °C and kept at this temperature for 75 minutes. Then substrates were taken out, washed with distilled water and dried.

Table 4.1 summarizes the deposition conditions

Compostion factor (x)	[Pb(CH <sub>3</sub> COO) <sub>2</sub> .2H <sub>2</sub> O] /ml	[Cd(CH <sub>3</sub> COO) <sub>2</sub> .2H <sub>2</sub> O] /ml	[(NH <sub>2</sub> ) <sub>2</sub> .CS] /ml	NH <sub>3</sub> / ml	Distilled water /ml
0.10	0.20	2.00	20.0	35.0	22.80
0.15	0.44	2.00	20.0	35.0	22.56
0.20	0.70	2.00	20.0	35.0	22.30
0.25	1.00	2.00	20.0	35.0	22.00
0.30	1.32	2.00	20.0	35.0	21.68

Figure 4.1 below shows a simplified diagram of a typical chemical bath.





Figure 4.1: Schematic diagram of the experimental set up

#### 4.6 MEASUREMENT OF THE ABSORPTION SPECTRA

Absorption spectra are usually registered by instruments known as spectrophotometers. Figure 4.2 shows a schematic diagram with the main elements of the simplest spectrophotometer. Basically, it consists of the following components: (i) a light source (usually a deuterium lamp for the UV spectral range and a tungsten lamp for the VIS and IR spectral ranges) that is focused on the entrance to (ii) a monochromator, which is used to select a single wavelength (frequency) from all of those provided by the lamp source and to scan over a desired frequency range. (iii) a sample holder, followed by (iv) a light detector, to measure the intensity of each monochromatic



beam after traversing the sample and finally (v) a computer, to display and record the absorption spectrum (Sole et al., 2005).

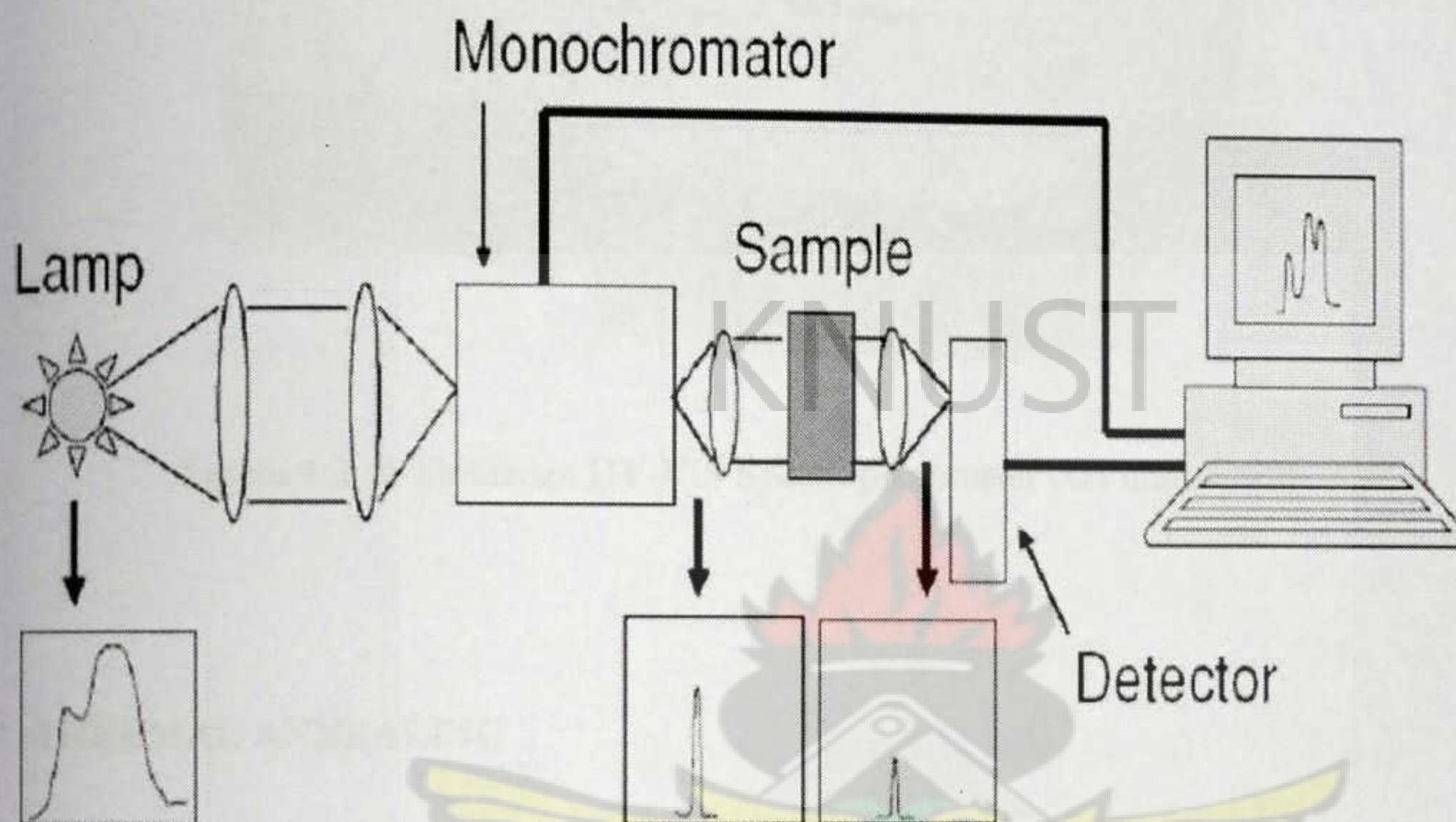


Figure 4.2: Schematic diagram of a single-beam spectrophotometer.

In this work, optical absorption spectra were recorded using a Shimadzu UV-VIS spectrophotometer (UVmini-1240) within the wavelength region of 900 – 200nm as indicated in Figure 4.3. The spectrophotometer also had attached a computer unit which made it possible to copy the absorbance reading for further analysis. A blank treated glass slide was initially scanned and used for baseline correction.





Figure 4.3: A Shimadzu UV-VIS Spectrophotometer (UVmini-1240)

#### 4.7 THERMAL ANNEALING

Annealing involves heating a material to above its critical temperature or maintaining a suitable temperature, and then cooling. Annealing can improve the crystallinity, reduce the structural imperfections and enlarge the grain size. The thin films were put in a tray, placed in a carbolite furnace and heated at temperatures of 200 °C and 300 °C for 75 minutes after which the furnace was switched off and allowed to cool to room temperature. The samples were then removed and again characterized by the same techniques.



#### 4.8 X-RAY DIFFRACTION MEASUREMENTS

There are many variables which affect the crystal structure of thin films, including the nature of the complex, the substrate and sometimes even stirring (Dekker,2002). X-ray diffraction studies were performed to study the crystal structure of the films, using secondary graphite monochromated Cu-K $\alpha$  radiation ( $\lambda = 0.15418$  nm) source over the diffraction angle  $2\theta$  between  $3^\circ$  and  $80^\circ$ , on a Brucker D8 powder X-Ray Diffractometer (40 kV, 40 mA) in Manchester. The scan time for each sample was three hours.

The penetration depth of an X-ray beam is typically a few tens of microns. In fact, polycrystalline films in this thickness range are quite easy to deal with using a regular powder diffractometer. Below one micron, the signal from the film can be seriously obscured by the signal from the substrate. At 100 nm, the signal from the film may be only 1% of the signal from the substrate and that approaches the limit of sensitivity of powder diffraction (Ryan, 2001). As 10 nm thickness is reached, things only get worse. Not only is the signal a factor of ten smaller, but diffraction broadening makes the diffraction peaks wider and peak intensities drop rapidly. The depth of penetration into the sample is given by the absorption length times the sine of the incidence angle. Since most of the diffraction peaks from a typical sample material lie in the region of  $20^\circ$  to  $100^\circ$ ,  $2\theta$  incidence angles are typically in the range of  $(30 \pm 20)^\circ$ . If the sample is a thin layer, most of the X-ray beam passes through the film and is scattered by the substrate. The technique in thin-film XRD is to choose an X-ray diffraction geometry that allows you to work at very small angles of incidence, increasing the path length of the X-rays in the film and reducing the amount of X-rays that penetrate through to the substrate. An incidence angle of  $6^\circ$  reduces the penetration depth by a factor of 10; an incidence angle of  $0.6^\circ$  leads to reduction by a



factor of 100 (Ryan, 2001). In this work a glancing angle of  $3^\circ$  was chosen since below this angle the resolution of the diffractometer was much reduced.

# KNUST





## CHAPTER FIVE

### 5.0 RESULTS AND DISCUSSION

#### 5.1 RESULTS OF THE OPTICAL ABSORPTION SPECTRA

In order to understand the optical behaviour of films, one must become familiar with the optical constants of materials, their origins; magnitudes and how they depend on the way films are processed. The unifying concept that embraces all optical properties is the interaction of electromagnetic radiation with the electrons of the material. The most direct and probably the simplest method of investigating the band structure of semiconductors is to measure the absorption spectrum.

The optical absorption spectra of the various deposited films were obtained and analyzed over wavelength range from 200 nm to 900 nm at room temperature using a Shimadzu UV-VIS Spectrophotometer (UV mini 1240). Figure 5.1, shows the optical absorption spectrum for  $\text{Pb}_x\text{Cd}_{1-x}\text{S}$  ( $0.1 \leq x \leq 0.3$ ) as-deposited thin films. Although the absorbance was measured within the wavelength range of 200 nm to 900 nm, the axis has been formatted to show the absorbance within the visible range of 350 nm to 750 nm because the band gap of the ternary thin film  $\text{Pb}_x\text{Cd}_{1-x}\text{S}$  lies within this range. The appearance of wiggles near the short wavelength (high photon energy region) may be attributed to the disorder that is caused by an increase in the composition of  $\text{Pb}^{2+}$  ions, the effect of which on the electronic states have been discussed by Anderson (1958) and Mott (1968, 1969, 1970).



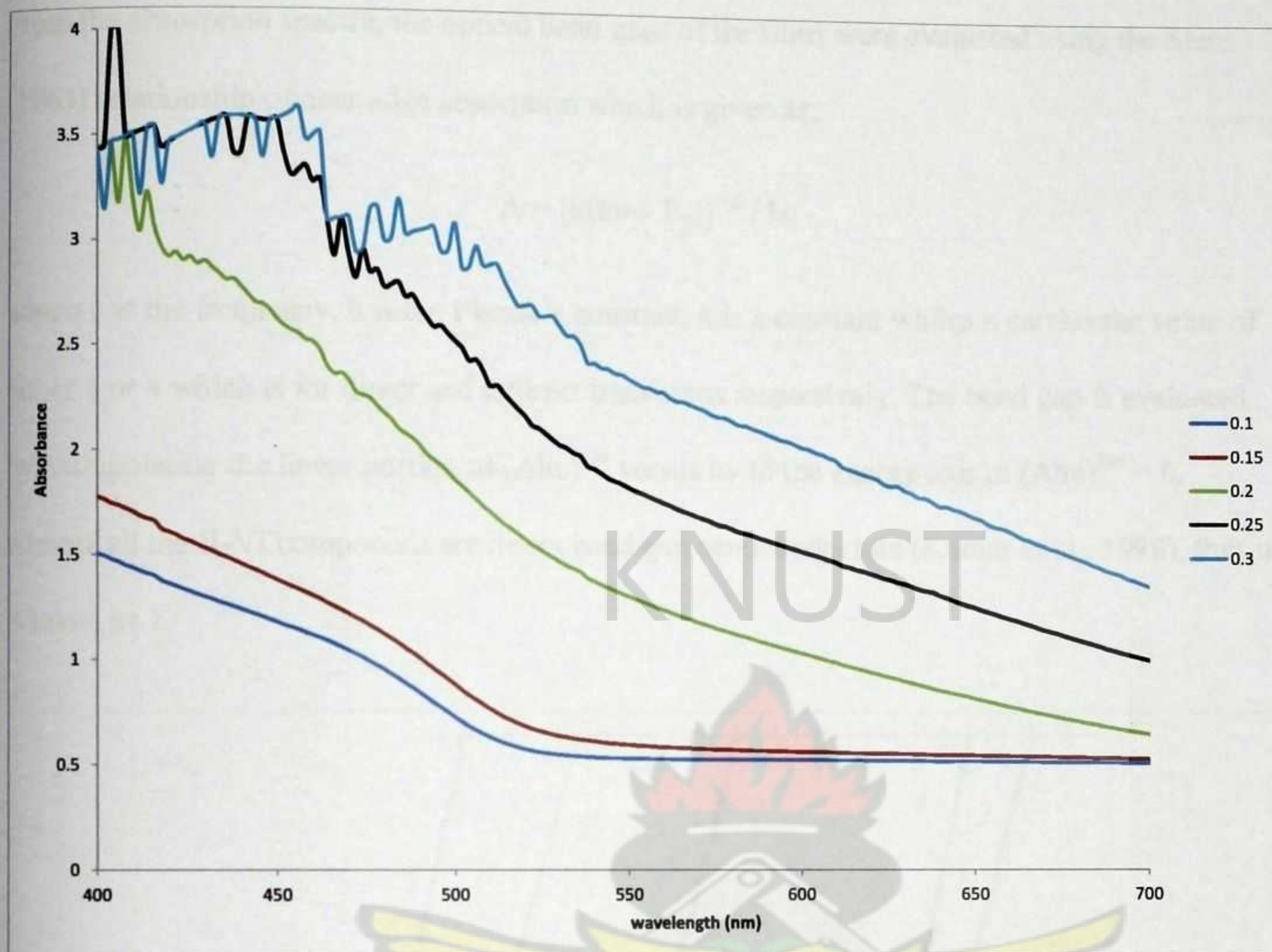


Figure 5.1: A plot of absorbance versus wavelength for  $\text{Pb}_x\text{Cd}_{1-x}\text{S}$  ( $0.1 \leq x \leq 0.3$ ) as-deposited thin films.

## 5.2 DETERMINATION OF THE OPTICAL BAND GAP

The electronic energy band parameters of semiconductor alloys and their dependence on alloy composition are very important. The energy band gap of a ternary alloy is dependent on the relative concentration of the constituent elements.



From the absorption spectra, the optical band gaps of the films were evaluated using the Stern (1963) relationship of near edge absorption which is given as;

$$A = [k(h\nu - E_g)]^{n/2} / h\nu$$

where  $\nu$  is the frequency,  $h$  is the Planck's constant,  $k$  is a constant while  $n$  carries the value of either 1 or 4 which is for direct and indirect transitions respectively. The band gap is evaluated by extrapolating the linear portion of  $(A h \nu)^{2/n}$  versus  $h \nu$  to the energy axis at  $(A h \nu)^{2/n} = 0$ .

Almost all the II-VI compounds are direct band gap semiconductors (Kumar et al., 1998), thus  $n$  is taken as 1.

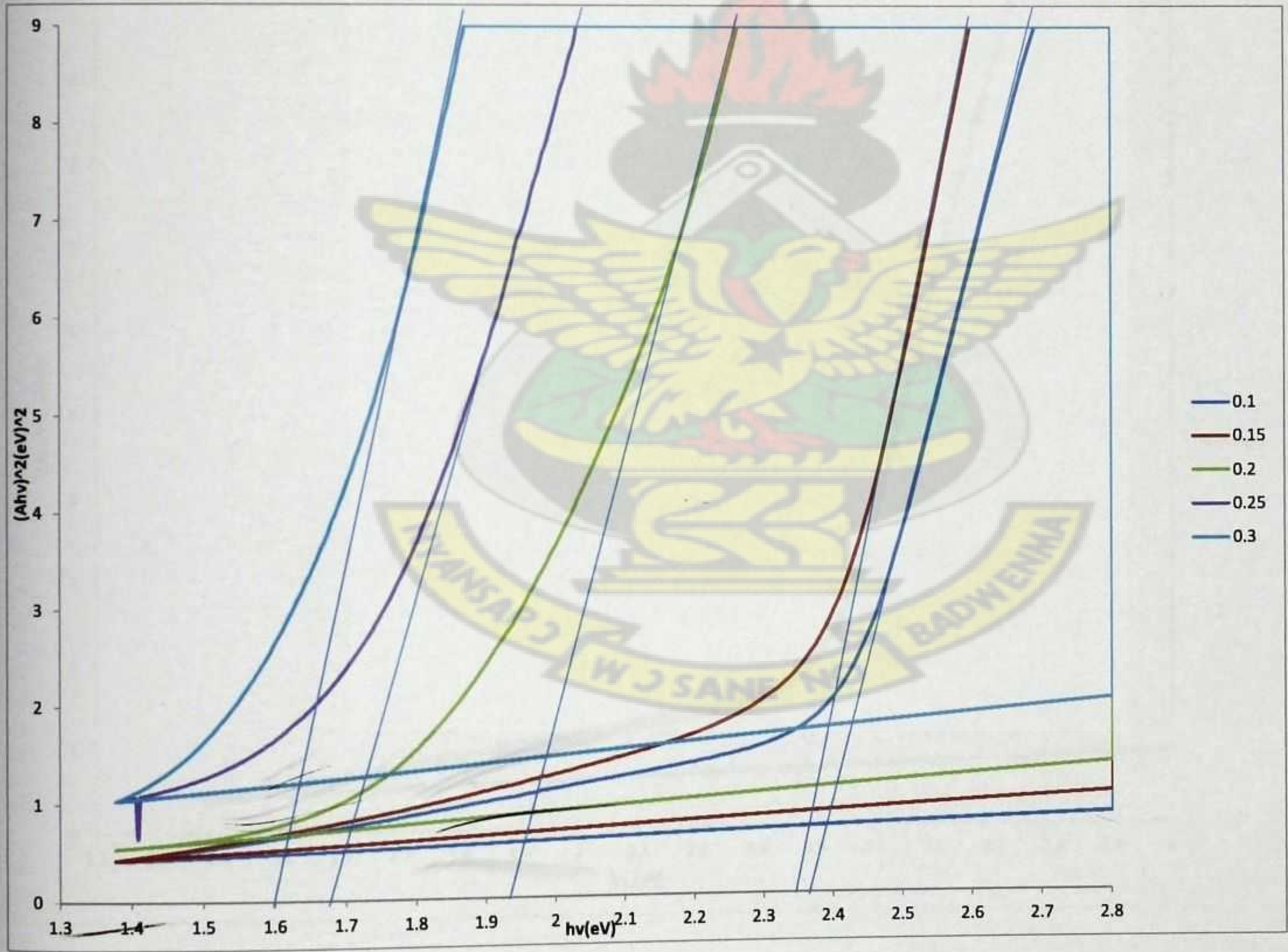


Figure 5.2: Plot of  $(A h \nu)^2$  versus  $h \nu$  for  $Pb_xCd_{1-x}S$  ( $0.1 \leq x \leq 0.3$ ) as- deposited thin films.



Figure 5.2 above shows the band gap of  $\text{Pb}_x\text{Cd}_{1-x}\text{S}$  ( $0.1 \leq x \leq 0.3$ ) thin films. The optical band gap of pure CdS is found to be 2.47 eV and decreases continuously down to 0.49 eV for PbS as the composition parameter 'x' is increased (Mohammed et. al, 2009). For this particular research the bandgap decreases monotonically from 2.36eV to 1.60eV as the composition of Pb is increased from 0.1 to 0.3. and this phenomenon can be attributed to the alloying of PbS and CdS, in agreement with the behavior shown previously by Skyllas-Kazacos et al. (1985). The other compositions have band gap between these values.

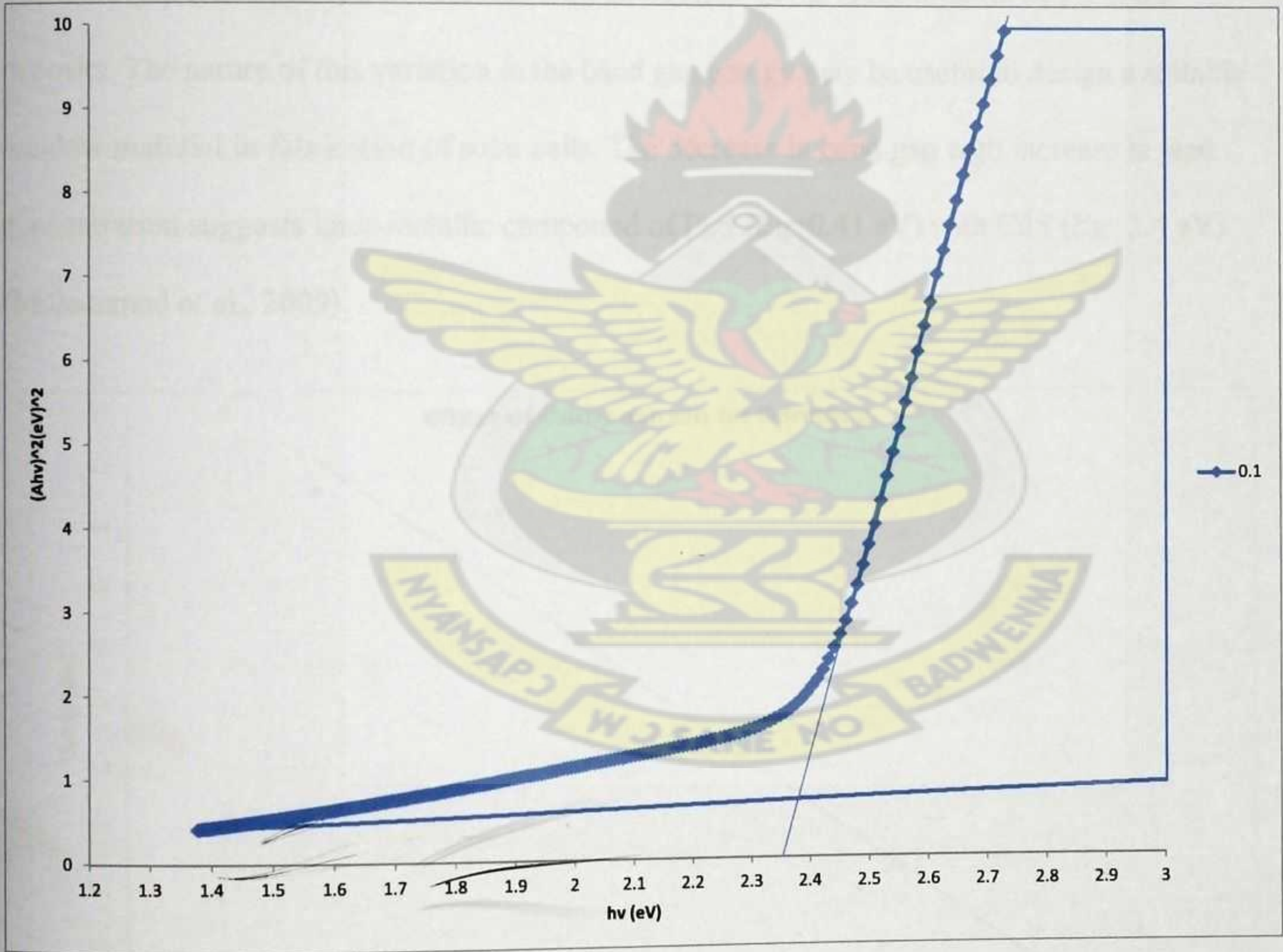


Figure 5.3: : Plot of  $(Ahv)^2$  versus  $h\nu$  for  $\text{Pb}_{0.1}\text{Cd}_{0.9}\text{S}$



Figure 5.3 above gives the band gap of the as-deposited  $\text{Pb}_{0.1}\text{Cd}_{0.9}\text{S}$ . The value obtained for the band gap is 2.36 eV which is close to the literature value of 2.47 eV (Barote et al., 2011). The marginally lower band gap value obtained in figure 5.3 could be ascribed to the presence of defect states in the band gap. The band gap of a semiconductor is affected by the residual strain, defects, charged impurities, disorder at the grain boundaries and also particle size confinement (Ramasamy, 2011).

The variation of band gap with the composition(x) is displayed in Figure 5.4 below. It is observed that small amount of Pb present in the films greatly affects the optical band gap of CdS. The band gap was observed to decrease with an increase in the concentration of Pb in the deposits. The nature of this variation in the band gap energy may be useful to design a suitable window material in fabrication of solar cells. The decrease in band gap with increase in lead concentration suggests inter-metallic compound of PbS ( $E_g=0.41$  eV) with CdS ( $E_g=2.4$  eV) (Mohammed et al., 2009).

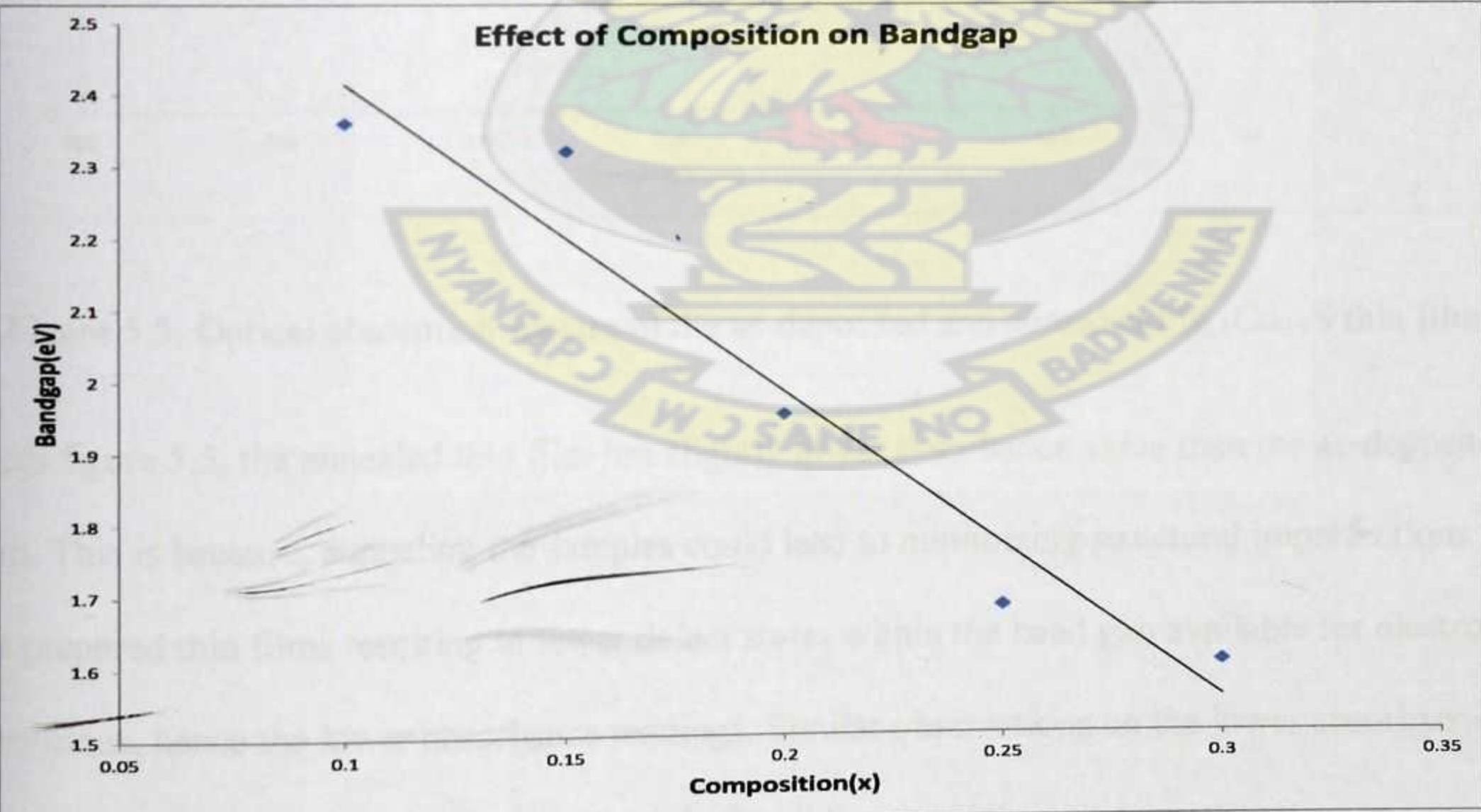


Figure 5.4 : A plot of band gap energy (eV) against composition (x)



### 5.3 EFFECT OF THERMAL ANNEALING ON THE OPTICAL PROPERTIES

The optical absorption spectra for the as-deposited and annealed PbCdS thin film is shown in Figure 5.5.

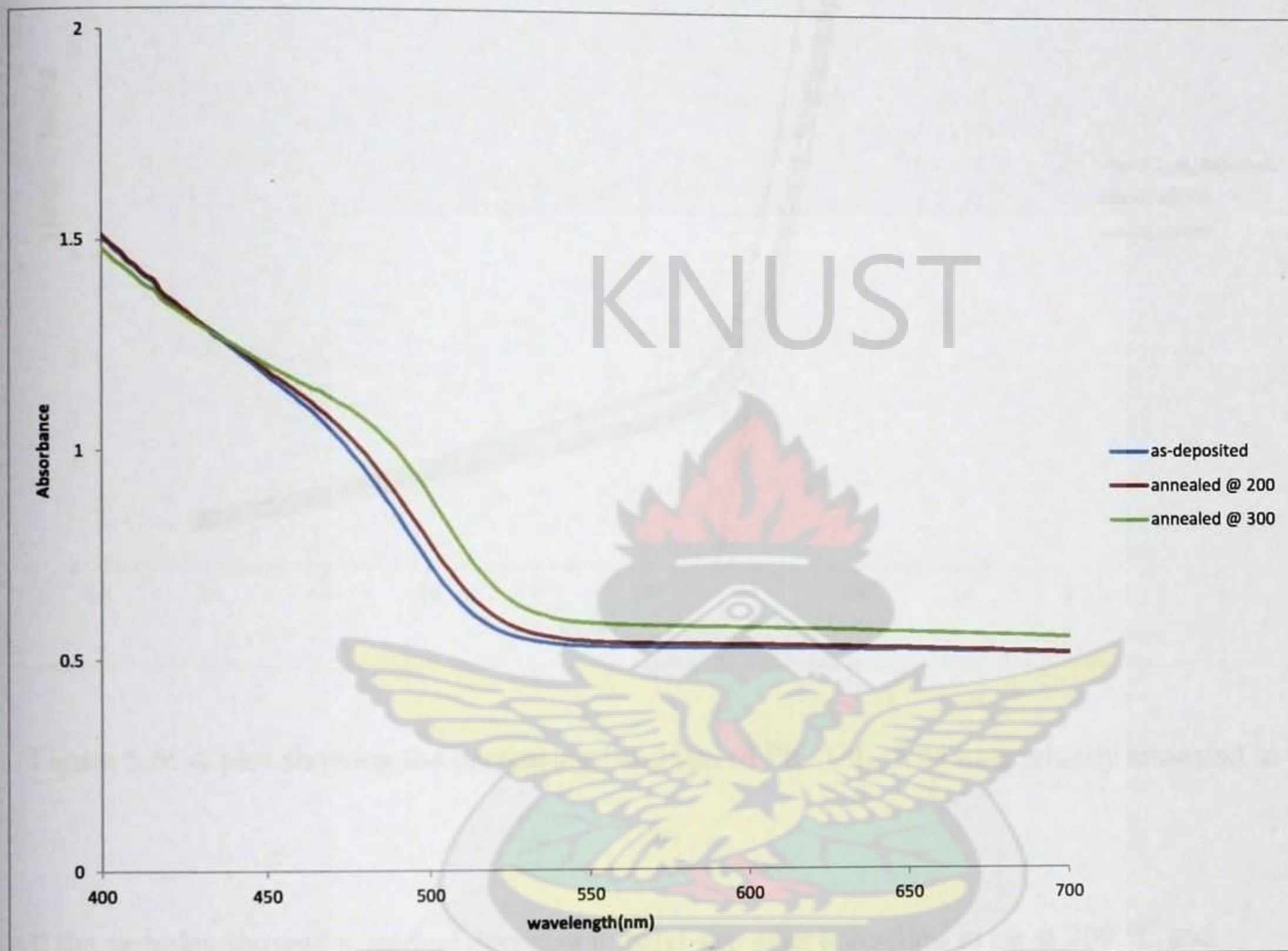


Figure 5.5: Optical absorption spectra of the as-deposited and annealed Pb<sub>0.1</sub>Cd<sub>0.9</sub>S thin film

From figure 5.5, the annealed thin film has slightly lower absorbance value than the as-deposited film. This is because, annealing the samples could lead to minimizing structural imperfections in the prepared thin films resulting in fewer defect states within the band gap available for electron transitions, hence the lower absorbance readings. Similar observations on the lower absorbance readings of the annealed thin films were made for all the samples.



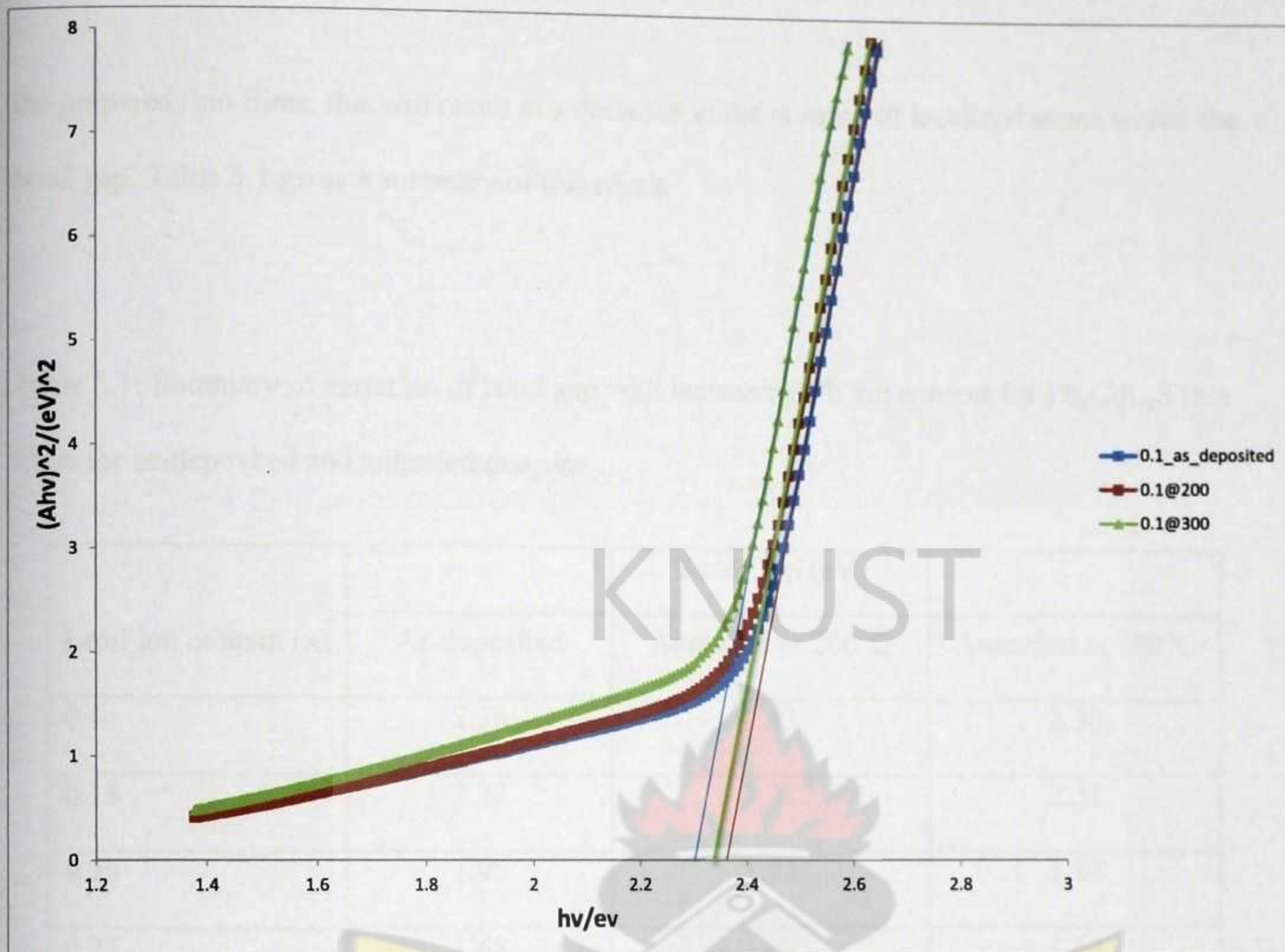


Figure 5.6: A plot showing the decreasing band gap of  $\text{Pb}_{0.1}\text{Cd}_{0.9}\text{S}$  as its gradually annealed in air.

All the samples showed a gradual decrease in band gap after annealing in air at 200 °C and 300 °C for 75 minutes. The decreased band gap of the films after annealing may be due to improvement in the structure, i.e., improving crystallinity or alternatively, a phase transformation taking place in the samples as a result of the heat treatment. Again, an increase in grain size after annealing could also cause a decrease in the band gap of the sample. Mott and Davis (1979), explained that the presence of high density of localized states in the band structure is responsible for the lower energy band gap. Annealing leads to improving the order of the atoms constituting



the prepared thin films, this will result in a decrease in the number of localized states within the band gap. Table 5.1 gives a summary of this result.

Table 5.1: Summary of variation of band gap with increasing Pb ion content for  $Pb_xCd_{1-x}S$  thin films for as-deposited and annealed samples.

Lead ion content (x)	Band Gap (eV)		
	As-deposited	Annealed at 200°C	Annealed at 300°C
0.1	2.36	2.33	2.30
0.15	2.32	2.31	2.31
0.20	1.95	1.93	1.84
0.25	1.68	1.67	1.64
0.3	1.60	1.59	1.58

It is worth noting here that the band gap can differ slightly depending on the method employed for the film deposition (Padam et al., 1988).



## 5.4 X-RAY DIFFRACTION PATTERNS OF THE THIN FILMS

The figures below show the x-ray diffraction pattern of the thin films. The horizontal axis of the graph is  $2\theta$ , twice the Bragg angle. The vertical axis is the intensity/X-ray count rate, this is a function of the crystal structure and the orientation of the crystallites. The space between diffracting planes of atoms determines peak positions. The peak intensity is determined by the type of atoms that are in the diffracting plane.

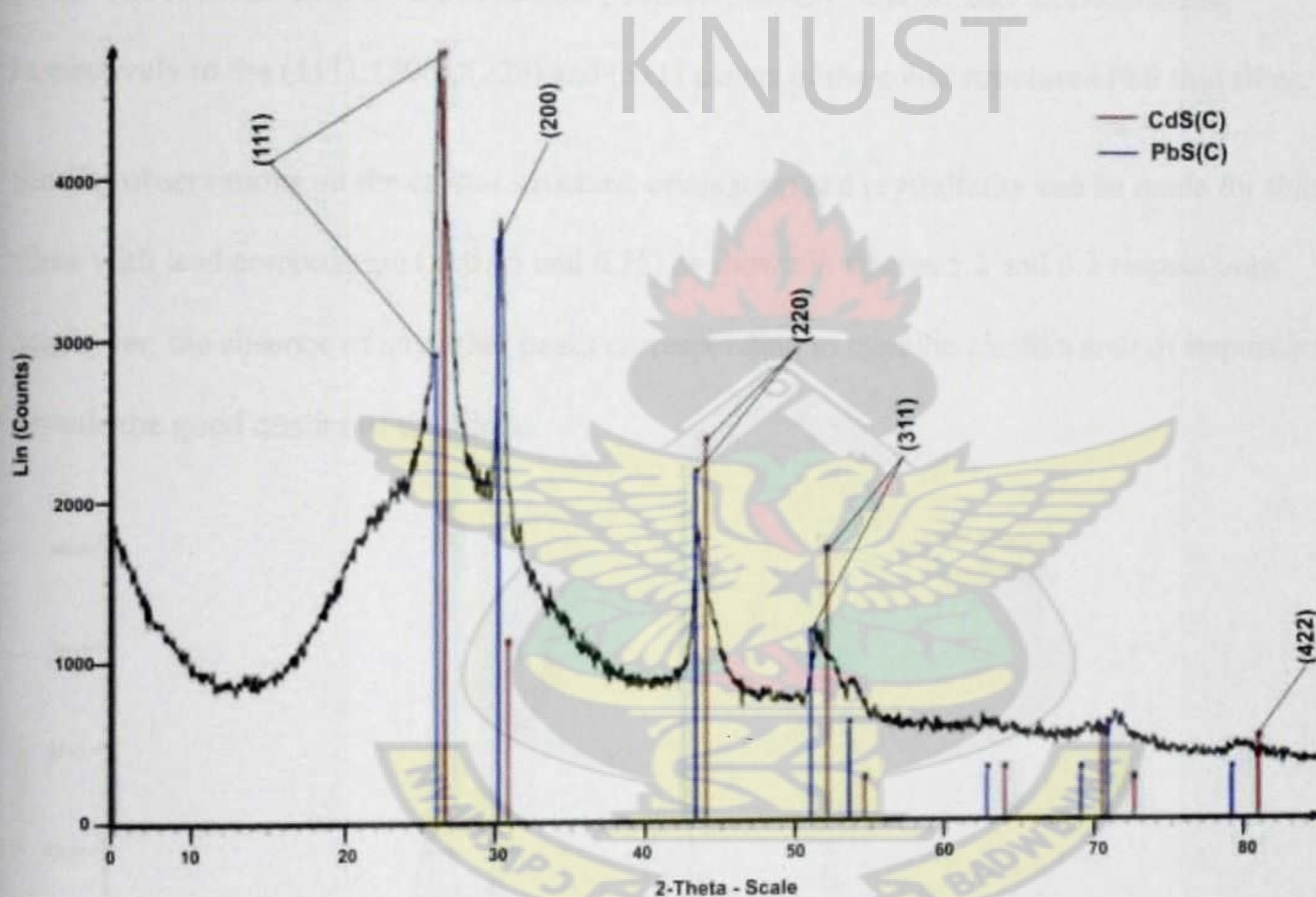


Figure 5.7: X-ray diffraction pattern of  $\text{Pb}_{0.1}\text{Cd}_{0.9}\text{S}$  (as-deposited)

The X-ray diffraction patterns of the  $\text{Pb}_{0.1}\text{Cd}_{0.9}\text{S}$  thin film is shown in Figure 5.7. The broad hump in the range  $20^\circ \leq 2\theta \leq 35^\circ$  is due to the glass substrate (Li et al., 2010). The presence of large number of peaks indicates that the films are polycrystalline in nature with cubic and hexagonal structure (Gorer and Hodes, 1994). The x-ray diffraction results show that the films



are of PbS-CdS composite with individual CdS and PbS planes. The diffraction patterns are compared with standards from the JCPDS data files with reference code, 00-010-0454. The reflection peaks at  $26.200^\circ$ ,  $44.221^\circ$ ,  $52.340^\circ$  and  $80.042^\circ$  correspond respectively to the (111), (220), (311) and (422) planes of the cubic structured CdS thin films.

Also peaks were identified for the PbS thin films and the corresponding diffraction patterns were compared with standards from the JCPDS data files with reference code, 00-02-1431. The observed reflection peaks were at  $26.200^\circ$ ,  $30.271^\circ$ ,  $43.491^\circ$  and  $50.206^\circ$  corresponding respectively to the (111), (200), (220) and (311) planes of the cubic structured PbS thin films.

Similar observations on the crystal structure, orientation and crystallinity can be made for thin films with lead composition ( $x=0.15$  and  $0.25$ ) as shown in figures 5.2 and 5.3 respectively.

Moreover, the absence of any other peaks corresponding to metallic clusters and/ or impurities reveals the good quality of the films.

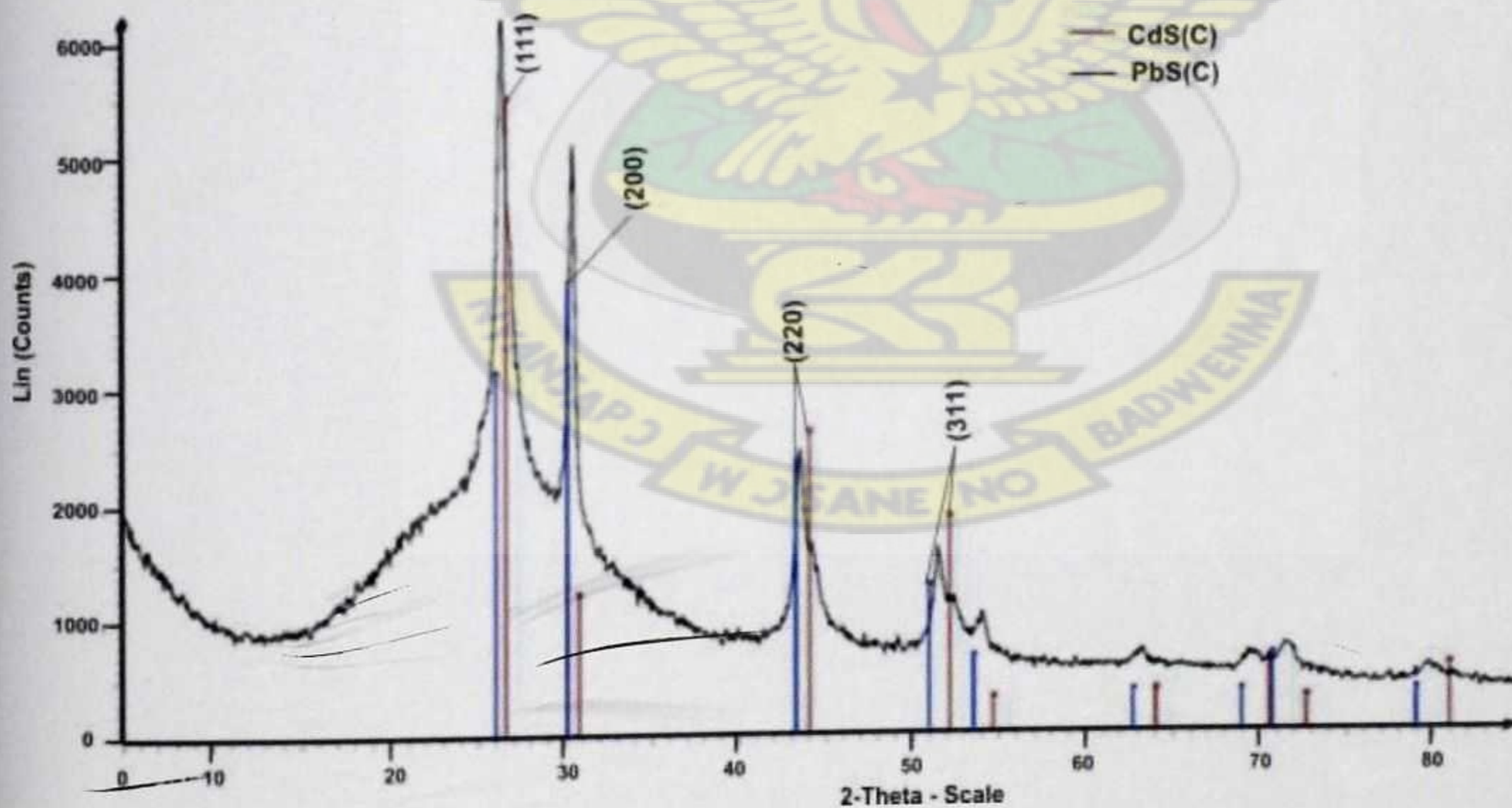


Figure 5.8: X-ray diffraction pattern of  $\text{Pb}_{0.15}\text{Cd}_{0.85}\text{S}$  (as-deposited)



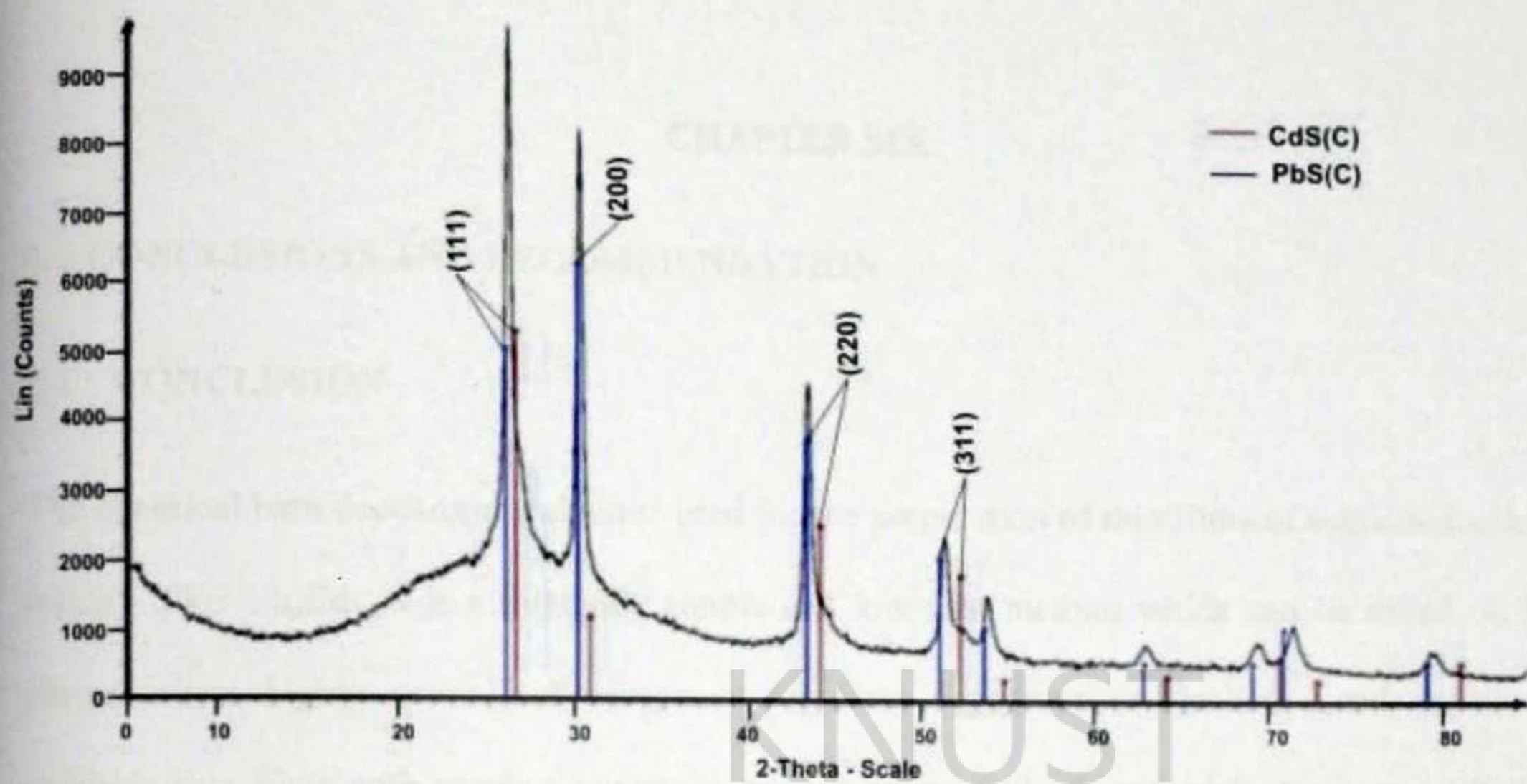


Figure 5.9: X-ray diffraction pattern of  $\text{Pb}_{0.25}\text{Cd}_{0.75}\text{S}$  (as-deposited)



## CHAPTER SIX

### 6. CONCLUSIONS AND RECOMMENDATION

#### 6.1 CONCLUSION

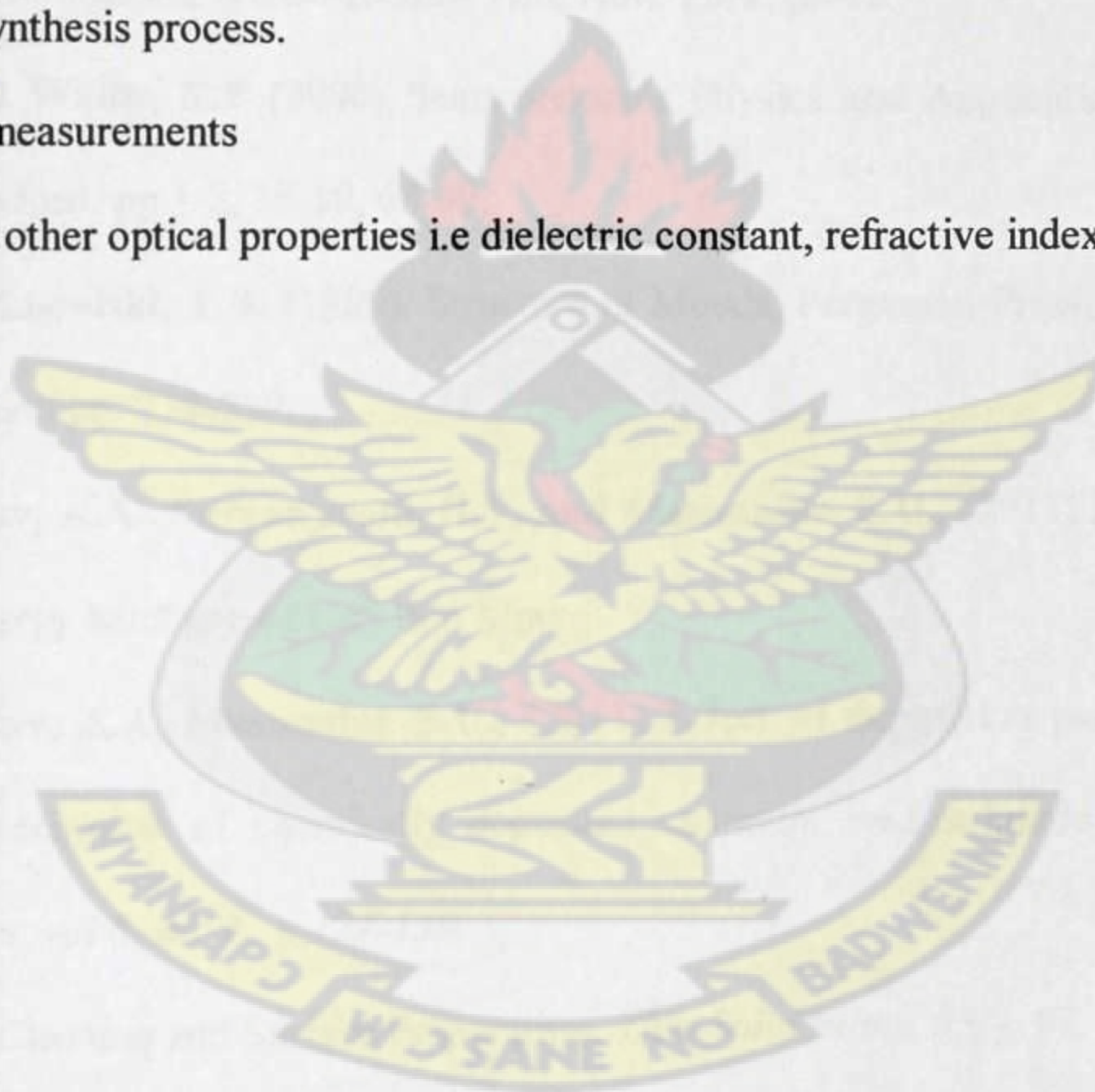
The chemical bath deposition technique used for the preparation of thin films of semiconducting ternary alloy  $\text{Pb}_x\text{Cd}_{1-x}\text{S}$  is a relatively simple and low cost method which can be relied on in places where highly specialized equipment for films deposition are lacked. Lead cadmium sulphide thin films with varying composition were successfully deposited from chemical baths containing lead acetate, cadmium acetate, thiourea and ammonia (as the basic medium). The thin films obtained using this method were smooth, uniform adherent bright yellow in color and changed to black with increasing lead content. The crystal structure was studied using powder X-ray diffraction (XRD). Optical absorption spectroscopy was used to investigate some of the optical properties of the films. The films were annealed in air at 200 °C and 300 °C for 75 minutes and the effect of annealing on the optical structure were studied. X-ray diffraction analysis of the thin films over the entire composition range ( $0.3 \leq x \leq 0.1$ ) showed that all the compositions exhibited the cubic phase of the CdS and PbS thin film. The band gap analysed from optical absorption spectroscopy varied linearly with composition between that of CdS (2.36 eV) and PbS (1.60 eV) for the as-deposited samples whiles the annealed at 300°C samples varied from (2.30 eV) for CdS to (1.58 eV) for PbS. The decrease in band gap after thermal annealing is an indication of improved crystallinity in the samples.



## 6.2 RECOMMENDATIONS

$\text{Pb}_x\text{Cd}_{1-x}\text{S}$  thin films with varying composition were successfully deposited on glass substrate from alkaline chemical baths. However, before this material can be used in device applications, further studies and research has to be conducted in the following areas:

- i. Photoconductivity measurements
- ii. Photoluminescence studies to investigate trap states.
- iii. X-ray photoelectron spectroscopy to investigate the possibility of oxide insertion during the synthesis process.
- iv. Hall Effect measurements
- v. Study of the other optical properties i.e dielectric constant, refractive index





## REFERENCES

1. **Adachi, S.** Cited in Singh, J. and Shimakawa, K., (2003). *Advances in Amorphous Semiconductors*, CRC Press, New York, pp 56.
2. **Adachi, S.**, (2009) *Properties of Semiconductor Alloys: Group-IV, III-V and II-VI semiconductors*, John Wiley & Sons.
3. **Advincula, R. and Knoll, W.**, (2011). *Functional Polymer Films*, Editors – Wiley.
4. **Anderson, F.** Cited in Mahajan, S. and Sree Harsha, K.S. (1999). *Principles of Growth and Processing of Semiconductors*, WCB/McGraw Hill, New York, pp 12.
5. **Balkanski, M. and Wallis, R.F** (2000) *Semiconductor Physics and Applications*. Oxford University Press. Oxford. pp.1-2, 18-19, 68-69.
6. **Barett, C.S. and Massalski, T.B.** (1980). *Structure of Metals*, Pergamon Press, New York, Third (revised) Edition pp. 238-239.
7. **Barote, M.A. Yadav, A.A. Suryawanshi, R.V. and Masumdar, E.U.**, (2011) Effect of Pb incorporation on energy band gap of CdS thin films.
8. **Barote, M.A. Yadav, A.A. Masumdar E.U.**, (2011) Effect of deposition parameters on growth and characterization of chemically deposited cadmium lead sulphide thin films, *Chalcogenide letters*, vol 8, no. 2 , p.129-138.
9. **Beal, S.E.**, (1978). Cleaning and Surface Preparation, *Thin Solid Films*, 53, p 97.
10. **Bindu, K. Lakshmi, M. Bini, S. Sudha Kartha, C. Vijayakumar, K. P. Abe, T. and Kashiwaba, Y.** (2002) Amorphous selenium thin films prepared using chemical bath deposition: optimization of the deposition process and characterization. *Semiconductor Science and technology*,. 17: p. 270-274.



11. Bindu, K. Kartha, C. S. Vijayakumar, K. P. Abe, T. and Kashiwaba, Y., (2003) CuInSe<sub>2</sub> thin film preparation through a new selenisation process using chemical bath deposited selenium. *solar Energy Materials and Solar Cells*,. 79: p. 67-79.
12. Bindu, K. Sudha Kartha, C. Vijayakumar, K. P. Abe, T. and Kashiwaba Y., (2002) structural, optical and electrical properties of In<sub>2</sub>Se<sub>3</sub> thin films formed by annealing chemically deposited Se and vacuum evaporated In stack layers. *Applied Surface Science*,. 191: p. 138-147.
13. Boakye, F. and Nusenu, D., (1996). The Energy Band Gap of cadmium sulphide, *Solid state Communication*, 102, 4, pp 323-326.
14. Bouroushian, M. Loizos, Z. Spyrellis, N. and Maurin G. Cited in Chavan, S.D. Senthilarasu, S. and Soo-Hyoung Lee, (2008). Annealing effect on the structural and optical properties of a Cd<sub>1-x</sub>Zn<sub>x</sub>S thin film for photovoltaic applications, *Applied Surface Science*, 254, pp 4539-4545.
15. Busch, G., (1983) "Early history of the physics and chemistry of semiconductors – from doubts to fact in a hundred years", *Eur. J. Phys.*, vol. 10, no. 4, pp. 254–263.
16. Cardoso, J. GomezDaza, O. Ixtilco, L. Nair, M. T. S. and Nair, P. K., (2001) Conductive copper sulfide thin films on polyimide foils. *Semiconductor Science and Technology*,. 16: p. 123-127.
17. Chopra, K.L. and Das, S.R., (1983) thin film solar cells, plenum press, New York.
18. Chopra, K.L. Kainthla, R. C. Pandya, D. K. and Thakoor, A. P., (1982) Chemical solution deposition of inorganic films, in *Physics of Thin Films*, G. Hass, Editor. 1982, Academic Press: New York. p. 167-235.



19. **Chopra, K.L. Kainthla, R.C. Pandya, D.K. and Thakoor, A.P.**, (1982). Chemical solution deposition of inorganic films. In: Hass, G. (Editor) *Physics of Thin Films*, Academic Press, New York, pp 167-235.
20. **Chopra, K.L. Paulson P.D. and Dutta V.**, (2004). Thin film Solar cells: An Overview, *Prog. Photovolt, Res. Appl.*, 12 pp 69-92.
21. **Chopra, K.L.**, (1969) *Thin Film Phenomena*, McGraw Hill, New York.
22. **Choudhary, S. Dolui, S.K. Avasthi, D.K. and Choudhary, A.**, (2005) *Indian J. Phys.* 79, 1019.
23. **Cody, G.D.**, (1984). *Semiconductors and Semimetals*, Academic Press, New York, 21, pp 11-14.
24. **Cohen M.H., Fritzsche H. and Ovshinski S.R.**, (1969) "Simple band model for amorphous semiconductor alloys", *Physical Review Letters*, 22, 1065-1072.
25. **Cullity, B. D.**, (1978) *Element of X-ray Diffraction*, Addison – Wesley Publishing Company Inc., Massachusetts.
26. **Das, V.D. and Bhat, K.S.**, (1990) *J. Mater. Sci.* 7, pg 169.
27. **Deshmukh, L.P. More, B.M. Holikatti, S.G. and Hankare, P.P.**, (1994) *Bull. Mater. Sci.* 17 455.
28. **Dunlap, W.C.**, (1961) Recent Developments in Semiconductors, *J. Chem. Educ.* No.5, 38, 238-241.
29. **Eckertova, L.**, (1977) *physics of thin films*.
30. **Elabd, H. and Steckl, A.J.**, (1980) *J. Appl. Phys.* 51(1), 726.
31. **Elango, T. Subramanian, S. and Murali, K.R.**, (2003) *Surf. Coat. Technol.*, pg 123, 8.
32. **Format, M. and Lincot, D.**, (1995) *Electrochim. Acta*, 40, 1293.



33. **Gadave, K.M. and Lokhande, C.D.** (1993) Formation of CuxS films through a chemical bath deposition process. *Thin Solid Films*,. 229: p. 1-4.
34. **Gellings, P.J. and Bouwmeester, H.J.M.**, (1997). The CRC Handbook of Solid State Electrochemistry, CRC Press, p 84.
35. **Gorer, S. and Hodes, G.** Cited in Hodes, G., (2002). Chemical Solution Deposition Mechanisms of semiconductor films, *Journal of Physical Chemistry*, 98, pp 533-5346.
36. **Grozdanov, I. Barlingay, C.K. and Dey, S.K.**, (1995) Novel applications of chemically deposited CuxS thin films. *Materials Letters*,. 23: p. 181-185.
37. **Grozdanov, I., Barlingay, C.K. Dey, S.K. Ristov, M. and Najdoski M.**, (1994) Experimental study of the copper thiosulfate system with respect to thin-film deposition. *Thin Solid Films*,. 250: p. 67-71.
38. **Hankare, P.P. Delekar, S.D. Asabe, M.R. Chate, P.A. Bhuse, V.M. Khomane, A.S. Garadkar, K.M. and Sarwade, B.D.**, (2006), Synthesis of CdSe thin films by simple chemical route and their characterization: *J. of Physics & chem of solids*, 67, pp 2506.
39. **Hodes, G.**, (2002) Chemical Solution Deposition of Semiconductor Films., New York: Marcel dekker, Inc. pp.2-3.
40. **Hogan, M. C.**, (2011). Sulfur. Encyclopedia of Earth, eds.
41. <http://mrsec.wisc.edu/Edetc/background/LED/>.
42. <http://www.southampton.ac.uk/~engmats/xtal/crystal/crystalline.html>.
43. **Hu, H. and Nair, P.K.**, (1996) Electrical and optical properties of poly(methyl methacrylate) sheets coated with chemically deposited CuS thin films. *Surface and Coatings Technology*,. 81: p. 183-189.



44. **Jagodzinski, H.** Cited in Boakye, F. and Nusenu., (1996). The Energy Band Gap of cadmium sulphide, *Solid State Communication*, 102, 4, pp323-326.
45. **Joachim, P et al.**, (2004) *Sensors* 4, pp.156.
46. **Joshi, R.K. Kanjilal, A. and Sehgal, H.K.**, (2004) *Appl. Surf. Sci.* 221,pg 43.
47. **Juster, N. J.**, (1963) Conduction and Semi conduction, *J. Chem. Educ.* No.9, 40, 489-496.
48. **Kanazawa, H. and Adachi, S.**, (1998) *J. Appl. Phys.* 83, 5997.
49. **Kasap S.O.**, "Photoreceptors: The Chalcogenides, Handbook of Imaging Materials Second Edition Revised and Expanded edited by Arthur S. Diamond and David S. Weiss", Marcel Dekker Inc., New York, 329-369, 2002.
50. **Kaur, I., Pandya, D.K. and Chopra, K.L.**, (1980) Growth kinetics and polymorphism of chemically deposited CdS films *Journal of the Electrochemical Society*, 1980. 127: p. 943-948.
51. **Kitaev, G. A. Uritaskaya, A. A. and Moksushin, S. G.** (1965) *Russ. J. Phys. Chem.* 39, 1101.
52. **Kittel, C.**, (2005). Introduction to Solid State Physics, Eighth Edition, John Wiley & Sons, Inc. p. 577.
53. **Korvink, J.G. and Greiner, A.**, (2002).Semiconductors for Micro and Nanosystems Technology, WILEY-VCH Verlag GmbH, Weinheim, ISBN 3-527-30257-3, pp 15-16.
54. **Kumar, V. Singh, V. Sharma, S.K. and Sharma, T.P.**, (1998). Structural and Optical Properties of Sintered CdZnS Films *Optical Materials*, 11, pp 29-34.
55. **Kunita, M.H., Girotto, E.M Radovanovic, E. Goncalves, M.C. Ferreira, O.P. Muniz, E.C. and Rubira, A.F.**, (2002) Deposition of copper sulfide on modified low-density



- polyethylene surface: morphology and electrical characterization. *Applied Surface Science*, 202: p. 223-231.
56. **Laeri, F. Schüth, F. Simon, U. and Wark, M.**, (2003) Host-Guest-Systems Based on nanoporous Crystals. Weinheim: Wiley, pp. 435–436.
57. **Li, S.S.**, (2006). Semiconductor Physical Electronics, Second Edition, pp.246-253, p.335.
58. **Li, Z.Q. Shi, J.H. Liu, Q.Q. Wang, Z.A. Sun, Z. and Huang, S.M.**, (2010). Effect of [Zn]/[S] ratios on the properties of chemical bath deposited zinc sulphide thin films, *Applied Surface Science* 257 pp 122-126.
59. **Lincot, D. Froment, M. and Cachet, H.**, (1999). Chemical deposition of chalcogenide thin films from solution. *Advances in Electrochemical Science and engineering*, 6, pp 165-235.
60. **Lokande, C.D.**, (1991) Chemical deposition of metal chalcogenide thin films. *Materials Chemistry and Physics*. 27: p. 1-43.
61. **Madan A. and Shaw M.P.**, (1988) "The Physics and Applications of Amorphous semiconductors", Academic Press Inc., San Diego,pg 4-10, 471-476.
62. **Mane, R.S. and Lokhande, C.D.**, (2000) Chemical deposition method for metal chalcogenide thin films. *Materials Chemistry and Physics*,. 65: p. 1-31.
63. **Marshall, J.M. and Owen, A.E.**, (1971). "Drift mobility studies in vitreous arsenic triselenide", *Philosophical Magazine*, 24, 1281-1290.
64. **Mattox, D.M.**, (1978). Surface Cleaning in Thin Film Technology, *Thin Solid Films*, 1, 53, p 81.
65. **McPeak, M.K.**, (2010). Chemical Bath Deposition of Semiconductor Thin Films & Nanostructures in Novel Microreactors, PhD Thesis, Drexel University, p1.



66. Mereno, I. Araiza, J.J. and Avendano – Alejo, M., (2005), Thin film spatial filters: *Optics letters* 30, 914.
67. Moazzami, R., (1992) *IEEE tras. Elct. dev.* 39 2044.
68. Mohammed, M.A. Mousa, A.M. and Ponpon, J.P., (2009). "Optical and Optoelectric properties of PbCdS Ternary Thin Films Deposited by CBD" *Journal of Semiconductor Technology and Science* 9, 117.
69. Molin, N. and Diksar, A., (1995) *Thin Solid Films* 265, 3.
70. Mondal, A. Chaudhari, T.K. and Pramanik, P., (1983) *Sol. Ener. Mater.* 7, 431.
71. Morigaki, K., (1999). *Physics of Amorphous Semiconductors*, Imperial College Press, London p. 1,7,67,3,9,10,11,4,8.
72. Mott, N.F., (1967) "Electrons in disordered structures", *Advances in Physics*, 16, 49-57.
73. Mott, N.F. and E.A. Davis, (1979). *Electronic processes in non-crystalline materials*, 2nd Ed., Clarendon Press, Oxford.
74. Mott, N.F. and Davis, E.A. Cited in Singh, J. and Shimakawa, K., (2003). *Advances in Amorphous Semiconductors*, CRC Press, New York, pp 56-63.
75. Nair, M.T.S. Alvarez-Garcia, G. Estrada-Gasca, C.A and Nair, P.K., (1993) Chemically deposited Bi<sub>2</sub>S<sub>3</sub>-Cu<sub>x</sub>S solar control coatings. *Journal of the Electrochemical Society*,. 140: p. 212-215.
76. Nair, M.T.S., Guerrero, L. and Nair, P.K., (1998) Conversion of chemically deposited CuS thin films to Cu<sub>1.8</sub>S and Cu<sub>1.96</sub>S by annealing. *Semiconductor Science and Technology*,. 13: p. 1164-1169.



77. **Nair, P.K. Garcia, V.M. Gomez-Daza, O. and Nair, M.T.S.,** (2001) High thin-film yield achieved at small substrate separation in chemical bath deposition of semiconductor thin films. *Semiconductor Science and Technology*,. 16: p. 855-863.
78. **Nair, P.K. and Nair, M.T.S.,** (1989), Versatile solar control characteristics of chemically deposited PbS-Cu<sub>x</sub>S thin film combinations. *Semiconductor Science and Technology*, 1989. 4: p. 807-814.
79. **Nair, P.K. Cardoso, J. Gomez-Daza, O. and Nair, M.T.S.,** (2001) Polyethersulfone foils as stable transparent substrates for conductive copper sulfide thin film coatings. *Thin Solid Films*,. 401: p. 243-250.
80. **Nair, P.K. Garcia, V.M. Fernandez, A.M. Ruiz, H.S. and Nair, M.T.S.,** (1991) Optimization of chemically deposited Cu<sub>x</sub>S solar control coatings. *Journal of Physics D: Applied Physics*,. 24: p. 441-449.
81. **Nayak, B. B. and Acharya, H. N.,** (1985) *J. of Mat. Sci. lett.* 4, 651.
82. **Neamen, D.,** (2003). *Semiconductor Physics and Devices, Basic Principles*, Third Edition pp 144-145.
83. **Neamen, D.,** (2006). *An Introduction to Semiconductor Devices* (1st ed.) McGraw-Hill.
84. **Nicolou, Y.F. and Dupuy, M.,** (1990) *J. Electrochemical soc.*, 137 2915.
85. **Ohring, M.** (1998) *Reliability and failure of electronic materials and devices* Academic Press, p. 310.
86. **Ohring, M.,** (1992). *The Materials Science of Thin Films*, Academic Press, San Diego. Pp. 195-199, 336-339.
87. **Okimura, H.,** (1980). 17 5359.



88. **Oladeji, I.O. and Chow, L.**, (2005) Synthesis and processing of CdS/ZnS multilayer films for solar cell application. *Thin Solid Films*,. 474: p. 77-83.
89. **Orozco-Teran, R.A. Sotelo-Lerma, M. Ramirez-Bon, R. Quevedo-Lopez, M.A. Mendoza-Gonzalez, O. and Zelava-Angel, O.**, (1999) Pbs-CdS bilayers prepared by the chemical bath deposition technique at different reaction temperatures. *Thin Solid Films*, 343-344: p. 587-590.
90. **Overhof, H. and Thomas, P.** Cited in Singh, J. and Shimakawa, K., (2003). Advances in Amorphous Semiconductors, CRC Press, New York, pp 56-63.
91. **Padam, G.K and Rao, S.U.M.**, (1986).Preparation and Characterization of chemically deposited CuInS<sub>2</sub> thin films, *Sol. Ener. Mater.* 13, pp 297-305.
92. **Patnaik, P.**,(2003). Handbook of Inorganic Chemical Compounds. McGraw-Hill. N.Y.
93. **Pentia, E. Draghici, V. Sarau, G. Mereu, B. Pintilie, L. Sava, F. and Popescu, M.**, (2004) structural, electrical, and photoelectrical properties of Cd<sub>x</sub>Pb<sub>1-x</sub>S thin films prepared by chemical bath deposition. *Journal of the Electrochemical Society*,. 151: p. G729-G733.
94. **Petterson, J.D. and Bailey, B.C.**, (2005). Solid State Physics: Introduction to the Theory, pp 293-294, 113, 637.
95. **Poole, C.P.Jr.**, (2004). *Encyclopedic Dictionary of Condensed Matter Physics*, vol.1 p. 66, 440, 1391.
96. **Poortmans, J. and Arkipov, V.**, (2006) thin film solar cells, John Wiley & sons publications.
97. **Ralf, M.**, (2001) "Photonics – Linear and Nonlinear Interaction of Laser Light and Matter", springer-Verlag Berlin Heidelberg, 1-9.



98. **Ramasamy K. Malik, M.A. Helliwell, M. Raftery J. and O'Brien P.**, (2011). Thio and dithio-biuret Precursors for Zinc Sulphide, Cadmium Sulphide and Zinc Cadmium Sulphide thin films, *chem. Mater.* 23, pg 1471-1481.
99. **Ray, S.C. Karanjai, M.K. and Dashupta, D.**, (1998) Thin Solid Films, 322 117.
100. **Rieke, P.C. and Bentjen, S.B.**, (1993), Deposition of cadmium sulfide films by decomposition of thiourea in basic solutions. *Chemistry of Materials*,. 5: p. 43-53.
101. **Rnjdar , R.M. and Ali, A.B.**, (2006) Optical Properties of Thin Film.
102. **Rose, R.M. Shepard, L.A. and Wulff, J.**, (1965) Electronic Properties, Wiley & sons. New York, pg 142 – 145.
103. **Ryan, T.**, (2001). The Development of Instrumentation for Thin Film X-ray Diffraction, *Journal of Chemical education*, 78, 5, pp 613-614.
104. **Sankagal, B.R. and Lokhande, C.D.**, (2002) Materials Chemistry and Physics; 14, 126.
105. **Schroder, D. K.**, (1998) semiconductor materials and device characterization (2<sup>nd</sup> edition), Wiley, N.Y.
106. **Seghaier, S. Kamoun, N. Brini, R. and Amara, A.B.**, (2006) *Mat. Chem. Phys.* 97, 71.
107. **Simmons, J.H. and Potter, K.S.**, (2000) "Optical Materials", Academic Press, San diego, CA (USA), xiii-xv.
108. **Singh, J. and Shimakawa, K.**, (2003). Advances in Amorphous Semiconductors, CRC Press, New York, pp 56-63.
109. **Singh, J.**, (2006). *Optical Properties of Condensed Matter and Applications*, John Wiley and sons, Ltd. pp. 2-4.
110. **Skyllas-Kazacos, M. Mccann, J.F. and Arruzza, R.**, (1985) *Application of Surface Science* 22/23 1091.



111. **Sole J.G., Bausa L.E and Jaque D.** (2005). An introduction to the optical Spectroscopy of inorganic Solids, pg. 11-12.
112. **Stern, F.** Cited in Anuar, K. Tan, W.T. Jelas, M. Ho, S.M. and Gwee, S.Y., (2010). Effects of deposition period on the Properties of FeS<sub>2</sub> Thin films by Chemical Bath Deposition Method, *Thammasat Int. J. Sc. Tech.*, 15,2, p 64.
113. **Tauc, J.**, (1974). Amorphous and Liquid Semiconductors, Plenum: New York, p. 159.
114. **Varkey, A.J.**, (1989) Chemical bath deposition of Cu<sub>x</sub>S thin films using ethylenediaminetetraacetic acid (EDTA) as complexing agent. *Solar Energy Materials*, 1989. 19: p. 415-420.
115. **Vaughan, D. J. and Craig, J. R.** (1978). Mineral Chemistry of Metal Sulfides. Cambridge: Cambridge University Press.
116. **Venables, J.A. Spiller, G.D.T. and Hanbucken, M.**, (1984), Nucleation and growth of thin films, *Rep.Prog.Phys.* 47 pp.399.
117. **Vossen, J. L.**, (1991) Thin film processes: Elsevier Publishing.
118. **Wikipedia, atomic spectroscopy**
119. **Wikipedia, energy band structure**
120. **Wikipedia, solid**
121. **Wikipedia, thin film**
122. **Yacobi, B. G.**, (2004) Semiconductor Materials: An Introduction to Basic Principles, pp.1-3, 154-157, 107.



123. **Yamamoto, T. Tanaka, K. Kubota, E. and Osakada, K.,** (1993) Deposition of copper sulfide on the surface of poly(ethylene terephthalate) and poly(vinyl alcohol) films in the aqueous solution to give electrically conductive films. *Chemistry of Materials*,. 5: p. 1352-1357.
124. **Yang, P.D. and Lieber, C.M.,** (1996), Nanarod-superconductor composites: a pathway to high critical current density: *Science* 273, 1836.

KNUST

